TEMPORAL EVALUATION OF SNOW DEPLETION CURVES DERIVED FOR UPPER EUPHRATES BASIN AND APPLICATIONS OF SNOWMELT RUNOFF MODEL (SRM)

A THESIS SUBMITTED TO
THE GRADUATE SCHOOL OF NATURAL AND APPLIED SCIENCES
OF
MIDDLE EAST TECHNICAL UNIVERSITY

BY

GÖKHAN MARIM

IN PARTIAL FULFILLMENT OF THE REQUIREMENTS
FOR
THE DEGREE OF MASTER OF SCIENCE
IN
GEODETIC AND GEOGRAPHIC INFORMATION TECHNOLOGIES

SEPTEMBER 2008

Approval of the thesis:

TEMPORAL EVALUATION OF SNOW DEPLETION CURVES DERIVED FOR UPPER EUPHRATES BASIN AND APPLICATIONS OF SNOWMELT RUNOFF MODEL (SRM)

submitted by **GÖKHAN MARIM** in partial fulfillment of the requirements for the degree of **Master of Science in Geodetic and Geographic Information Technologies Department, Middle East Technical University** by,

Prof.Dr. Canan Özgen _____
Dean, **Gradute School of Natural and Applied Sciences**

Assoc.Prof.Dr.Şebnem Düzgün _____
Head of Department, **Geodetic and Geographic Inf. Tech.**

Prof.Dr.A.Ünal Şorman _____
Supervisor, **Civil Engineering Department, METU**

Examining Committee Members

Prof. Dr. Alparslan Arıkan _____
Hydrogeology Dept., Hacettepe University,

Prof.Dr.A.Ünal Şorman _____
Civil Engineering Dept., METU

Prof.Dr.Vedat Toprak _____
Geological Engineering Dept., METU

Assoc.Prof.Dr Nuri Merzi _____
Civil Engineering Dept., METU

Özgür Beşer _____
Proland Engineering Company Ltd.

Date: **05.09.2008**

I hereby declare that all information in this document has been obtained and presented in accordance with academic rules and ethical conduct. I also declare that, as required by these rules and conduct, I have fully cited and referenced all material and results that are not original to this work.

Name, Last name: Gökhan Marım

Signature :

ABSTRACT

TEMPORAL EVALUATION OF SNOW DEPLETION CURVES DERIVED FOR UPPER EUPHRATES BASIN
AND
APPLICATIONS OF SNOWMELT RUNOFF MODEL

Marım, Gökhan

M.S., Department of Geodetic and Geographic Information Technologies

Supervisor: Prof.Dr.A.Ünal Şorman

September 2008, 112 pages

Water is becoming very important issue day by day with descending usable water and energy resources. In the aspect of water resources management, especially for the optimum reservoir management, predicting runoff for large reservoirs by applying hydrologic model is a recent and crucial topic. The most important model input and predictor parameters to estimate runoff for the mountainous regions are to be distribution of rainfall; temperature and snow cover area, (SCA). It is seen that many predictor variables should be integrated with Geographic Information Systems (GIS) and Remote Sensing Techniques especially for hydrologic model variable preparation. Satellite products have the potential for obtaining those kinds of data in near real time. In this study, the changes of SDC are generated by the analysis of optical satellite and by using SDC as an input to hydrological models runoff is simulated for Upper Euphrates Basin (10215.7 km2) which is a sub basin of Euphrates Basin. Largest dams of Turkey; Keban, Karakaya and Atatürk are located on Euphrates River. Optimum operations of these dams depend on forecasting incoming water in early summer season. Euphrates River is fed mainly from snowmelts in spring or early summer time.65-70 % of the annual flow is contributed

from snowmelt in that region. Main objective of this study is to obtain the spatially and temporally distributed SCA percentages from optical satellite, which are required as one of the main input variables of the hydrological model used in the application. SCA percentages and SDC are obtained for snowmelt years 2004-2007 by using high temporal resolution optical remote sensing data: Terra Moderate Resolution Imaging Spectroradiometer (MODIS). In this study, Terra MODIS snow cover map product, MOD10A1 which has a spatial resolution of 500 m is used. As a hydrological model Snowmelt Runoff Model (SRM) was applied. SRM was built up on the well-known degree day approach. In this study SRM is simulated for two years 2006 and 2007.The simulation results are compared and resultant model parameters are obtained for future runoff forecast studies. In this study, beside recommendations, discussions on the variables and SRM parameters are also provided.

Keywords: Snow Cover Depletion Curves, Snowmelt Runoff Model, MODIS, Upper Euphrates Basin

ÖZ

YUKARI FIRAT HAVZASI İÇİN ELDE EDİLEN KAR ÇEKİLME EĞRİLERİNİN ZAMANSAL ANALİZİ VE KAR ERİME AKIM MODELİ UYGULAMALARI

Marım,Gökhan

Yüksek Lisans, Jeodezi ve Coğrafi Bilgi Teknolojileri Bölümü

Tez Yöneticisi: Prof.Dr.A.Ünal Şorman

Eylül 2008, 112 sayfa

Azalan su ve enerji kaynakları düşünüldüğünde su, her geçen gün daha önemli bir konu haline gelmektedir. Su kaynaklarının yönetimi, özellikle barajların verimli yönetimi için hidrolojik modellerin uygulanarak büyük baraj haznelerine gelen akımın tahmin edilmesi güncel ve kaçınılmaz bir hale gelmiştir. Dağlık bir alanda akım benzeşiminin yapılmasında kullanılan ve hidrolojik modellere girdi oluşturan model değişkenlerinin en önemlileri yağışın, sıcaklığın ve karla kaplı alanların dağılımıdır. Hidrolojik model girdi değişkenlerinin oluşturulmasının Coğrafi Bilgi Sistemleri ve Uzaktan Algılama Teknikleri ile bütünleşmesi gerektiği görülmüştür. Gerçek zamanlı mekansal ve zamansal değişim gösteren karla kaplı alan dağılımının uydu ürünleri ile elde edilmesi mümkündür. Bu çalışmada, kar çekilme eğrileri, optik uydu görüntülerinin analizleri ile oluşturulmuş ve hidrolojik model girdisi olarak kullanılarak Fırat havzasının alt havzası olan Yukarı Fırat Havzası (10,195 km^2) için akım simulasyonu yapılmıştır. Türkiyenin en büyük barajları; Keban, Karakaya ve Atatürk Fırat Havzası içerisindedir.Bu barajların optimum yonetimi erken yaz dönenminde gelen suların tahminine bağlıdır. Fırat nehri genel olarak bahar ve

erken yaz ayları kar erimesinden beslenmektedir. Bu bölgede yılık ortalama akımın % 65-70'i kar erimesindendir. Bu çalışmanın ana amacı, uygulanan hidrolojik model için önemli bir değişken olan, optik uydudan elde edilmiş, zamansal ve mekansal dağılımlı karla kaplı alan yüzdelerinin elde edilmesidir. 2004–2007 yılları için, karla kaplı alan yüzdeleri ve kar çekilme eğrileri yüksek zamansal çözünürlüğe sahip optik uzaktan algılama verileri: "Terra Moderate Resolution Imaging Spectroradiometer (MODIS)" ile elde edilmiştir. Bu çalışmada, Terra MODIS'in karla kaplı harita ürünü olan ve 500 m alansal çözünürlüğe sahip MOD10A1 kullanılmıştır. Hidrolojik model olarak Kar Erime Akım Modeli; SRM (Snowmelt Runoff Model) kullanılmıştır. SRM, kar erimesi hesaplarında derece gün yaklaşımını kullanmaktadır. Bu çalışmada SRM 2006 ve 2007 simule edilmiştir. Simulasyon sonuçları karşılaştırılmış ve model parametreleri akım tahmin çalışmaları için elde edilmiştir. Bu çalışmada tavsiyelerle birlikte değişkenler ve SRM parametreleri ile ilgili tartışmalar da sunulmuştur.

Anahtar kelimeler: Kar Çekilme Eğrisi, Hidrolojik Modelleme, MODIS, Yukarı Fırat Havzası

To My Parents and Friends…

ACKNOWLEDGEMENTS

My great thanks are to Prof. Dr. A. Ünal Sorman whom I see as a man full of enthusiasm to learn, to search and to teach. I would like to appreciate to him for his encourage to finish this study even I don't believe i will finish this study. I acknowledge supervision and valuable suggestions of him .It was more than honoring to be part in the projects that are guided by him.

Many thanks are also extended to Asst. Prof. Dr Aynur Şensoy Şorman. The contributions made throughout the thesis and publications can not be over simplified. Her important and valuable suggestions make the most difficult things simplify. It was honor and enjoyable to have a chance to study even from Eskisehir. I owe special thanks to Asst. Prof. Dr .Zuhal Akyürek for her valuable support throughout master study of mine. I also owe special thanks to Prof.Dr.Vedat Toprak, Assoc. Prof.Dr.Nuri Merzi, Prof.Dr.Alpaslan Arıkan, Prof.Dr.İbrahim Gürer for their valuable assessments on this thesis.

My deepest thanks goes to my collogue, roommate in laboratory, course mate, my traveling companion in Switzerland, the person that makes this study enjoyable :Serdar Sürer.I wish he will realize his dreams. Many thanks are also extended to my great friends "Ortillerim" Yılmaz Brothers (Hazım and Serkan Yılmaz) and to my second brother "double S" Suat Doğan. I want to thank my dear lovely small motion flatmate; Yavuz for his patient to me. I also appreciate A.M.'s important and interesting contribution to my life and to my thesis especially while correcting each chapter. I also owe special thanks to my companions in the Chamber of Civil Engineers ; İlker Gündez, Taylan Ulaş Evcimen, Eylem Bilge Yazıcıoğlu, Ferhat Yaşar Arıkan. I thank all of my friends while they are encouraging me in this study both positively and negatively.

TABLE OF CONTENTS

LIST OF TABLES

TABLES

LISTS OF FIGURES

FIGURES

LIST OF SYMBOLS

A	: Area of zone
Dv	: Percentage of volume difference between the measured and the simulated runoff
DEM	: Digital Elevation Model
DMI	: State Meteorological Organization
DMSP	: Defense Meteorological Satellite Program
DSI	: State Hydraulic Works
EIE	: General Directorate of Electrical Power Resources Survey and Development Administration
EOS	: Earth Observing System
GIS	: Geographic Information Systems
GOES	: Geostationary Operational Environmental Satellite
HDF	: Hierarchical Data Format
HDF-EOS	: Hierarchical Data Format- Earth Observing System
IMS	: Interactive Multisensor Snow and Ice Mapping System
IRBMC	: International River Basin Management Congress
L	: Time Lag
M	: Snowmelt rate
MDC	: Modified depletion curves
MOD...	: Generated from EOS Terra Spacecrafts
MODIS	: Medium Resolution Imaging Spectroradiometer
MODIS10A1	: MODIS/Terra Snow Cover Daily L3 Global 500m Grid
MRT	: MODIS Reprojection Tool
MYD	: Generated from EOS Aqua Spacecrafts
NDSI	: Normalized Difference Snow Index
NDVI	: Normalized Difference Vegetation Index

NESDIS	: National Environmental Satellite, Data, and Information Service
NOAA-AVHRR	: National Oceanic and Atmospheric Administration – Advanced Very High Resolution Radiometer
NE(delta)T	: Noise-equivalent temperature difference
NOHRSC	: National Operational Hydrologic Remote Sensing Centre
NSIDC	: National Snow and Ice Data Center
P	: Precipitation falling as rain in the zone
R2	: Nash-Sutcliffe coefficient
RCA	: Rainfall Contributing Area
RS	: Remote Sensing
RMS	: Root Mean Square
S	: Ratio of Snow Covered area to the total area
SCA	: Snow Covered Area
SDC	: Snow Depletion Curve
SDS	: Scientific Data Set
SNR	: Signal-to-noise ratio
SRM	: Snowmelt Runoff Model
SSM/I	: Special Sensor Microwave/Imager
SWE	: Snow Water Equivalent
T	: Number of Degree Days
Ta	: Average Daily Temperature
Tb	: Base Temperature
Tcrit	: Critical Temperature
Q	: Average daily discharge
Qi	: Measured dailly discharge
Q'_i	: Simulated dailly discharge
$\overline{Q}$	: Average dailly discharge for simulation year
QA	: Quality assurance
VR	: Measured runoff model
V'_R	: Simulated runoff model

WMO	: World Meteorological Organization
ΔT	: The adjustment by temperature lapse rate
a	: Degree day factor
cS	: Correction factor for snow
cR	: Correction factor for rain
$\bar{h}$	: Hypsometric mean elevation of a zone
hst	: Height of temprature station
k	: Recession coefficient
ρs	: Density of Snow
ρw	: Density of Water
γ	: Temperature Lapse Rate

CHAPTER 1

INTRODUCTION

1.1. Problem Definition

Water is becoming very important issue day by day with decreasing fresh water resources and increasing population of the world. The critical importance of water for countries can not be denied. It is an international argument that water is potentially going to be reason for wars between countries. As it wouldn't be forgotten in all of the studies that each humanbeing has human right reach to water. Water can not be tolerable with any material in the world. That is why the issue; managing the water resources efficiently is becoming very important day by day.

The climate of Turkey is semi-arid with extremities in temperature. The climate and precipitation shows great variance in Turkey and this also makes difficult to manage water resources. In International River Basin Management Congress, 2007 (IRBMC) book, it is written that Turkey is located on the crossroads of Asia and Europe and surrounded with 8300 km coastline. Turkey has a total surface area of 779452 km^2, of which 765152 km^2 is land and remaining 14300 (1.83 %) is water surface. Turkey gross and exploitable potentials are 234 and 112 billion m^3 respectively (IRBMC, 2007). Water available per person per year is 3162 m^3 according to gross potential in Turkey. Water available per capita per year is 1430 m^3 (45 % of gross potential) according to exploitable potential in Turkey. Moreover Turkey can use only % 36.5 of this 112 billion m^3 exploitable potential for year 2003 .It is defined that below

1000 m^3 per capita per year is defined as water deficit country. Turkey is water stress country however Turkey is going to be water deficit country in few years with that population increase (IRBMC, 2007).

The water management with those potential is an important governmental issue in Turkey. Turkey is divided into 25 basins. The Euphrates and Tigris basin account for the 28.5 % of the potential of the country (IRBMC, 2007) and they are located in eastern part of Turkey. Largest dams of Turkey; Keban, Karakaya and Atatürk are located on this river. Optimum operations of these dams depend on forecasting incoming water in early summer season. This river is fed mainly from snowmelts in spring and early summer time.65-70 % of the annual flow is contributed from snowmelt and rain on snow during spring and early summer months in that region. In the eastern part of Turkey snow stays half of a year.

The hydrological models are the main necessities for efficient water resources managements. Predicting inflow to reservoir by applying hydrological modelling is a recent and important topic. The most important variable to such models is temporarily and spatial distributed snow cover area information especially in mountainous regions. To obtain temporarily and spatial distributed snow cover area (SCA) information, Remote Sensing Techniques (RS) and Geographic Information Systems (GIS) are essential as tools for computations. Satellite data has the potential for obtaining those kinds of data in real time. Remote sensing integrated with GIS serve valuable information for snowmelt runoff models. Those new technologies improve the accuracy of the models consequently runoff predictions. A suitable integration between RS, GIS and a snowmelt runoff model would provide accurate estimates for efficient water management, energy production and flood mitigation.

1.2. Scope and Purpose of the Study

In this study, Snow Cover Area (SCA) and Snow Depletion Curves (SDC) are generated by the analysis of optical satellite and by using SDC as an input to Snowmelt Runoff Model (SRM) is simulated for Upper Euphrates Basin (10215.7

km^2) which is a sub basin of Euphrates Basin. SRM was built up on the well-known degree day approach. SRM is also famous due to the ability of using SCA percentages directly. Temporarily and spatially distributed SCA percentages, precipitation and temperature variables are main input to applied SRM used in this application for snowmelt years 2004-2007. In order to obtain SDC, high temporal resolution optical remote sensing data: Terra Moderate Resolution Imaging Spectroradiometer (MODIS) is used.

The main aim of this study is simulating SRM for two years 2006 and 2007 by calibrating model parameters. Obtaining resultant model parameters is aimed in order to forecast incoming flow to basin but forecasting is not performed. Beside these, to obtain the spatially and temporally distributed SCA percentages from optical satellite, which are required as one of the main input variables of the hydrological model used in this application is important for this study. SDC for 5 elevation zone and for years 2004, 2005, 2006 and 2007 are obtained by Remote Sensing Techniques and GIS applications. SDC for years 1997 and 1998 are obtained from previous studies made in this basin area (Şensoy, 2000 and Tekeli 2000).To gather all of them and to compare for each elevation zone is also aimed in this study.

The subjects described in the following chapters are given below:

In chapter 2, the pilot basin area is introduced. The reason for choosing that area is detailed in this chapter. The snow hydrology in that region is mentioned. Many created maps of basin area which display different properties of basin area are shown. Social, geostrategically importance of basin area and especially reservoirs is also described. The location and instrumentation of Meteorological Stations is presented in detail. Beside this, previous studies made in that basin area and literature about this topic are also mentioned.

In chapter 3, application of remote sensing and geographic information system in snow hydrology is introduced. Spectral characteristic of snow is also described in this chapter. After the importance of snow in hydrology is mentioned, the remote

sensing history in snow hydrology is detailed. MODIS data, MODIS snow products and MOD10A1 which is used to obtain SCA percentages are introduced in this chapter.Beside these, MODIS snow detection algorithm is described in detail. Application of geographic information system integrated with remote sensing is presented in and how to obtain temporarily-spatially distributed SCA percentages is described. The GIS and MODIS tools and applications that are used to get useful information from MOD10A1 are described in detail.

Chapter 4 mainly describes the hydrological model that is used in this study. In this chapter, the general information about SRM is mentioned. Purpose of SRM is described and the model structure and formula is defined. The necessary data to run SRM is discussed. Area-elevation curve of Karasu Basin, main variables input to hydrological model are described in that chapter. The methodology to obtain necessary data for SRM is also presented.

In chapter 5, the performed SRM runs are presented after obtaining necessary data for SRM and SRM parameters in chapter 4.The SRM result for the year 2006 that are applied with SRM parameters obtained in chapter 4 from calculations or from previous studies are presented. The model result obtained from calibrated parameters for year 2006 is presented. The methodology of calibration of SRM parameter for the year 2006 is described also in this chapter. The result of SRM run for the year 2007 which is applied with the model parameters that are calibrated for the year 2006 is presented. After that, the result of one more calibration made for the year 2006 and 2007 is presented in detail. The resultant parameters are same for both year and are tabled in this chapter.

Chapter 6 includes conclusions and recommendations. Recommendations are purposed to be guideline to future snow detection and hydrological modelling studies.

CHAPTER 2

STUDY AREA, KARASU BASIN

2.1. Introduction

Many civilizations are developed in Mesopotamia “the land between two rivers”; Euphrates and Tigris River. Mesopotamia is the region between Euphrates and Tigris Rivers and lies on South East Anatolia Region of Turkey to Persian Gulf (Figure 2.1). This area is still keeping its importance. Euphrates and Tigris Rivers are very important for Mesopotamia agriculture, energy, industry sector and economy of region. The study area is chosen as a pilot area; Karasu Basin which is Upper Euphrates River Basin (Figure 2.2).

There are 5 riparian countries sharing the Euphrates-Tigris basin as shown in Figure 2.1 Turkey, Syria Iran, Iraq and Saudi Arabia. Those rivers crossing national boundaries are always main international issue between those countries especially for Turkey, Syria and Iraq.

Euphrates River starts from Turkey pass through two downstream country; Iraq and Syria. Euphrates River is the longest river of South West Asia with 2700 km length and 35.6 milliard cubic meter average runoff (Aytemiz, 2006). The surface area that each country contributes is given in Table 2.1 (UNEP, 2001). 21.1% of Euphrates Basin area and 14.3% of Tigris Basin area is in Turkey .However 98% of Euphrates runoff and 53% of the discharge of the Tigris are contributed from Turkey.

Table 2.1 Area and percent of the Euphrates-Tigris drainage basin in riparian countries (UNEP, 2001)

	Tigris Basin		**Euphrates Basin**	
Country	**km^2**	**%**	**km^2**	**%**
Turkey	**53052**	**14.30**	**121787**	**21.10**
Syria	948	0.20	95405	16.50
Iran	175386	47.20	-----	------
Iraq	142175	38.30	282532	49.00
Saudi Arabia	-----	------	77090	13.40
Total	371561	100.00	576814	100.00

The characteristic property of the rivers regime is: their flows are irregular. Fluctuations in a year occur in the flows of these two rivers. The large floods are common in spring times due to snowmelt. That is why monitoring snow cover and using it in runoff modelling is important for that region for the water resources management point of view.

Eastern part of Turkey is mountainous and major contributor to runoff in that region is snowmelt. There are three important dams for Turkey on the Euphrates River sequentially Keban, Karakaya and Atatürk (Figure2.2) .That is why snowmelt runoff modelling and snow detecting studies are important for that region.

Because of the geopolitical and snow hydrological importance of this area, an important number of thesis studies were carried out for that basin. In both master and doctorial thesis Karasu Basin is studied by Tekeli (2000, 2005).These two previous studies are about integrating snowmelt runoff with snow cover area detected by satellite products. Beside these, Şensoy's master and doctorial thesis (2000, 2005) are both about physical snowmelt modelling and GIS applications. Furthermore Şorman (1999, 2005) had also studied on the subject GIS and Remote Sensing applications on hydrological modelling for that area.

2.2. Upper Euphrates River Basin; Karasu Basin

Karasu Basin is sub basin area of Euphrates River Basin. Euphrates River has two branch; Murat and Karasu. Karasu Basin is geographically in between $39^0$7'39'' – $41^0$34'21''latitude and $39^0$27'1.50'' – $40^0$19'38'' longitude. Total Karasu basin area is 10195.24 km^2. Karasu Basin is spread on a mountainous region between the 1125-3487 m elevation ranges and the average altitude of the basin is 1977 m.

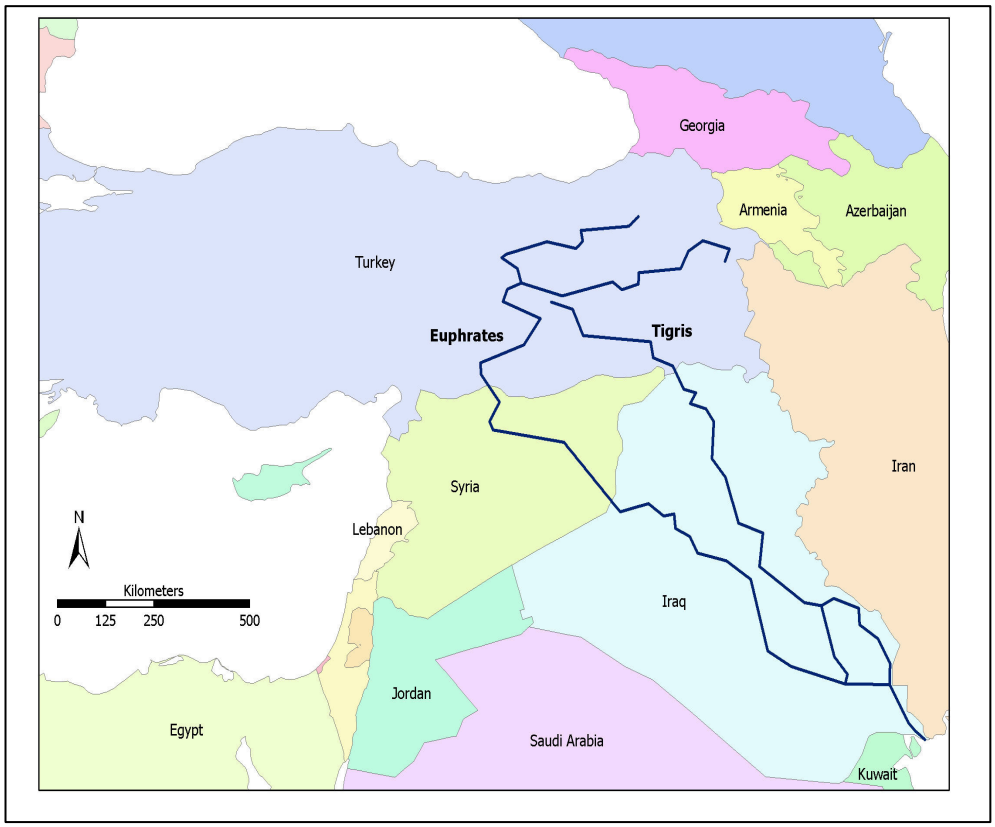

Figure 2.1 Mesopotamia, Euphrates and Tigris River

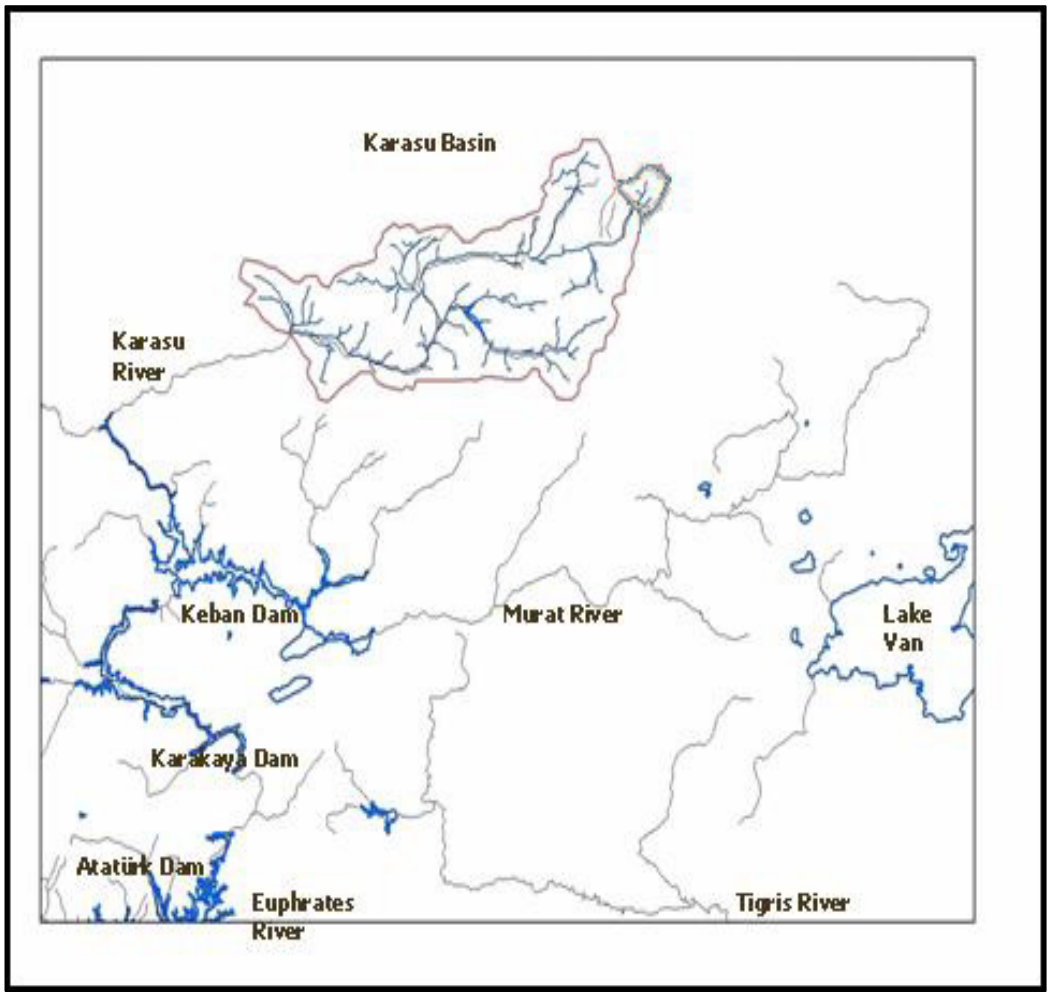

Figure 2.2 Upper Euphrates River Basin

The Figures 2.3 and 2.4 shows the slope and aspect map of basin area. The Figure 2.5 is obtained by combining slope map with aspect map of basin area. An aspect-slope map simultaneously shows the aspect (direction) and degree (steepness) of slope for Karasu Basin. The coloring is based on improvements made on MKS-ASPECT method which is performed by Moellering and Kimerling in 1990.This map helps to recognize and imagine the altitude property of basin area. The aspect has an important effect on microclimate of the region. For instance, because the sun rays are hottest at afternoon, the west facing slope areas are warmer. This can have big influence on vegetation of the area. Moreover east–facing slopes are protected from dry west winds.

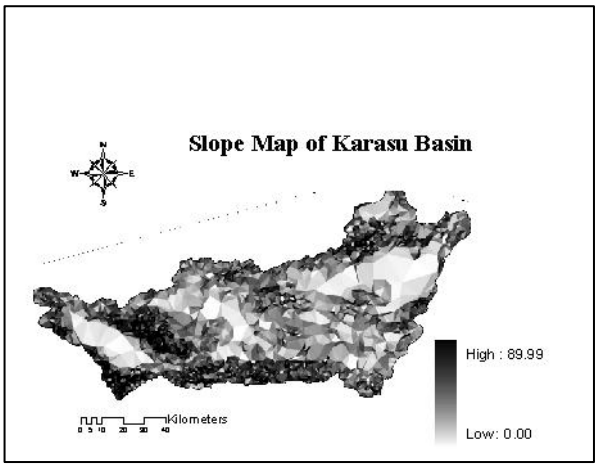

Figure 2.3 The slope map of basin

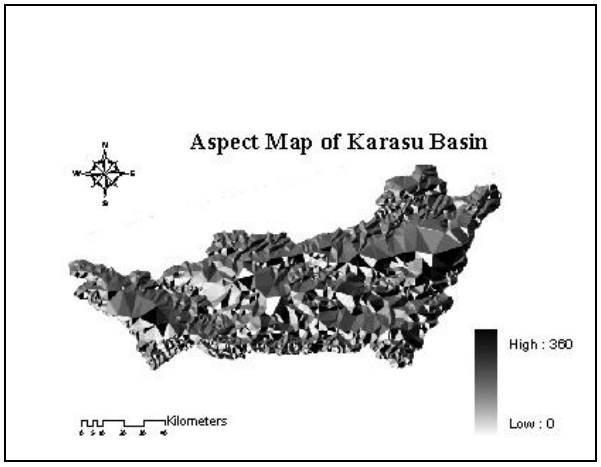

Figure 2.4 The aspect map of basin

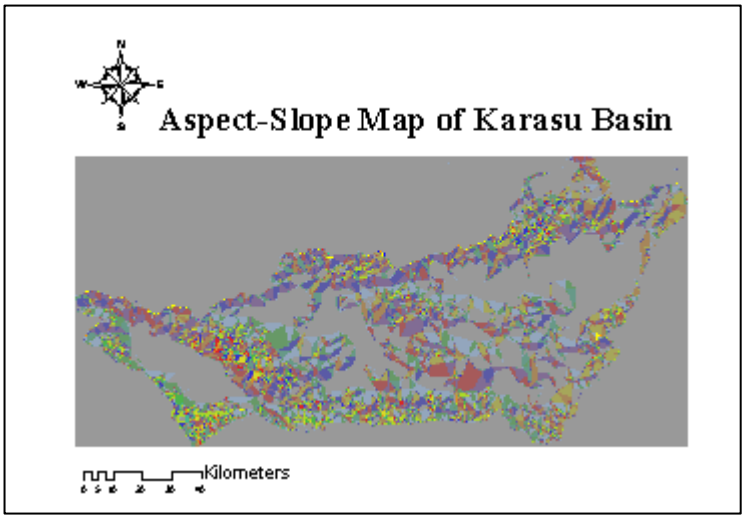

Figure 2.5 The aspect-slope map of basin

The Figure 2.6 shows the 3D view of Digital Elevation Model (DEM) of basin area. Triangulated Irregular Network (TIN) is generated from DEM of basin area. The Figure 2.7 is the TIN of basin area with coloured according to elevation zones in Table 2.1 .Moreover Figure 2.8 is generated from TIN and shows 5 times exaggerated hillshade of basin area. All of these Figures are aimed to give information about cartographic property of basin area. Different types of visualizing technique are used by the help of GIS softwares.

As it can be seen from elevation ranges and elevation maps of basin area, Karasu Basin is a big mountainous area. That is why to represent the all basin is not easy. In snow hydrology altitude information and representation is very important in terms of recognizing the snow cover area by remote sensing technique. The Karasu Basin is divided into 5 elevation zones to represent temporal and spatial distribution with regard to altitude of basin. The topographic information about elevation zones are given in Table 2.1.

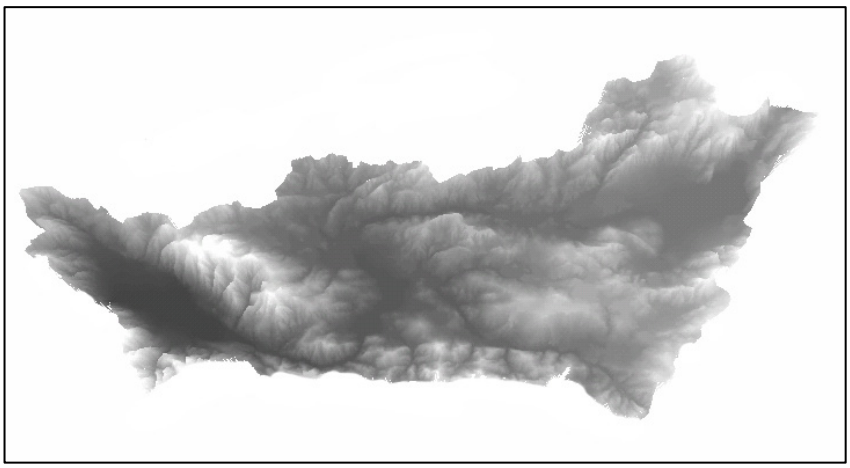

Figure 2.6 3D view of DEM of basin area

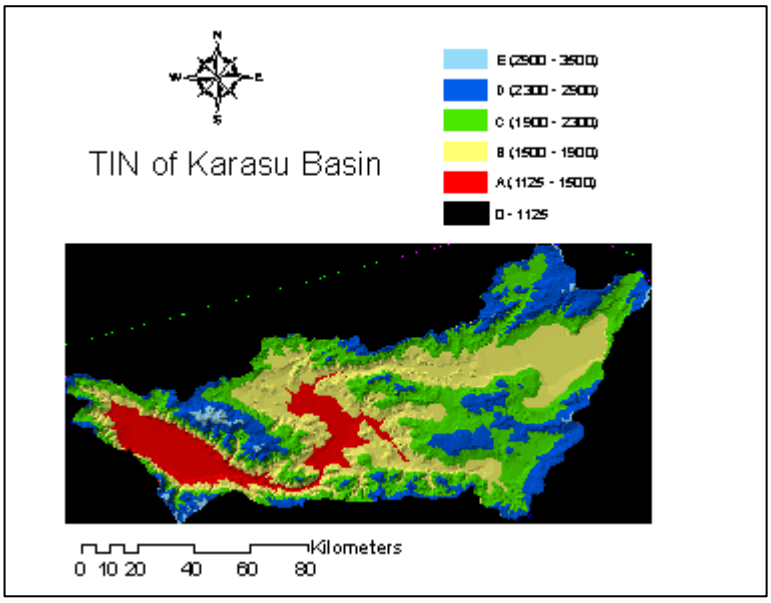

Figure 2.7 TIN map of basin area

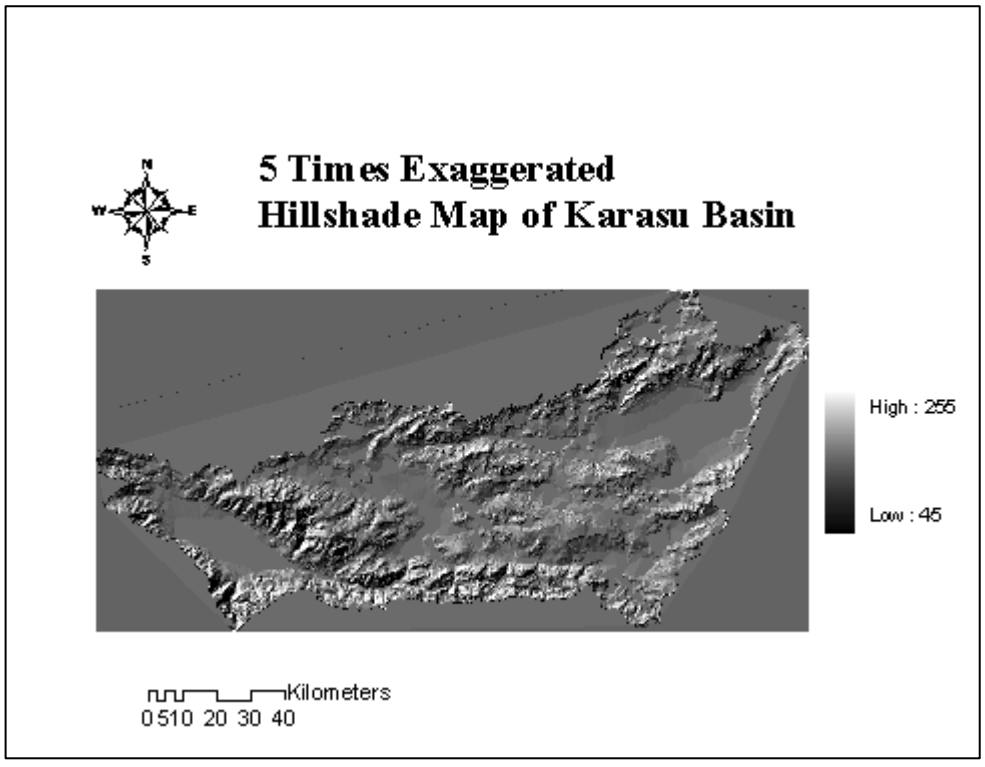

Figure 2.8 With 45 altitude and 345 azimuth angle 5 times exaggerated hillshade map of basin area

Contour and DEM maps of Karasu Basin are shown in Figure 2.9 and 2.10. They are coloured and divided according to 5 elevation zone. It can be seen from Figures 2.7, 2.9, 2.10 and Table 2.1 that the largest segment of the basin area is C and B elevation zone respectively 34 % and 32 % of total basin area. Therefore, 66 % of basin area consists of B and C elevation zone. Thus the contribution to runoff from this elevation zones determined total runoff a lot. However in this region, yearly runoff volume is fed by mainly snowmelt and snow stays on the ground more than half of the year in the elevation zones D and E. That is why their contribution to runoff is very important also. All of the modelling applications, spatial and temporal distribution of precipitation and temperature data is done according to this division of elevation zones (Figure 2.10, Table 2.2).

Table 2.2 Topographic characteristics of elevation zones

ZONE	Elevation Range (m)	Area (km^2)	Area (%)	Hypsometric Mean Elevation(m)	Mean Slope (%)
A	1125-1500	1123,2	11	1352	6,1
B	1500-1900	3268,5	32	1751	11,5
C	1900-2300	3459,3	34	2097	18,1
D	2300-2900	2196,8	21	2482	21,3
E	2900-3487	167,9	2	2989	26,3
Whole Basin	1125-3487	10215,7	100	1977	15,5

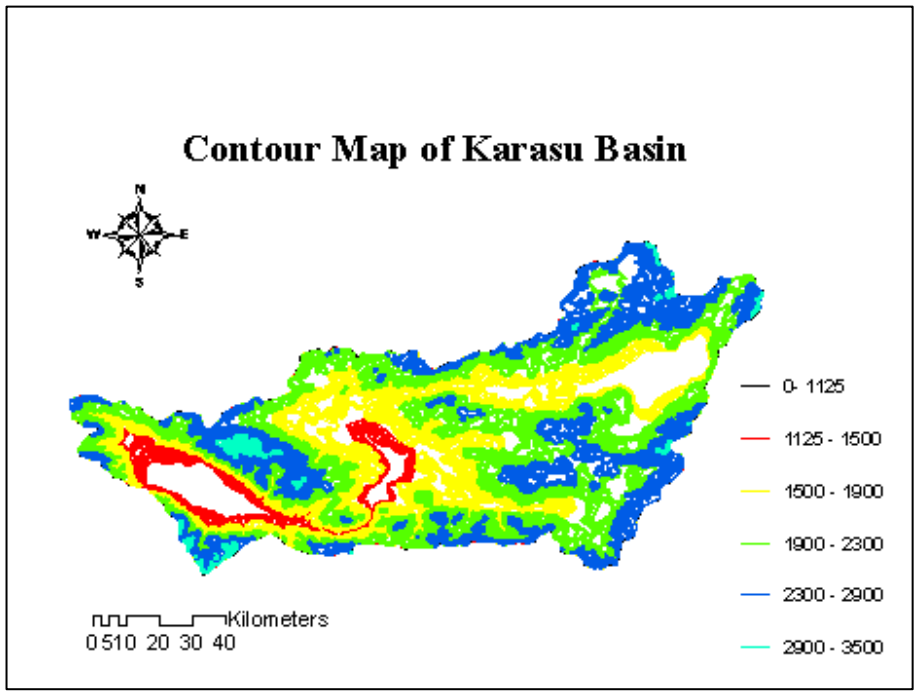

Figure 2.9 Divided into 5 elevation zone contour map of basin area

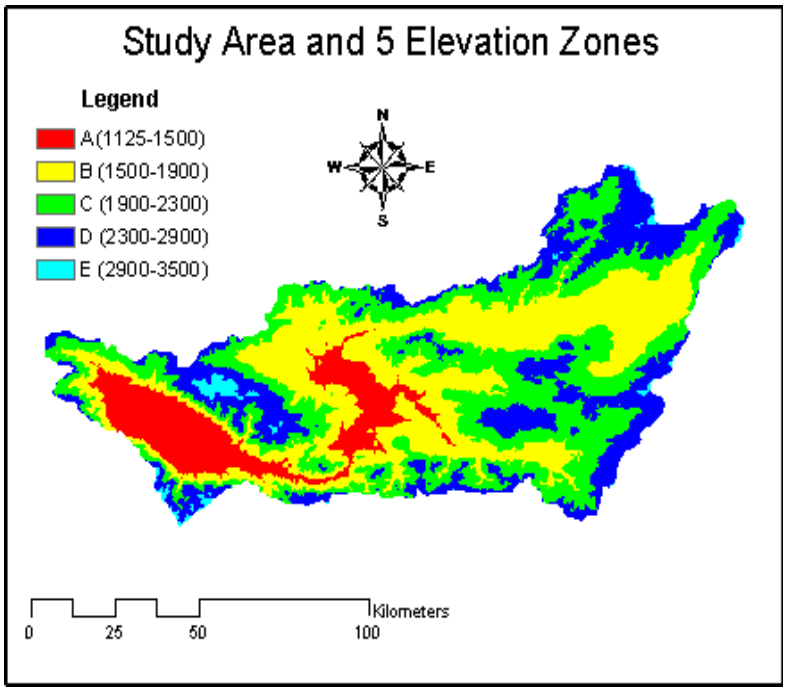

Figure 2.10 Divided into 5 elevation zone DEM of basin area

Table 2.3 gives some information about Karasu Basin. The properties of dams Kuzgun, Tercan, Erzincan is shown in Table 2.4

The mountainous character of basin can be realized from average slope of basin area which is 15.5 % (Table 2.3). Basin maps also give idea about topographic characteristic of basin area. There are two important cities located at that basin area (Table 2.3). It is recognizable that all of dams located in Karasu Basin are irrigation dams (Table 2.4).That is why reservoir management performance is important for this region economy.

Karasu basin outlet is controlled by the stream gauging station EIE 2119 under the supervision of General Directorate of Electrical Power Resources Survey and Development Administration (EIE) in Turkey. The runoff measurements obtained from EIE 2119 at Figure 2.11 for the year 1998, 2006 and 2007 show that the % 60-70 of the incoming flow is due to snowmelt and rainfall during spring and early summer months (Tekeli, 2005).

Generally snow is started to accumulate in December. During the winter time most of the precipitation type is snowfall however partial areal precipitation is also common. During spring time mixed rain-snow precipitation type occurs generally. According to these climatic properties, low flows occur in wintertime. With the following spring time, high flows occur due to melting of accumulated snow and rain on snow events. After that period flow declines in early summer.

The area can be defined as predominantly steppe. It is similar to a prairie, although a prairie is generally reckoned as being dominated by tall grasses, while short grasses are said to be the norm in the steppe (Şensoy, 2005). It may be semi-desert, or covered with grass or shrubs, or both depending on the season (Şensoy, 2005).

Table 2.3 The information about Karasu Basin

Basin Area	10,215.7 km2
Elevation Range	1125 - 3487 m
Mid Altitude	1977 m
Average Slope	15.50%
Cities in Basin	Erzurum, Erzincan
Dams in Basin	Kuzgun, Tercan, Erzincan

Table 2.4 Properties of dams

Dams	Kuzgun	Tercan	Erzincan
Location	Erzurum	Erzincan	Erzincan
Aim	Irrigation and Energy	Irrigation and Energy	Irrigation
The Constracting time	1985-1996	1969-1988	1991-1997
Lake Volume	312 hm^3	178 hm^3	8.39 hm^3
Lake Area	11.20 km^2	8.85 km^2	0.46 km^2

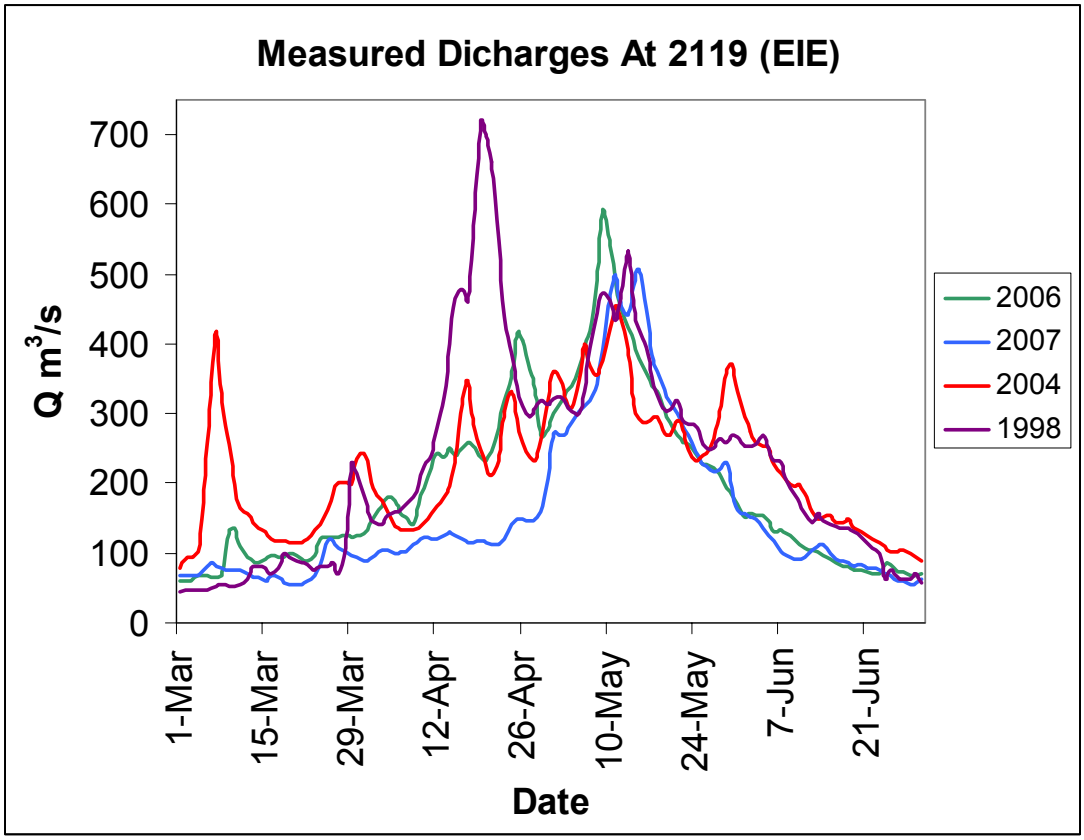

Figure 2.11 Measured discharges at 2119 (EIE)

2.3. Location and Instrumentation of Meteorological Stations

In modelling studies temperature and precipitation data are main input variable. Most of the measurements obtained are point measurements. Consequently they have to be distributed temporally and spatially. The method that is used for distribution is detailed in the Chapter 4. The accuracy of these point measurements is very important for the precision and accuracy of those distribution results.

The temperature measurements are most common, since it is easier to measure at anywhere. Ideally, these measurements should be made at a specified height above the snow surface especially, shielded from the effects of radiation or conduction from sources other than the atmosphere (Şorman, 2005). This problem is maximized when wind speeds are low and mixing of the air is small (Şorman, 2005).

Collecting hydrometerological data at high elevations is very difficult and expensive especially in extreme climatic conditions. There are not so many meteorological stations above 1850 m and generally they are not continuous. In Karasu Basin, the highest meteorological station is located at 2130 m for precipitation measurements and 2340 m for temperature measurements .Before 1999, the highest meteorological station was located 1758 m in Erzurum on the other hand, the highest point in Karasu Basin is 3487 m.

Precipitation in Karasu Basin falls mainly as snow during November through March and rain at other times. But sleet (mixed rain and snow) is also quite frequent in the transition periods between rain and snow depending on air temperature (Şorman, 2005).

In Figure 2.12 there is the map of station used in this study and located in or close to Karasu Basin. Both daily average temperature and daily total precipitation data which are measured from stations are used for obtaining spatial and temporal distribution of input variable to SRM. It is shown in Table 2.5 that there are 12 meteorological stations in between 1154 – 2340 m elevation range. Both precipitation and temperature values are measured in 9 of all stations. Only temperature values are measured in 3 of all stations.

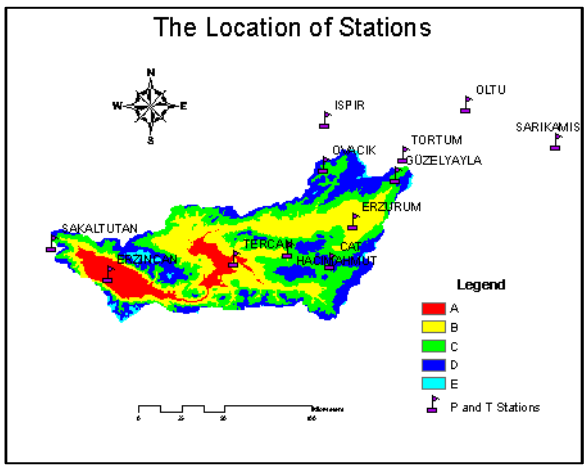

Figure 2.12 Precipitation and temperature measured stations

Table 2.5 Autometed and non-automed Meteorological stations

Stations	Elevation (m)	Precipitation (mm)	Temprature (^{0}C)
Erzincan	1154	√	√
İspir	1222	√	√
Oltu	1322	√	√
Tercan	1425	√	√
Tortum	1572	√	√
Erzurum	1758	√	√
Hacımahmut	1965		√
Güzelyayla	2065	√	√
Sarıkamış	2102	√	√
Ovacık	2130	√	√
Sakaltutan	2150		√
Çat	2340		√

CHAPTER 3

REMOTE SENSING IN SNOW HYDROLOGY

3.1. Introduction and Spectral Characteristic of Snow

Snowmelt has an important role in hydrological cycle in the wide areas of world. Snowmelt is a dominant water resource for runoff and groundwater recharge. Therefore, forecasting of snowmelt is beneficial for management of water resources regarding magnitude and timing of snowmelt. Large volume of water is released during melting seasons. Sudden runoff raises may causes floods in certain times.

Snowmelt runoff is important especially for water supply, flood control, hydropower generation and irrigation. The hydrologists and managers of water resources want to know how much water is stored in their basin in the form of snow. There are numerous applications of snow detecting, snow water equivalent assessments and snowmelt runoff predictions. For each study, detecting snow cover with remote sensing is very vital and can be achieved by gamma rays, visible and near infrared, thermal infrared and microwaves (Rango, 1993).

Snow is the occurrence of precipitation in a solid form. Snow is a key component of global hydrological cycle. It affects the overlying air and the underlying ground with its radioactive and thermal characteristics. Snow reflects 80 % or more of incident solar radiation. This affects near-surface atmosphere temperatures. The insulating properties of snow, owing to its relatively low thermal conductivity create a large

extent permafrost conditions. The high albedo property of snow affects the earth's radiation budget for several months as an important climatologically factor. Through sublimation processes, a snow cover constitutes a sink of energy near the surface and a source of atmospheric moisture (Dery et. al., 2005).

Snow acts as a deposit during winter period. With melting season, snow turns into water and feed water resources. In the eastern part of Turkey snow stays about six months. About 60 % of yearly discharge in that region is contributing from snowmelt. Recognizing snow cover areas and using them in hydrological modelling studies is becoming vital and important at those regions especially.

3.2. History of Remote Sensing In Snow Hydrology

Detecting snow cover area had begun in 1930s by aerial photographs in order to make runoff prediction (Potts, 1937). A satellite derivation became available with National Oceanic and Atmospheric Administration – Advanced Very High Resolution Radiometer (NOAA-AVHRR) since 1972 (Rango, 1996). At the beginning of 1990s, a 1 km snow-cover product for the conterminous USA and portions of Canada has been operationally produced by the National Operational Hydrologic Remote Sensing Center (NOHRSC) (Lee, Klein, Over, 2005). A number of new satellite-derived snow-cover maps covering all or portions of the Northern Hemisphere are currently produced, including: the NOAA's 23 km Interactive Multisensor Snow and Ice Mapping System (IMS) charts (Ramsay, 2000), the 25 km near real-time SSM/I EASE-grid daily global ice concentration and snow extent from the National Snow and Ice Data Center (NSIDC) made from Defense Meteorological Satellite Program (DMSP) F13 Special Sensor Microwave/Imager (SSM/I) passive microwave measurements (Chang et al., 1987; Armstrong and Brodzik, 2001), and new automated 5 km snow-cover maps produced by the National Environmental Satellite, Data, and Information Service (NESDIS) using Geostationary Operational Environmental Satellite (GOES) and SSM/I data (Romanov, Gutman, Csiszar, 2000; Bitner et al., 2002).

Earth Observing System (EOS) Terra and Aqua spacecraft are launched in 1999 and 2002 respectively. NASA's MODIS began collecting science data from onboard the Terra (formerly known as EOS-AM1) spacecraft on 24 February 2000 and from onboard the Aqua (formerly known as EOS-PM1) spacecraft on 24 June 2002.

3.3. Moderate Resolution Imaging Spectroradiometer (MODIS)

Nowadays, many instruments are convenient for detecting and measuring snow especially by kinds of spaceborne sensors with various spectral, spatial and temporal resolutions. However each sensor has some limitations. For instance, visible-band and near-infrared imagery, only offers the possibility to map the evolution and extent of snow cover (Pivot et al., 2002). Among many satellite products, MODIS offers the best potential for snow mapping on a regular basis with respect to temporal and spatial resolution and data availability (Rango et al., 2003).

Both Terra and Aqua carry a MODIS instrument that probes the Earth's atmosphere and surface using 36 visible and thermal infrared channels viewing the entire Earth's surface every 1 to 2 days (Barnes et al., 1998). Terra's orbit around the Earth is timed so that it passes from north to south across the equator in the morning, while Aqua passes south to north over the equator in the afternoon. Technical specifications in Table 3.1 are obtained on the internet site of MODIS:
http://modis.gsfc.nasa.gov/about/specifications.php

Table 3.1 Technical specifications of MODIS

Orbit:	705 km, 10:30 a.m. descending node (Terra) or 1:30 p.m. ascending node (Aqua), sun-synchronous, near-polar, circular
Scan Rate:	20.3 rpm, cross track
Swath Dimensions:	2330 km (cross track) by 10 km (along track at nadir)
Telescope:	17.78 cm diam. off-axis, afocal (collimated), with intermediate field stop
Size:	1.0 x 1.6 x 1.0 m

Table 3.1 Continued

Weight:	228.7 kg			
Power:	162.5 W (single orbit average)			
Data Rate:	10.6 Mbps (peak daytime); 6.1 Mbps (orbital average)			
Quantization:	12 bits			
Spatial Resolution:	250 m (bands 1-2)			
	500 m (bands 3-7)			
	1000 m (bands 8-36)			
Design Life:	6 years			
Primary Use	**Band**	**Bandwidth1**	**Spectral Radiance2**	**Required SNR3**
Land/Cloud/Aerosols Properties	1	620 - 670	21.8	128
	2	841 - 876	24.7	201
Land/Cloud/Aerosols Properties	3	459 - 479	35.3	243
	4	545 - 565	29	228
	5	1230 - 1250	5.4	74
	6	1628 - 1652	7.3	275
	7	2105 - 2155	1	110
Ocean Colour/ Phytoplankton/ Biogeochemistry	8	405 - 420	44.9	880
	9	438 - 448	41.9	838
	10	483 - 493	32.1	802
	11	526 - 536	27.9	754
	12	546 - 556	21	750
	13	662 - 672	9.5	910
	14	673 - 683	8.7	1087
	15	743 - 753	10.2	586
	16	862 - 877	6.2	516
Atmospheric Water Vapour	17	890 - 920	10	167
	18	931 - 941	3.6	57
	19	915 - 965	15	250

Table 3.1 Continued

Primary Use	Band	Bandwidth1	Spectral Radiance2	Required NE[delta]T(K)4
Surface/Cloud Temperature	20	3.660 - 3.840	0.45(300K)	0.05
	21	3.929 - 3.989	2.38(335K)	2
	22	3.929 - 3.989	0.67(300K)	0.07
	23	4.020 - 4.080	0.79(300K)	0.07
Atmospheric Temperature	24	4.433 - 4.498	0.17(250K)	0.25
	25	4.482 - 4.549	0.59(275K)	0.25
Cirrus Clouds Water Vapour	26	1.360 - 1.390	6	150(SNR)
	27	6.535 - 6.895	1.16(240K)	0.25
	28	7.175 - 7.475	2.18(250K)	0.25
Cloud Properties	29	8.400 - 8.700	9.58(300K)	0.05
Ozone	30	9.580 - 9.880	3.69(250K)	0.25
Surface/Cloud Temperature	31	10.780 - 11.280	9.55(300K)	0.05
	32	11.770 - 12.270	8.94(300K)	0.05
Cloud Top Altitude	33	13.185 - 13.485	4.52(260K)	0.25
	34	13.485 - 13.785	3.76(250K)	0.25
	35	13.785 - 14.085	3.11(240K)	0.25
	36	14.085 - 14.385	2.08(220K)	0.35

Note: Performance goal is 30-40% better than required

[1] Bands 1 to 19 are in nm; Bands 20 to 36 are in µm
[2] Spectral Radiance values are (W/m^2 -µm-sr)
[3] SNR = Signal-to-noise ratio
[4] NE(delta)T = Noise-equivalent temperature difference

3.3.1. MODIS Data Products

There are many standard MODIS data products that scientists are using to study global changes of atmosphere, land**,** cryosphere and ocean etc. These products are being used by scientists from a variety of disciplines, including oceanography,

biology, and atmospheric science. MODIS data products are grouped in 5 groups; calibration, atmosphere, land**,** cryosphere and ocean.

Calibration

MOD 01 - Level-1A Radiance Counts

MOD 02 - Level-1B Calibrated Geolocated Radiances

MOD 03 - Geolocation Data Set

Atmosphere

MOD 04 - Aerosol Product

MOD 05 - Total Precipitable Water (Water Vapour)

MOD 06 - Cloud Product

MOD 07 - Atmospheric Profiles

MOD 08 - Gridded Atmospheric Product

MOD 35 - Cloud Mask

Land

MOD 09 - Surface Reflectance

MOD 11 - Land Surface Temperature & Emissivity

MOD 12 - Land Cover/Land Cover Change

MOD 13 - Gridded Vegetation Indices (Max NDVI & Integrated MVI)

MOD 14 - Thermal Anomalies, Fires & Biomass Burning

MOD 15 - Leaf Area Index & FPAR

MOD 16 - Evapotranspiration

MOD 17 - Net Photosynthesis and Primary Productivity

MOD 43 - Surface Reflectance

MOD 44 - Vegetation Cover Conversion

Cryosphere

MOD 10 - Snow Cover

MOD 29 - Sea Ice Cover

Ocean

MOD 18 - Normalized Water-leaving Radiance

MOD 19 - Pigment Concentration

MOD 20 - Chlorophyll Fluorescence

MOD 21 - Chlorophyll_a Pigment Concentration

MOD 22 - Photosynthetically Available Radiation (PAR)

MOD 23 - Suspended-Solids Concentration

MOD 24 - Organic Matter Concentration

MOD 25 - Coccolith Concentration

MOD 26 - Ocean Water Attenuation Coefficient

MOD 27 - Ocean Primary Productivity

MOD 28 - Sea Surface Temperature

MOD 36 - Total Absorption Coefficient

MOD 37 - Ocean Aerosol Properties

MOD 39 - Clear Water Epsilon

3.3.2. MODIS Snow Products

The MODIS snow products are created as a sequence of products beginning with a swath (scene) and progressing, through spatial and temporal transformations to global gridded product (Salomonson, Hall, Riggs, 2006). The summary of 13 MODIS snow products is listed in the Table 3.2.

Table 3.2 The summary of MODIS snow data products

MODIS Snow Products *	Product Level	Dimension of Arrays	Spatial Resolution	Temporal Resolution	Map Projection	Data Format **
MOD10_L2	L2	1354 km by 2000 km	500 m	swath(scene)	None	HDF-EOS
MYD10_L2	L2	1354 km by 2000 km	500 m	swath(scene)	None	HDF-EOS
MOD10L2G	L2G	1200 km by 1200 km	500 m	n^{th} day	Sinusoidal	HDF-EOS
MYD10_L2G	L2G	1200 km by 1200 km	500 m	n^{th} day	Sinusoidal	HDF-EOS
MOD10A1	**L3**	**1200 km by 1200 km**	**500 m**	**daily**	**Sinusoidal**	**HDF-EOS**
MYD10A1	L3	1200 km by 1200 km	500 m	daily	Sinusoidal	HDF-EOS
MOD10A2	L3	1200 km by 1200 km	500 m	8-day	Sinusoidal	HDF-EOS
MYD10A2	L3	1200 km by 1200 km	500 m	8-day	Sinusoidal	HDF-EOS
MOD10C1	L3	360^o by 180^o global arrays	0.05^o	daily	Geographic	HDF-EOS
MYD10C1	L3	360^o by 180^o global arrays	0.05^o	daily	Geographic	HDF-EOS
MOD10C2	L3	360^o by 180^o global arrays	0.05^o	8-day	Geographic	HDF-EOS
MYD10C2	L3	360^o by 180^o global arrays	0.05^o	8-day	Geographic	HDF-EOS
MOD10CM	L3	360^o by 180^o global arrays	0.05^o	monthly	Geographic	HDF-EOS

*MOD...: Generated from EOS Terra Spacecrafts

MYD…: Generated from EOS Aqua Spacecrafts

** HDF-EOS: Hierarchical Data Format- Earth Observing System

According to validation processes, MODIS Products are grouped in three groups; **beta, provisional and validated** products. Beta products are first publicly available products. They are minimally validated. Therefore they can contain significant errors. Provisional products are partially validated. But they are useful for exploratory and process scientific studies. Furthermore, validated products have high quality with well-defined uncertainties. Validated products have 3 stages they are divided into stages according to their improvements. For more information the website can be checked: http://modis-snow-ice.gsfc.nasa.gov/val-df.html.

3.3.3. MOD10A1

MODIS/Terra Snow Cover Daily L3 Global 500m Grid (MOD10A1) contains snow cover and quality assurance (QA) data in HDF-EOS format. MOD10A1 consists of 1200 km by 1200 km tiles of 500 m resolution data gridded in a sinusoidal map projection. MODIS snow cover data are based on a snow mapping algorithm that employs a Normalized Difference Snow Index (NDSI) and other criteria tests. The Terra product, MOD10A1 is validated stage 2 product. For more information the websites can be checked: http://nsidc.org/cgi-bin/get_metadata.pl?id=mod10a1 - http://modis-snow-ice.gsfc.nasa.gov/MOD10A1.html

3.3.4. MODIS Snow Detection Algorithm

MODIS snow detection algorithm is based on Normalized Difference Snow Index (NDSI). NDSI is evaluated according to MODIS bands 4 (0.545–0.565 μm) and 6 (0.628–0.652 μm) (Hall et al., 1995; 2002a) as it can be seen in Equation 3.1:

$$NDSI = \frac{(\text{MODIS4} - \text{MODIS6})}{(\text{MODIS4} + \text{MODIS6})} \tag{3.1}$$

Non-forested pixels whose NDSI ≥0.4 and reflectance in MODIS band 2 (0.841–0.876 μm) is >11% will be mapped as snow. However, snow-covered forests may have lower NDSI values. However, snow-covered forests may have lower NDSI values. To map these snow-covered forests well, a combination of the normalized

difference vegetation index (NDVI),(Equation3.2) is computed using MODIS bands 1 (0.620–0.670 μm) and 2 (0.841–0.876 μm) and the NDSI are used. Pixels falling in a polygon region in NDVI–NDSI space may be mapped as snow for NDSI <0.4 (Lee S. et al, 2005).

$$NDSI = \frac{(\text{NIR} - \text{VIS})}{(\text{NIR} + \text{VIS})} = \frac{\text{Band2} - \text{Bandl}}{\text{Band2} + \text{Bandl}} \tag{3.2}$$

High values of NDVI indicate dense vegetation. By using the NDSI and NDVI in combination, it is possible to lower the NDSI threshold in forested areas without compromising the algorithm performance in other land covers (Hall et al., 2001). If the NDVI ≈ 0.1, the pixel may be mapped as snow even if the NDSI is lower than 0.4 (Klein et al., 1998).To prevent the erroneous classification of dark targets as snow, however, a grid point is not classified as snow if MODIS band 4 reflectance is less than 10 %, even if the first criteria are met (Dery et al, 2005). MODIS thermal bands 31 (10.780–11.280 μm) and 32 (11.770–12.270 μm) are used to mask misclassified pixels whose temperature is too high to contain snow (Lee S. et al, 2005). A pixel is not mapped as snow if the estimated surface temperature is greater than 277°K especially in tropical regions.

Cloud and land/water masks supply the final criteria used in the generation of MODIS snow cover maps (Ackerman et al., 1998). Clouds are masked using MODIS cloud mask data product MOD35 (Riggs et al., 2003). MODIS snow algorithm is executed on land and inland lake pixels. In this content, oceans are skipped using the land/water mask in MODIS geolocation product MOD03 (Şorman, 2005). Detail information about snow detection algorithm can be found in Hall et al study (1995, 2001).

3.4. Geographic Information Systems in Remote Sensing

Geographic Information Systems (GIS) are computer-based systems that are used to store and manipulate geographic information (Aronoff, 1993). A GIS is an organized collection of computer hardware, software and geographic data designed to

efficiently capture, store, update, manipulate, analyze and display all forms of geographically referenced information (Johnson et al., 1992).

GIS has become a particularly useful and important tool for hydrologists in the scientific study and management of resources. GIS, alone can not serve useful maps to users. However, if the data is put into GIS, the hydrologic data can be easily stored and manipulated. That would be much easier than handling data with manual techniques.

GIS is necessary for successful application of remote sensing. Beyond the initial computer data processing of the digital remote sensing imagery, GIS are used to supply all other important information (spatial, temporal and statistical) and further integrate and analyze the remote sensing information (Baumgartner and Apfl, 1996).

Remote sensing technology and GIS are both tools for managing spatially distributed information in large quantities for different scales. Both increasing the capabilities of human decision-makers and planners, grasping relationships at large scales have become available. Complex settings have been more possible than before (Rango, 1998).

3.5. Obtaining Temporal and Spatial Distribution of SCA

As the MODIS data become available, the data should be converted to meaningful information. In this study, MOD10A1, which is described in the section 3.3.3, is processed to obtain temporal and spatial distribution of SCA. The daily MODIS snow product; MOD10A1 has some pixel values which represent snow, cloud, inland water, land etc.

In this study, the images that have more than **30 %** cloud are not evaluated. Before downloading MOD10A1 pre-elimination was made from one of NASA's web pages which allow quicklook of MOD10A1: http://landweb.nascom.nasa.gov/cgi-bin/browse/browse.cgi

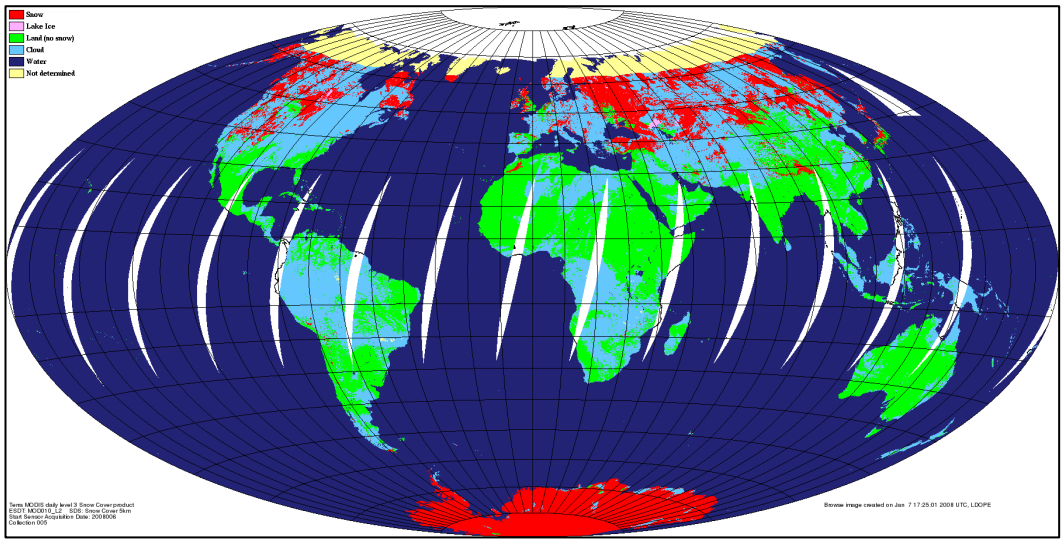

Figure 3.1 Quick look, 08.01.2008 dated image of MOD10A1. Red coloured places are snow covered, green coloured places are land covered, dark blue coloured places are water surfaces, cyan coloured places are cloud covered, Pink coloured places are lake ice.

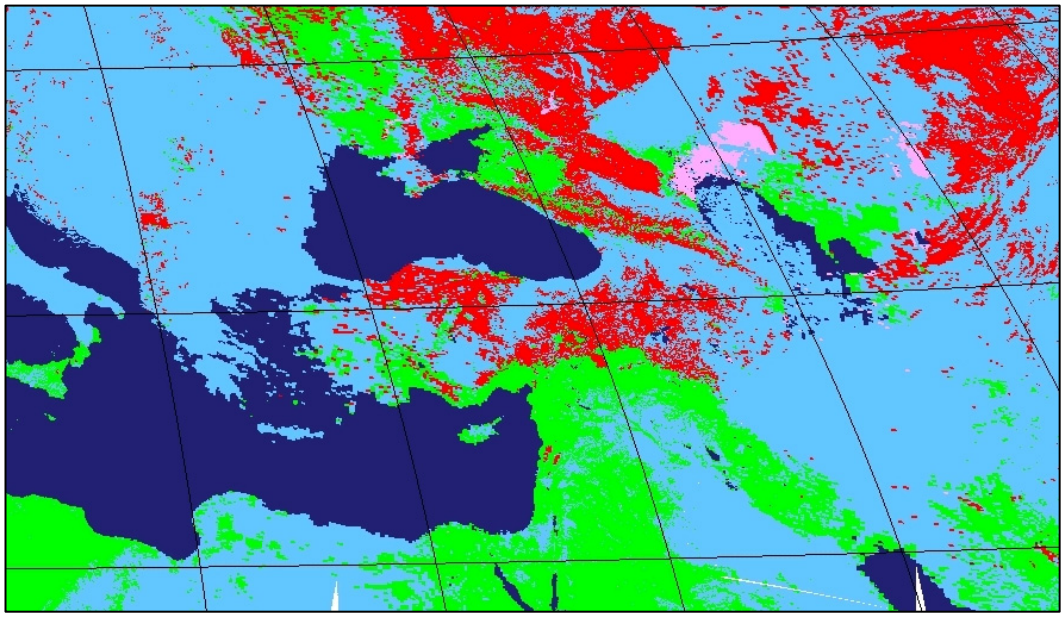

Figure 3.2 Zoomed quick look image of study area

After deciding cloud free days, MOD10A1 is downloaded from National Snow and Ice Data Center (NSIDC) website:
http://nsidc.org/~imswww/pub/imswelcome/index.html

The Figure 3.3 describes the general procedure that is followed to obtain meaningful information from downloaded **MODIS10A1.**

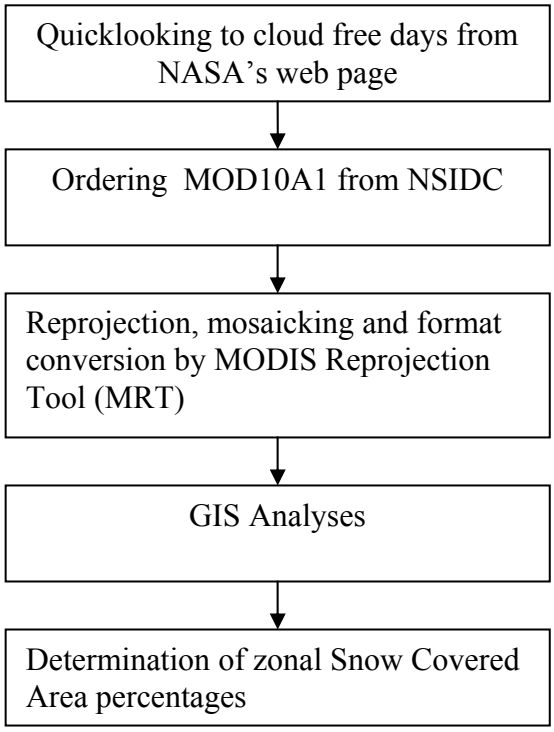

Figure 3.3 Flow chart of obtaining information from MODIS10A1

3.5.1. MODIS Reprojection Tool

In this study, MODIS Reprojection Tool is used for converting downloaded data to the suitable data for GIS software. Land Processes DAAC USGS Center for Earth Resource Observation and Science (EROS) in collaboration with the Department of Mathematics and Computer Science South Dakota School of Mines and Technology composed MODIS Reprojection Tool User's Manual in 2006.

The MODIS Reprojection Tool (MRT) is software designed to help individuals work with MODIS data by reprojecting MODIS images into more standard map projections and conversion of the HDF-EOS data format into different data formats that are supported by GIS softwares. Native MODIS data files are stored in (Hierarchical Data Format – Earth Observing System), a file format that does not currently have wide support. The MODIS Reprojection Tool supports both versions and projections.

The MODIS Reprojection Tool allows the user to reproject to and from the following map projections:

- Albers Equal Area
- Equirectangular
- Geographic
- Hammer
- Integerized Sinusoidal
- Interrupted Goode Homolosine
- Lambert Azimuthal
- Lambert Conformal Conic
- Mercator
- Mollweide
- Polar Stereographic
- Sinusoidal
- Transverse Mercator
- **Universal Transverse Mercator**

A limited number of input and output datums are supported by the MRT for datum conversions. Supported datums are NAD27, NAD83, WGS66, WGS72, and WGS84. The MODIS Reprojection Tool supports 8-bit, 16-bit, and 32-bit integer data (both signed and unsigned), as well as 32-bit float data. HDF-EOS and raw binary files are supported on input; HDF-EOS, GeoTIFF, and raw binary files are supported on

output. Moreover, the MRT provides an option to mosaic several tiles together before reprojecting them.

MOD10A1 consists of 1200 km by 1200 km tiles. Tiles are 10 degrees by 10 degrees at the equator. The tile coordinate system starts at (0, 0) (horizontal tile number, vertical tile number) in the upper left corner and proceeds right (horizontal) and downward (vertical). The tile in the bottom right corner is (35, 17). The study area is in eastern part of Turkey and it is in h21v04 and h21v05 tiles **(Figure 3.4).** MODIS Reprojection Tool is used to mosaick, reproject images and convert HDF EOS data format to GeoTIFF format. Two tile images are mosaicked and are reprojected into World Geodetic System 1984 (WGS 84), Universal Transverse Mercator (UTM) Zone 37 with a cell size of 500 m.

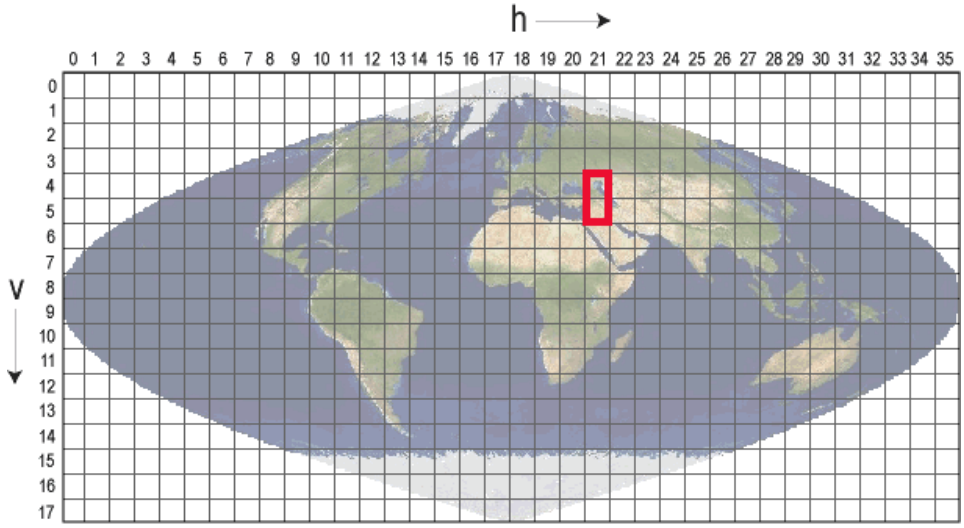

Figure 3.4 MODIS Tiles

3.5.2. GIS Analyses

The mosaicked, reprojected and converted images are imported to ArcGIS software. Simple ArcGIS model is constructed to get the snow covered area from output of MRT. Figure 3.5 shows the flow chart of model. By GIS applications, MRT output image was cropped according to interest area of elevation zones. The extracted raster images were converted to polygon format. Then the polygon images were dissolved and the snow covered area was calculated.

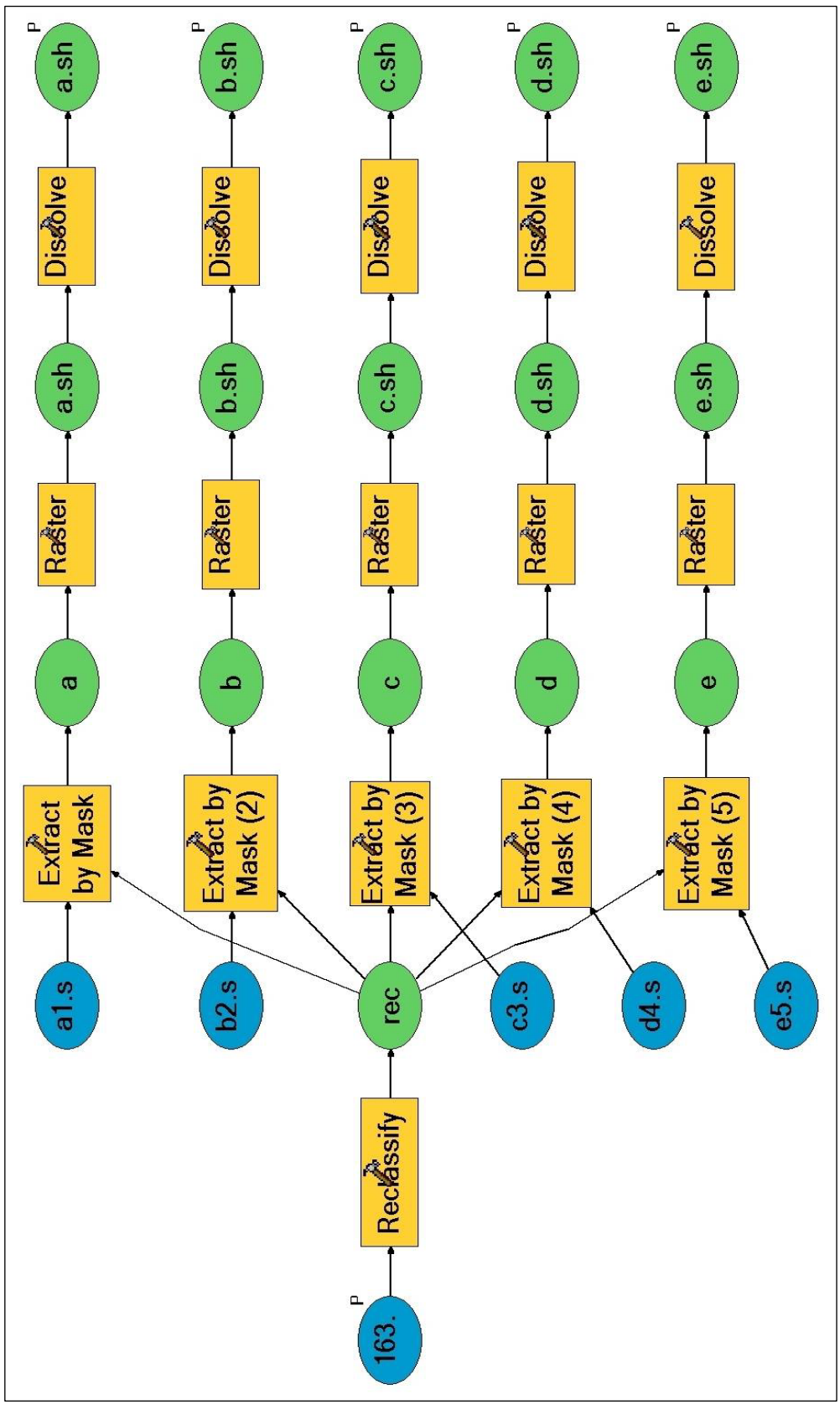

Figure 3.5 Flow chart of GIS model

CHAPTER 4

SNOWMELT RUNOFF MODEL (SRM)

4.1. Introduction

All over the world, the runoff caused by snowmelt is an important water resource potential. Detecting snow cover area in the river basins is very important for the magnitude and timing of water incoming to dam. The common precipitation type is snow in the mountainous region like in Turkey where the average altitude is around 1130 m .This makes the detecting snow cover area and using it in model studies are very important .The eastern part of Turkey is snow covered during the half of the year. According to the long years period, analysis of 2119 flow observation station at that region shows that 60-70 % of incoming flow is because of snowmelt in spring and first months of summer especially rainfall falling on snow cover area.

The usage of snow cover area percentages in modelling studies and evaluating model results is very important for regarding water resources management. Among many snowmelts runoff models that use snow cover information, the deterministic Snowmelt Runoff Model (SRM) is one of the most widely used model. SRM is a degree-day-based model for daily runoff simulations and forecasts runoff in the mountainous areas in which snowmelt is the major runoff contributor (Rango and Martinec, 1981; Martinec and others; 1998; Mitchell and DeWalle, 1998).

SRM which is known as “Martinec Model” or “Martinec-Rango Model” in the literature, also deal with the effect of climate change on snow cover and runoff (Rango and Martinec, 1998). SRM was developed for small basins in Europe by Martinec in 1975. After usage of satellite products of snow cover, the model is started to be applied to larger basins. Figure 4.1 illustrates the locations where SRM has been tested.

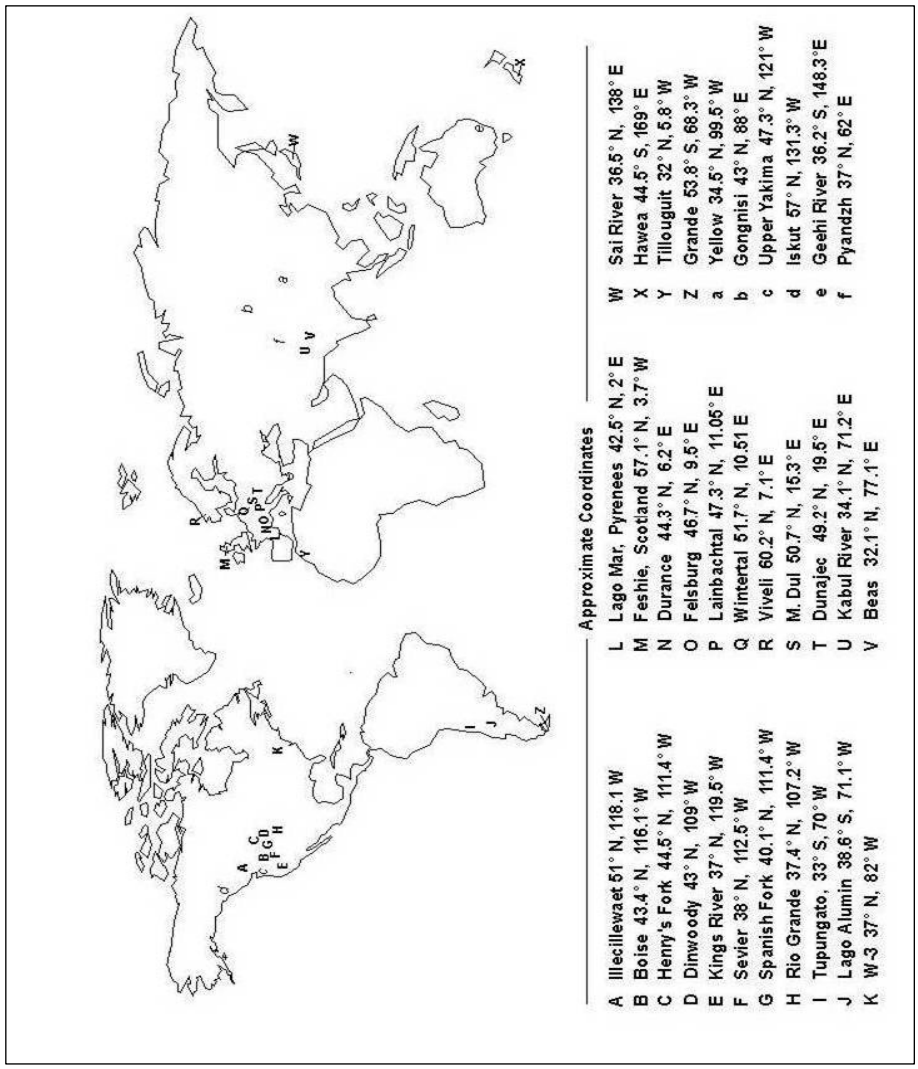

Figure 4.1 Selected locations where SRM has been tested.

SRM can be applied to different locations, in different sizes; 0.76 to 120 000 km^2, in different elevation ranges; 305 to 7690 m.a.s.l (Table 4.1) If input variables temperature, precipitation, snow cover area and model parameters are provided,

SRM can be applied to obtain runoff hydrographs. Since the publication of the 1994 Edition (Martinec *et al.,* 1994), SRM has been applied by independent investigators in Chile, Ecuador, China, Austria, Switzerland, **Turkey** and Spain (Rango and Martinec, 1998). Totally, 81 different basins, 454589.51 km^2 area are modelled by SRM.

Table 4.1.SRM applications and results (Rango A. and Martinec J., 1998)

Country	Basin	Size (km^2)	Elevation Range (m.a.s.l.)	Zones	Years (seasons)	R^2 *	Dv [%] *
Germany	Lange Bramke (Harz)	0.76	540-700	1	1	N/A	N/A
Germany	Wintertal (Harz)	0.76	560-754	1	1	N/A	N/A
Czech Republic	Modry Dul (Krkonose)	2.65	1000-1554	1	2	0.96	1.70
Ecuador	Antisana (Andes)	3.72	4500-5760	3	1	N/A	N/A
Spain	Lago Mar (Pyrenees)	4.50	2234-3004	1	1	N/A	N/A
Spain	Llauset dam (Pyrenees)	7.80	2100-3000	2	1	0.69	5.50
USA	W-3 (Appalachians)	8.42	346-695	1	10	0.81	8.80
Germany	Lainbachtal (Alps)	18.70	670-1800	1	5	N/A	N/A
Spain	Salenca en Baserca (Pyrenees)	22.20	1460-3200	3	3	0.72	4.30
Spain	Noguera Ribagorzana en Baserca (Pyrenees)	36.80	1480-3000	3	3	0.71	3.70
Switzerland	Rhone-Gletsch (Alps)	38.90	1755-3630	4	1	N/A	N/A
Switzerland	Dischma (Alps)	43.30	1668-3146	3	10	0.86	2.50
Japan	Sai (Japan Alps)	57.00	300-1600	3	3	0.86	N/A
Austria	Rofenache (Alps)	98.00	1890-3771	8	1	0.88	2.40
United Kingdom	Feshie (Cairngorms)	106.00	350-1265	1	2	0.88	N/A
Switzerland	Sedrun (Alps)	108.00	1840-3210	3	2	0.79	1.90
Australia	Geehi River (Snowy Mtns,)	125.00	1032-2062	3	6	0.70	6.60
USA	American Fork	130.00	1820-3580	4	1	0.90	1.70

Table 4.1 continued

Switzerland	Landwasser (Alps)	183.00	1500-3146	3	1	N/A	N/A
India	Kulang (Himalayas)	205.00	2350-5000	N/A	N/A	N/A	N/A
Switzerland	Tavanasa (Alps)	215.00	1277-3210	4	2	0.82	3.10
USA	Dinwoody (Wind River)	228.00	1981-4202	4	2	0.85	2.80
USA	Salt Creek (Utah)	248.00	1564-3620	5	1	N/A	2.56
Italy	Cordevole (Alps)	248.00	980-3342	3	1	0.89	4.60
India	Beas-Manali (Himalayas)	345.00	1900-6000	N/A	4	0.68	12.00
Norway	Laerdalselven (Lo Bre)	375.00	530-1720	5	1	0.86	5.20
Norway	Viveli (Hardangervidda)	386.00	880-1613	N/A	N/A	N/A	N/A
Japan	Okutadami (Mikuni)	422.00	782-2346	3	3	0.83	5.40
USA	Bull Lake Creek (Wind River)	484.00	1790-4185	4	1	0.82	4.80
Switzerland	Tiefencastel (Alps)	529.00	837-3418	5	2	N/A	N/A
USA	South Fork (Colorado)	559.00	2506-3914	3	7	0.89	1.10
Argentina	Las Cuevas (Andes)	600.00	2500-7000	N/A	N/A	N/A	N/A
USA	Independence R, (Adirondacks)	618.00	261-702	1	1	0.81	5.00
Chile	Mapocho (Andes)	630.00	1024-4450	3	1	0.42	29.90
Poland	Dunajec (High Tatra)	700.00	577-2301	3	1	0.73	3.80
India	Saing (Himalayas)	705.00	1400-5500	N/A	N/A	N/A	N/A
USA	Conejos (Colorado)	730.00	2521-4017	3	7	0.87	1.10
Switzerland	Ilanz (Alps)	776.00	693-3614	5	2	N/A	N/A
China	Toutunhe	840.00	1430-4450	6	3	0.81	2.00
Austria	Ötztaler Ache (Alps)	893.00	670-3774	6	1	0.84	9.18
Argentina	Lago Alumin (Andes)	911.00	1145-2496	N/A	N/A	N/A	N/A
China	Urumqi (Tien Shan)	924.00	1920-4000	N/A	N/A	N/A	N/A
Uzbekistan	Angren	970.00	1400-3800	5	1	0.30	-13.90
India	Parbati (Himalayas)	1154.00	1500-6400	5	1	0.73	7.50
Canada	Illecillewaet (Rocky Mtns,)	1155.00	509-3150	4	4	0.86	7.00
Spain	Segre en Seo d'urgel (Pyrenees)	1217.00	360-2900	5	N/A	N/A	N/A

Table 4.1 continued

India	Buntar (Himalayas)	1370.00	1200-5000	N/A	N/A	N/A	N/A
Chile	Tinguiririca Bajo Briones (Andes)	1460.00	520-4500	3	1	0.88	-0.30
New Zealand	Hawea (S,Alps)	1500.00	300-2500	N/A	N/A	N/A	N/A
Switzerland	Ticino-Bellinzona (Alps)	1515.00	220-3402	5	1	0.86	-0.60
USA	Spanish Fork (Utah)	1655.00	1484-3277	4	1	0.85	1.00
Argentina	Tupungato (Andes)	1800.00	2500-6000	8	1	0.63	6.40
Switzerland	Inn-Martina (Alps)	1943.00	1030-4049	2	1	0.82	4.30
Argentina	Chico (Tierra del Fuego)	2000.00	N/A	N/A	N/A	N/A	N/A
China	Gongnisi (Tien Shan)	2000.00	1776-3200	N/A	N/A	N/A	N/A
USA	Boise (Idaho)	2150.00	983-3124	3	3	0.84	3.30
France	Durance (Alps)	2170.00	786-4105	5	5	0.85	2.60
USA	Madison (Montana)	2344.00	1965-3234	2	2	0.89	1.50
Uzbekistan	Pskem	2412.00	800-4300	7	1	0.84	0.50
Morocco	Tillouguit (Atlas)	2544.00	1050-3411	3	1	0.84	0.50
Austria	Salzach-St,Johann (Alps)	2600.00	570-3666	N/A	N/A	N/A	N/A
USA	Henry's Fork (Idaho)	2694.00	1553-3125	3	2	0.91	1.50
USA	Cache la Poudre (Colorado)	2732.00	1596-4133	3	1	N/A	N/A
Chile	Aconcagua (Andes)	2900.00	900-6100	3	1	0.91	0.90
USA	Sevier R (Kingston, Utah)	2929.00	1823-3260	4	1	0.75	5.10
Switzerland	Rhine-Felsberg	3249.00	562-3425	5	7	0.70	7.20
Switzerland	Rhone-Sion (Alps)	3371.00	491-4634	7	1	0.95	0.02
USA	Rio Grande	3419.00	2432-4215	3	13	0.84	3.80
USA	Kings River	4000.00	171-4341	7	5	0.82	3.20
Chile	Maipo en el Manzano (Andes)	4960.00	850-5600	3	2	0.77	0.90
India	Beas-Thalot (Himalayas)	5144.00	1100-6400	6	2	0.80	1.50
USA	Upper Yakima (Cascades)	5517.00	366-2121	5	1	0.92	2.80
Uzbekistan	Chatkal	6309.00	800-4500	7	1	0.70	-7.40
Canada	Sturgeon (Ontario)	7000.00	N/A	N/A	N/A	N/A	N/A
Argentina	Grande (Tierra del Fuego)	9050.00	N/A	N/A	N/A	N/A	N/A
Canada	Iskut (Coast)	9350.00	200-2556	5	N/A	N/A	N/A

Table 4.1 continued

USA	Sevier (Juab, Utah)	13380.00	1506-3719	4	1	0.93	4.00
USA	Snake River (Idaho)	14897.00	1524-4196	N/A	11	0.90	0.40
Pakistan	Kabul (Himalayas)	63657.00	305-7690	1	1	0.66	6.00
Tajikistan/Afghanistan	Pyandzh (Pamirs and Hindu Kush)	120534.00	2141-5564	8	3	0.65	5.60
China	Yellow (Anyemogen Shan)	121972.00	2500-5224	3	N/A	N/A	N/A

If more than one year is modelled, the average of R^2 and D_v [%] is listed.

*The accuracy criteria is defined as:

$$R^2 = 1 - \frac{\sum_{i=1}^{n}(Q_i - Q'_i)^2}{\sum_{i=1}^{n}(Q_i - \overline{Q})^2}$$

$$Dv = \frac{V_R - V'_R}{V_R} \bullet 100 \qquad (4.1)$$

R^2 = a measure of model efficiency

Q_i = measured dailly discharge

Q'_i = simulated dailly discharge

$\overline{Q}$ = average dailly discharge for simulation year

n = number of dailly discharge values

D_V = percentage of volume difference between the measured and the simulated runoff (%)

V_R = measured runoff model

V'_R = simulated runoff model

4.2. Purpose of SRM

Model can be run for snowmelt seasons, a year or consequent years. The daily runoff results can be compared with measured runoff .This would help to determine model accuracy, model performance and to verify model parameters. Basin characteristics such as forested area, soil conditions if available are also useful for determination of model parameters. Seasonal and short term runoff forecasts can be done after

determination of model parameters. Modified depletion curves (MDC) which relates snow covered areas to cumulative snow depths can be derived. Moreover, potential effects of climate change on the seasonal snow cover and runoff can be detected.

4.3. Model Structure

SRM uses snow cover area percentages as a direct model variable with a degree-day method. Three important SRM variables are daily average temperature, daily total precipitation and snow covered area percentages (Figure 4.2).

SRM gives users a freedom to modify the values which are used at different times during the melt season, unlike other calibration models (Ferguson, 1999). Related to these characteristics of SRM, SRM falls in between the fully calibration-based hydrological models which are fitted from data and have no physical interpretations, and the fully physics-based models which are physical constants or measurable real-world quantities so that no fitting is involved (Ferguson, 1999).

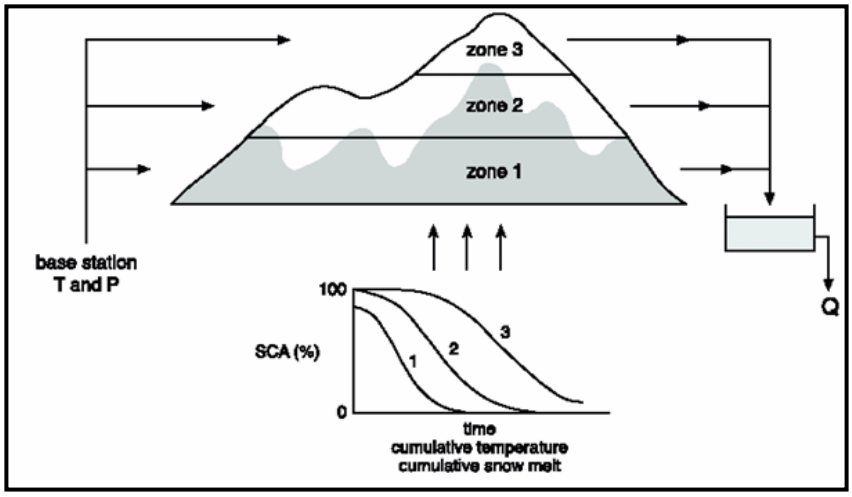

Figure 4.2 Flow chart of SRM

The basic equation of SRM can be formulized as;

$$Q_{n+1} = [C_{Sn} \cdot a_n (T_n + \Delta T_n) S_n + C_{Rn} \cdot P_n] (A.10000/86400) (1-k_{n+1}) + Q_n k_{n+1}] \quad (4.2)$$

where;

n : is the number indicating the day

Q : average daily discharge from the basin [$m^3 \cdot s^{-1}$]

T : extrapolated air temperature to the hypsometric elevation of each zone [$^oC \cdot d$]

P : precipitation falling as rain in the zone [cm]

S : snow covered area in the zone

A : area of the zone

ΔT : the adjustment by temperature lapse rate [$^oC \cdot d$]

k : recession coefficient

a : degree day factor [$cm \cdot ^oC^{-1} \cdot d^{-1}$]

C_S : correction factor for snow

C_R : correction factor for rain

T, P and S are model variables should be determined for each day whereas k, T_{CRIT}, ΔT, lag time, a, C_S, C_R are parameters and they are characteristics for given basin and climate. If the elevation range of the basin exceeds 500 m, it is recommended that the basin be subdivided into elevation zones of about 500 m each (Rango A. and Martinec J. ,1998). In this study basin area is divided in 5 elevation zones. For 5 elevation zones A, B, C, D and E, model equation becomes as:

$$\begin{aligned} Q_{n+1} = {} & [C_{SAn} \cdot a_{An} (T_n + \Delta T_n) S_{An} + C_{RAn} \cdot P_{An}] (A_A.10000/86400) + \\ & C_{SBn} \cdot a_{Bn} (T_n + \Delta T_n) S_{Bn} + C_{RBn} \cdot P_{Bn}] (A_B.10000/86400) + \\ & C_{SCn} \cdot a_{Cn} (T_n + \Delta T_n) S_{Cn} + C_{RCn} \cdot P_{Cn}] (A_C.10000/86400) + \\ & C_{SDn} \cdot a_{Dn} (T_n + \Delta T_n) S_{Dn} + C_{RDn} \cdot P_{Dn}] (A_D.10000/86400) + \\ & C_{SEn} \cdot a_{En} (T_n + \Delta T_n) S_{En} + C_{REn} \cdot P_{En}] (A_E.10000/86400)] (1-k_{n+1}) + Q_n k_{n+1} \end{aligned} \quad (4.3)$$

4.4. Input Data For SRM Runs

4.4.1. Area – Elevation Curve

In addition to model variables, area – elevation curve is needed for running the model. Area-elevation (hypsometric) curve is plotted as shown in the Figure 4.3. Hypsometric elevation was obtained automatically by the help of digital elevation data and GIS software. It can be also obtained from area - elevation curve.

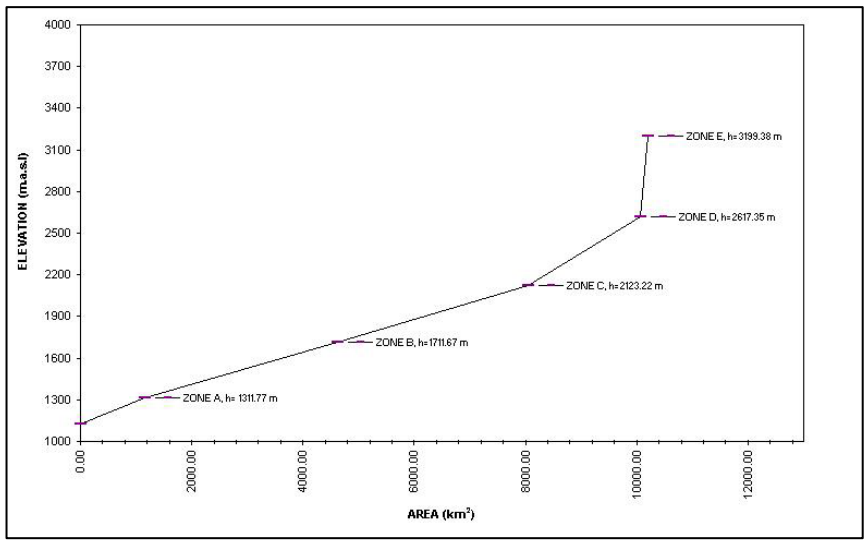

Figure 4.3 Area - elevation curve of Karasu Basin

4.4.2. The Model Variables; Temperature, Precipitation, Snow Cover Area

The variables; temperature, precipitation, snow cover area percentages should be measured for running SRM. The variables; temperature and precipitation are distributed by the Detrended Kriging method. For each elevation zone the daily average temperature and precipitation values are obtained by distributing temperature measurements derived from stations with Detrended Kriging Program (DK) (Garen, 2003).

4.4.2.1.Kriging Procedure and Detrended Kriging Program

Kriging Procedure

Two of the classical methods that are used to estimate mean areal distribution of temperature and precipitation from point measurements are the Thiessen polygons and the Isohyetal method. Although these methods are simple and straightforward, they can not handle orographic effects. A more recent technique for estimating mean areal distribution of temperature and precipitation is the use of kriging, an optimal spatial interpolation procedure for estimating the values of a variable at unmeasured points from nearby measurements (Garen et al, 1994).
Kriging is objective, statistically rigorous and performs as well as or better than other estimation techniques (Tabios and Salas, 1985).

Rectangular grids for all basins should be constructed by hand or by the help of GIS software. Each grid should have the location and elevation information. The weights that are going to be used for estimating value at grid cell should be determined. Kriging requires the situation that there should be no systematic spatial trend in the mean or variance of the process .This is not the case in the mountainous regions because there is a trend through elevation; precipitation and temperature. There are different types of application of kriging procedure such as cokriging, detrended kriging etc. Detrended kriging is subtracting a precipitation –elevation trend from the data before performing procedure and is calculating mean areal precipitation or temperature.

Detrended Kriging Program

The program estimates spatial fields of precipitation, temperature and snow water equivalent by interpolating among point measurement from stations. The program can be used daily and other temporal resolutions. The program is most appropriate for mesoscale watersheds, approximately 100-10000 km^2. The implicit assumption is that there is a homogeneous relationship between the hydrometeorological variable

and elevation within this domain, hence other factors such as slope, aspect, differing orographic regimes, etc. are not considered. For large regions where climatic regimes do differ, the DK program would have to be applied to sub-regions where homogeneity could be assumed (Garen, 2003). The algorithm is based on detrended kriging (Garen, 2003). Program needs location of stations, DEM of each elevation zone to use it in constructing gridded files, precipitation and temperature measurements from stations. For more information, Detrended Kriging Program (DK) User's Guide (2003) can be inquired.

4.4.2.2.Temperature

The number of degree days should be determined from temperature measurements for deriving the daily snowmelt depth. There are two choices how temperature measurements or temperature forecasts can be entered to model:

1. Maximum and minimum temperature values in a day
2. Daily average temperature values

For Option 1, the average temperature is computed for each zone as:

$$\overline{T} = \frac{T_{MAX} + T_{MIN}}{2} \tag{4.4}$$

The ΔT; the adjustment by temperature lapse rate [$^{o}C \cdot d$] in Equation (4.2) is computed as follows:

$$\Delta T = \gamma \bullet (h_{st} - \overline{h}) \bullet \frac{1}{100} \tag{4.5}$$

where

γ = temparature lapse rate [$^{\circ}C$ per 100 m]

h_{st} = height of temparature station [m]

$\overline{h}$ = hypsometric mean elevation of a zone

The model accepts temperature data in two choices:

1. Basin wide
2. By zone

In Option 1, the height of the station is entered and the temperature data is extrapolated by the help of hypsometric mean elevations of all zones and the calculated lapse rates. In Option 2, the separate stations for each elevation zone are thought to be used and already lapse rated to mean hypsometric elevation.

In this study daily average temperature data is used. By zone option is applied for the study area. The detrended kriging method defined in section 4.4.2.1 is used to calculate the daily average temperature data by measurements obtained from the stations described in chapter 2. That is why; there is no need to lapse rate temperature data to hypsometric mean elevation of each elevation zone .The daily average temperature values for each elevation zone and years 2006, 2007 are calculated by Detrended Kriging Program . The SRM variable, temperature values are entered to SRM .The graphics for each elevation zone and years 2006, 2007 are obtained (Figure 4.4 and 4.5).The decreasing trend of temperature values through higher zones can be detected from the Figures 4.4 and 4.5.

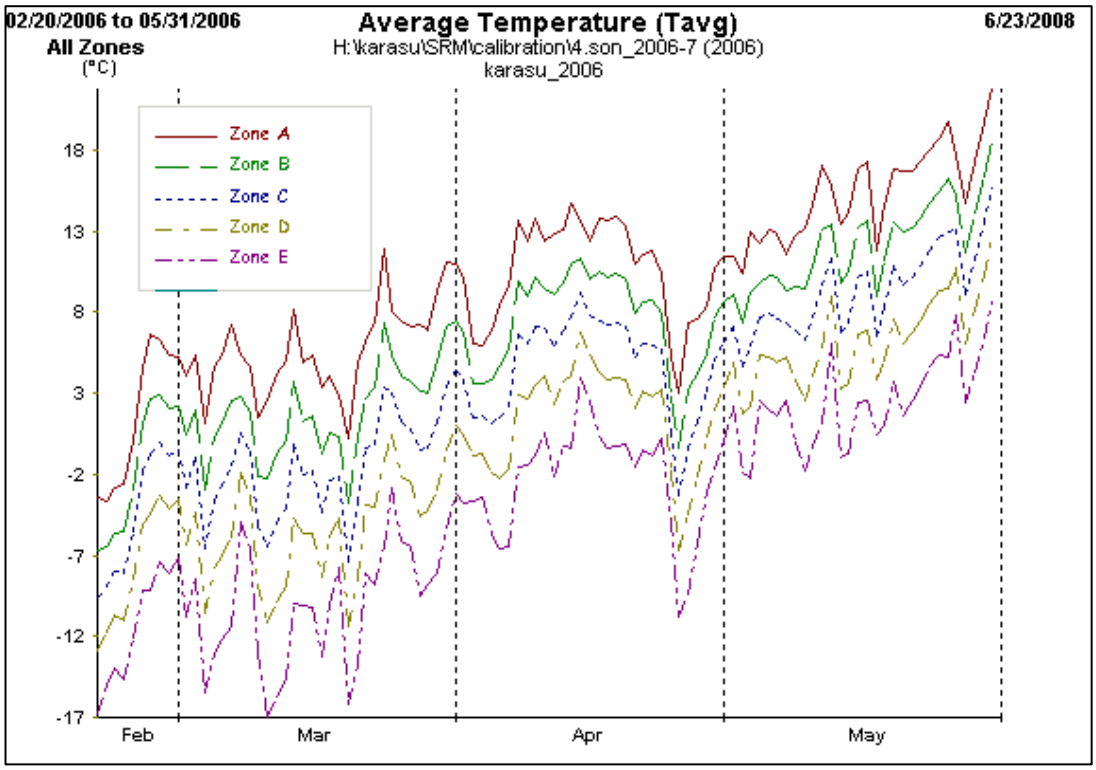

Figure 4.4 The graphic of average daily temperature values for year 2006

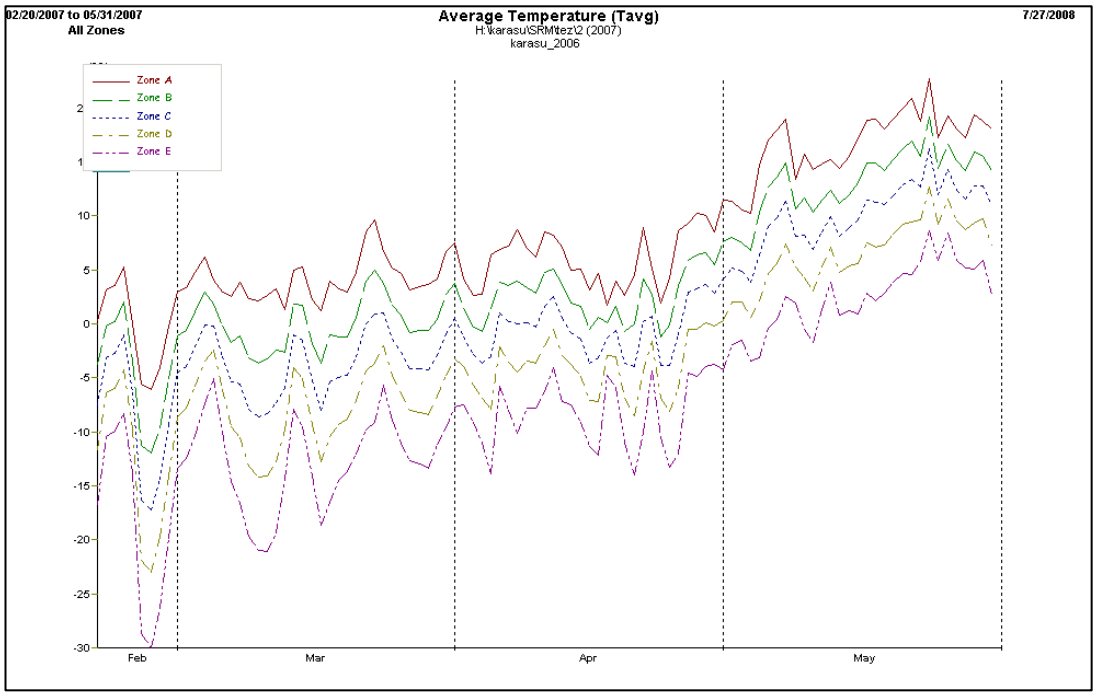

Figure 4.5 The graphic of average daily temperature values for year 2007

4.4.2.3.Precipitation

Obtaining daily total precipitation is not easy in the mountainous regions. There are not so many stations in the mountainous regions. In this study, the maximum altitude of precipitation measured stations in the Karasu Basin is 2130 m. However the maximum height of the basin area is 3487 m. There is no precipitation measured station in the D and E elevation zones. In these types of basins snowmelt generally prevails over the rainfall component (Tekeli, 2000; Rango and Martinec, 1998). However, sharp runoff peaks from occasional heavy rainfalls must given particular attention and the SRM includes a special treatment of such events (Rango and Martinec, 1998).

There are two choices that precipitation measurements can be entered to model:

1. Basin wide
2. By zone

In option 1, one precipitation station represents all basin can be thought off that it is located in the mean hypsometric elevation of basin. In option 2, different measured or extrapolated precipitation values represent each elevation zone.

In basins with a great elevation range, the precipitation input may be underestimated if only low altitude precipitation stations are available. It is recommended to extrapolate precipitation data to the mean hypsometric altitudes of the respective zones by an altitude gradient, for example 3 % or 4 % per 100 m. If two stations at different altitudes are available, it is possible to assign the averaged data to the average elevation of both stations and to extrapolate by an altitude gradient from this reference level to the elevation zones (Rango and Martinec, 1998).

By zone; Option 2 is applied for the study area. The detrended kriging method defined in section 4.4.2.1 is used to calculate the daily average precipitation data by the measurements obtained from the stations described in chapter 2. All of the

precipitation stations are used to find daily average precipitation values for each elevation zone.

A critical temperature (T_{CRIT}) is used to define if precipitation type is snow or rain.

- If $T \geq T_{CRIT}$, precipitation is defined as rain.
- If $T \leq T_{CRIT}$, precipitation is defined as new snow.

When the precipitation is defined as a snow in ***snowmelt season,*** it is treated in two different ways. If it falls on snow covered area, it becomes the part of seasonal snowpack. It affects like how normal depletion curve affect. However, if it falls on snow free area, it is defined as precipitation to be added snowmelt. This precipitation is stored by SRM and then melted as soon as a sufficient number of degree-days have occurred (Rango and Martinec, 1998).

In winter time, especially from October to March for Northern Hemisphere to assess snow coverage is more difficult. Satellite data, if available, are not frequent enough to distinguish the stable snow cover from frequent transitory snowfalls which are subsequently melted.(Rango and Martinec, 1998).There are two different options to deal with this problem:

Option 1: Put S=0, therefore each precipitation event defined by T_{CRIT} is stored. This method is applicable if the precipitation data is in good quality .In the mountains area like Karasu Basin it is hard to catch at that level quality. That is why, SRM uses snow cover area for calculating runoff.

Option 2: In January and February S is 1 generally. If S=1 or less than 1, put S=1 or interpolate S for march. Normally option 2 is preferable for higher elevation zones whereas option 1 is applicable for lowest elevation zone.

Sharp peaks of discharge are typical for rainfalls. It is not common to see such events when there is a regular snowmelt. SRM has been adapted to better simulate these

rainfall peaks whenever the average daily rainfall calculated over the whole basin equals or exceeds 6 cm (Rango A. and Martinec J., 1998). This value can be adapted according to basin area. The maximum average daily rainfall in Karasu Basin for the years 2006 and 2007 is 2.5 cm.

Some local rainfalls may be missed if the stations are not located dense enough. Moreover in some cases; the timing of rainfall is unknown that is why precipitation data must be shifted backwards by one day before input to SRM (Rango and Martinec, 1998).

Regarding those precautions, the daily average precipitation values for each elevation zone and years 2006, 2007 are calculated by detrended kriging program .Then the SRM variable, precipitation values are entered to SRM .The graphics for each elevation zone and years 2006, 2007 are obtained (Figure 4.6 and 4.7).The increasing trend of precipitation values through higher zones can be detected from the Figures 4.6 and 4.7. In Figures 4.6 and 4.7 some parts are magnified to recognize increasing trend of precipitation values through higher zones.

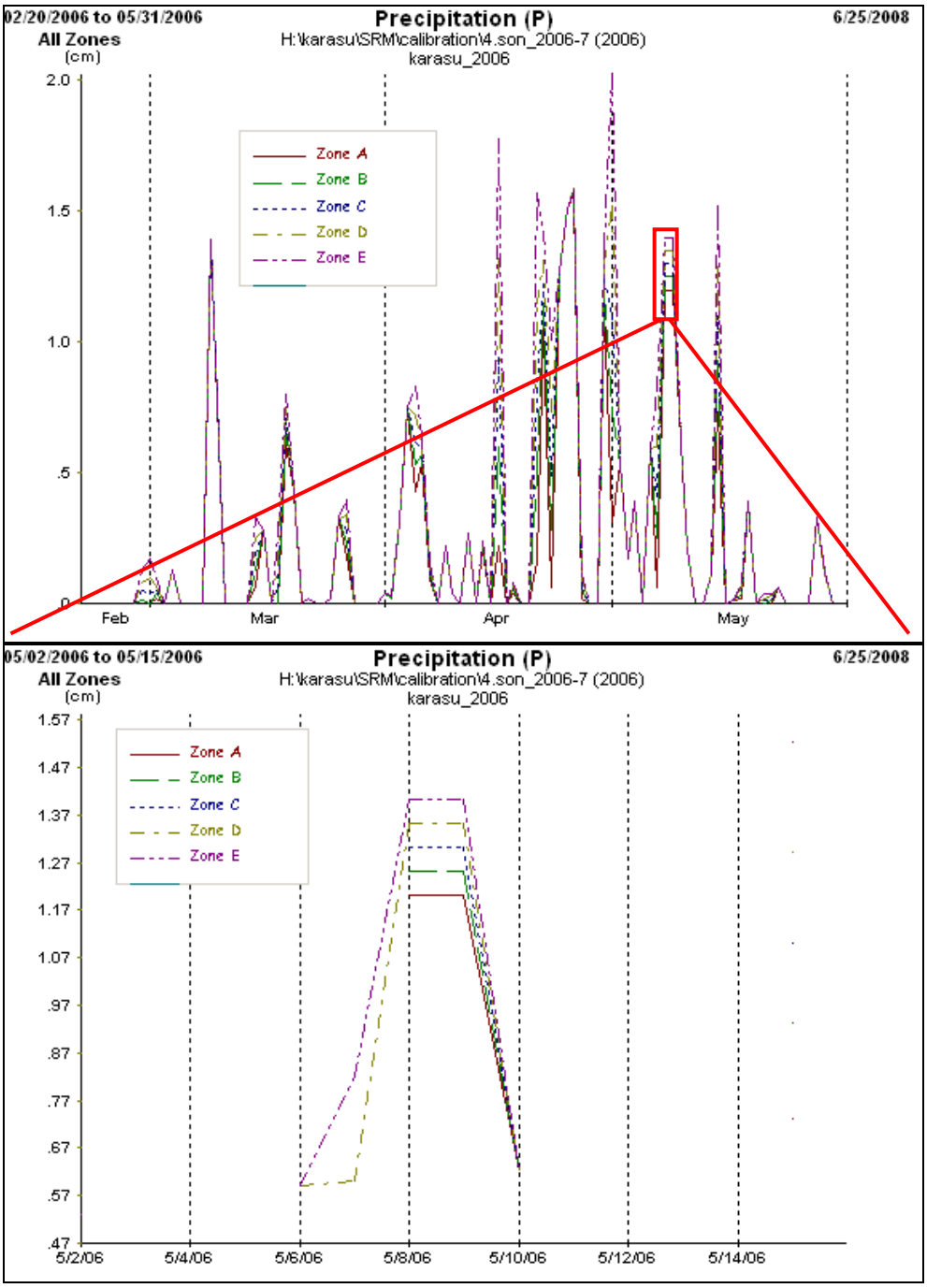

Figure 4.6 Average daily precipitation values for year 2006 and zoomed view

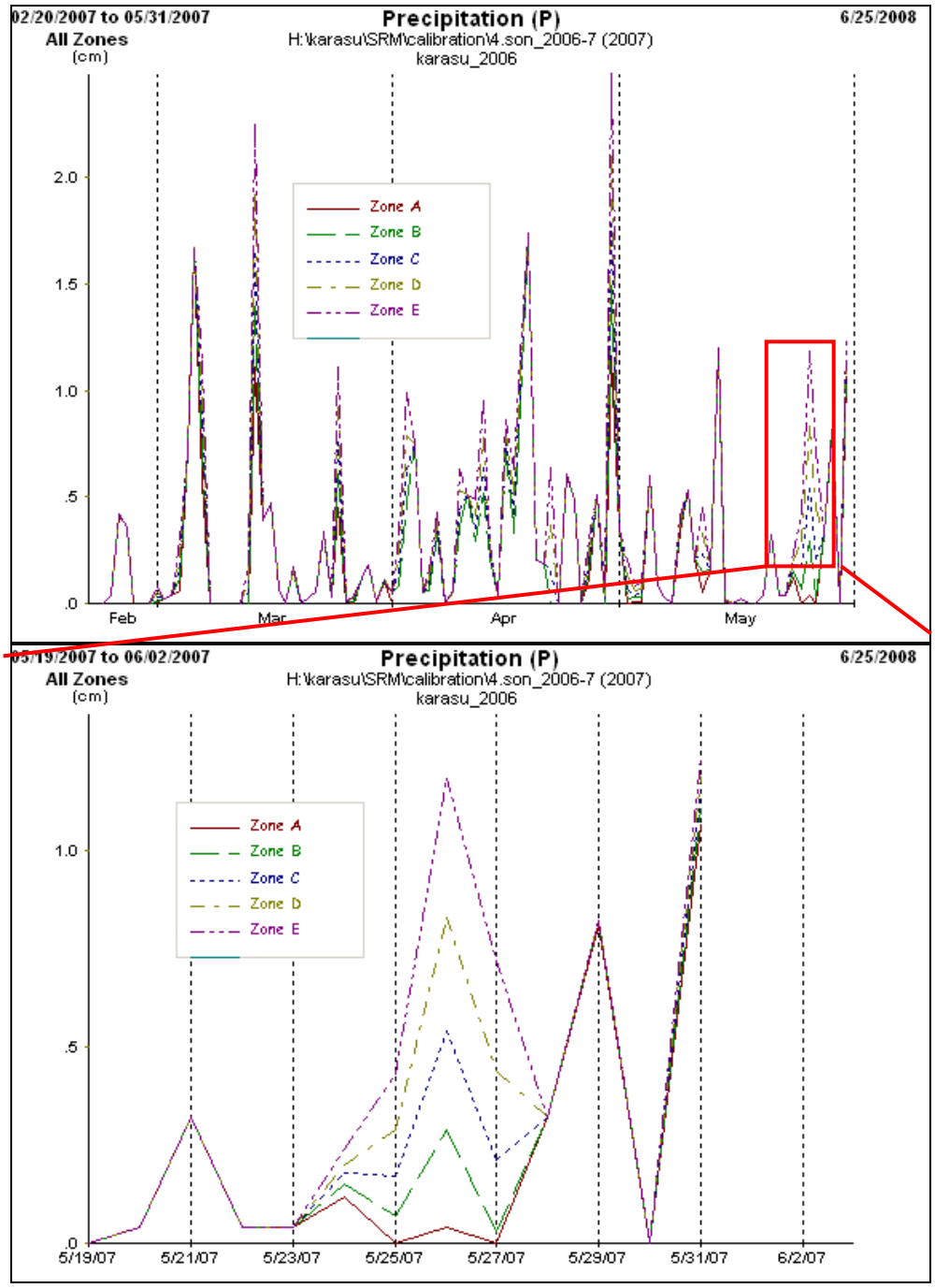

Figure 4.7 Average daily precipitation values for year 2007 and zoomed view

4.4.2.4.Snow Cover Area

In the mountain basins such as Karasu Basin; snow cover areas decrease gradually during snowmelt period. In section 3, how to obtain snowmelt depletion curves for each elevation zone is defined. One of the important things in SRM is that it uses snowmelt depletion curves directly in the model. Snowmelt depletion curves of each elevation zone are interpolated to use in SRM. In this way, daily percentage of snow cover area is obtained.

Figures 4.8, 4.9, 4.10, and 4.11 show the snow ,cloud and land coverage changes of Karasu Basin detected by satellite imaging for the years 2004,2005,2006 and 2007. As it is seen from the changing colours of bars, the spatial and temporal snow coverage have characteristic behaviour. Snowmelt procedure starts at the second half of February. In the basin area, snow can be seen till second half of June.

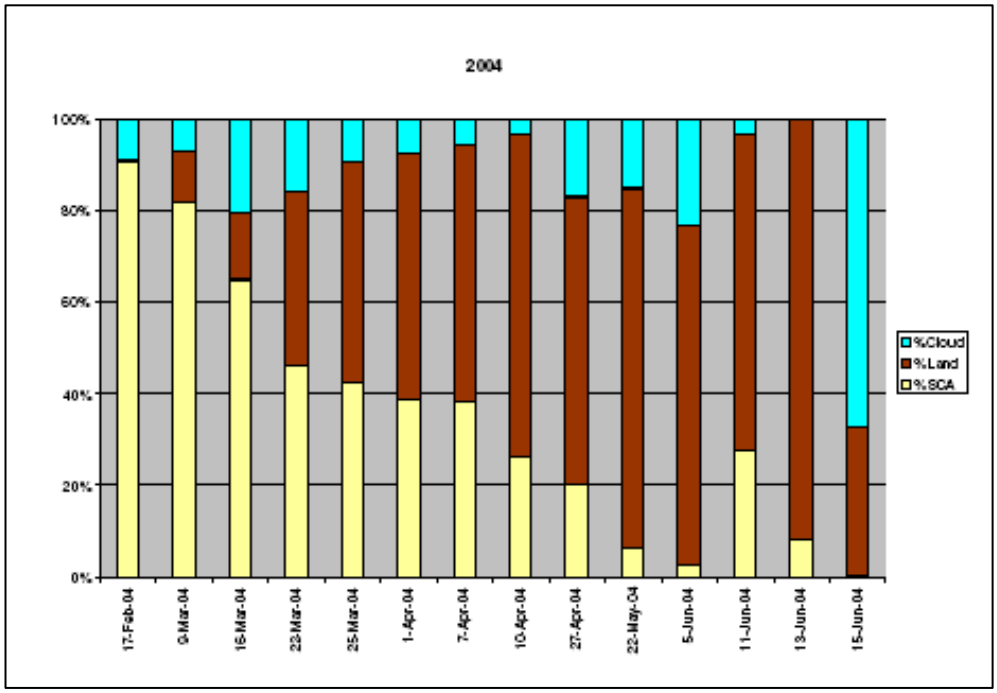

Figure 4.8 Bar chart of snow, cloud and land coverage of Karasu Basin for the year 2004

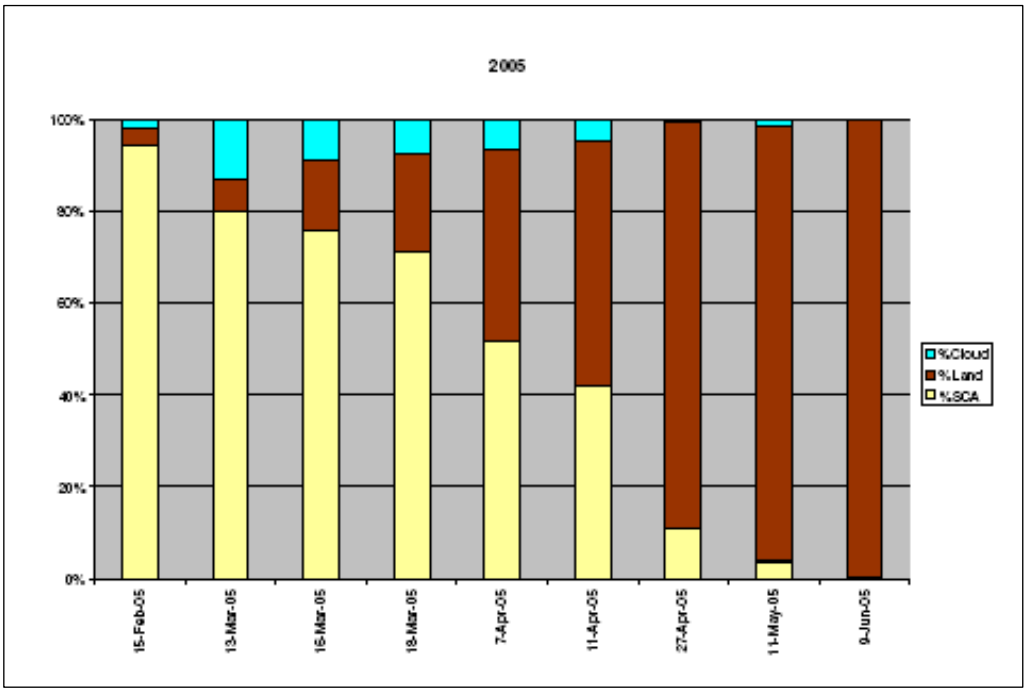

Figure 4.9 Bar chart of snow, cloud and land coverage of Karasu Basin for the year 2005

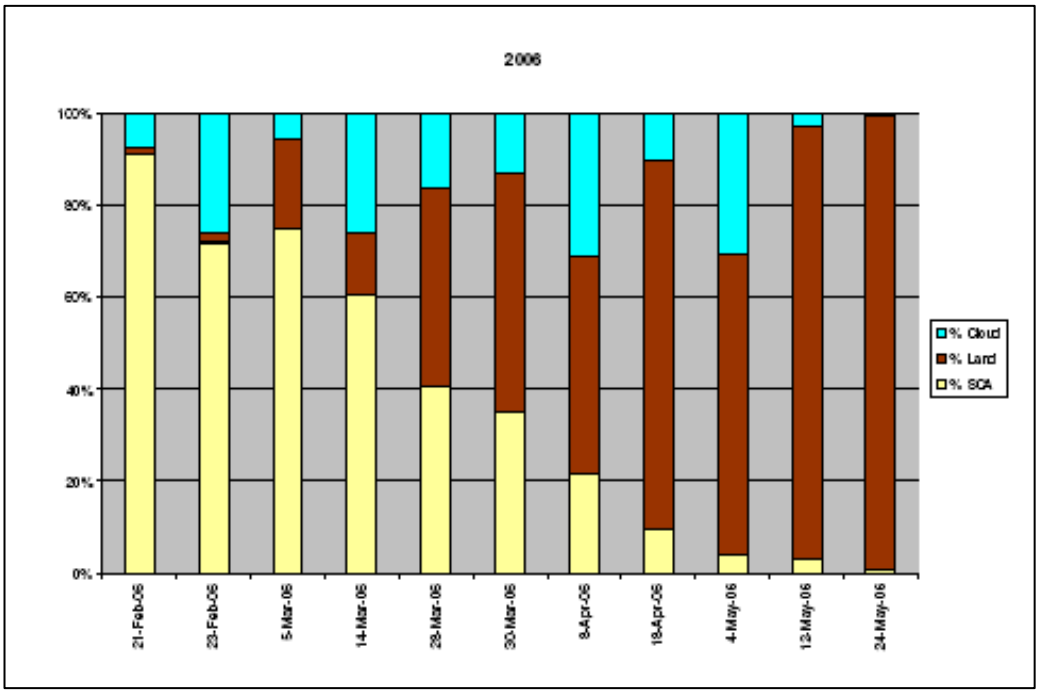

Figure 4.10 Bar chart of snow, cloud and land coverage of Karasu Basin for the year 2006

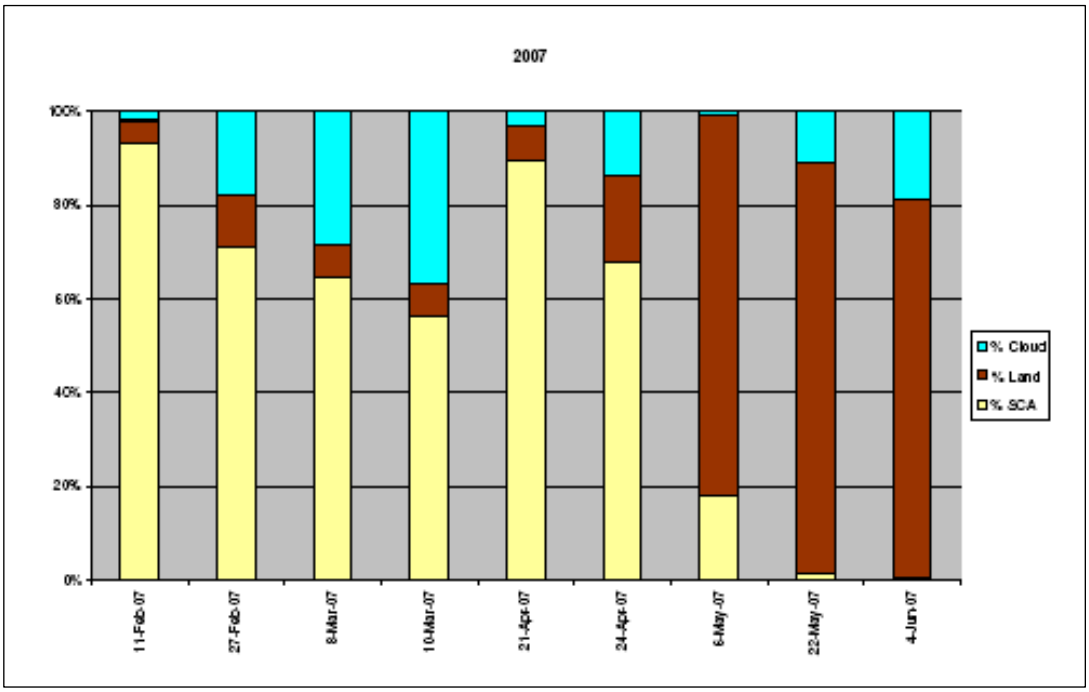

Figure 4.11 Bar chart of snow, cloud and land coverage of Karasu Basin for the year 2007

The snowmelt period can be detected for each year from Figures 4.8, 4.9, 4.10 and 4.11.The snowmelt period is generally from 20 February to 30 May of each year for Karasu Basin. The MODIS detect clouds in clouded days. Those images which have higher cloud percentages from 30 % of basin area are not used to define snow depletion curves in this study and also previous studies. SRM uses those added snow coverage as an input variable after cloud percentages is distinguished according to land and snow coverage and added to previous snow coverage. Based on those calculations snow depletion curves are drawn for years 2004, 2005, 2006 and 2007 (Figures 4.14, 4.15, 4.16 and 4.17). Moreover, in Figures 4.12 and 4.13 SDC for years 1997 and 1998 can be seen and are obtained from the previous studies for Karasu Basin (Kaya, 1999 and Tekeli, 2000).

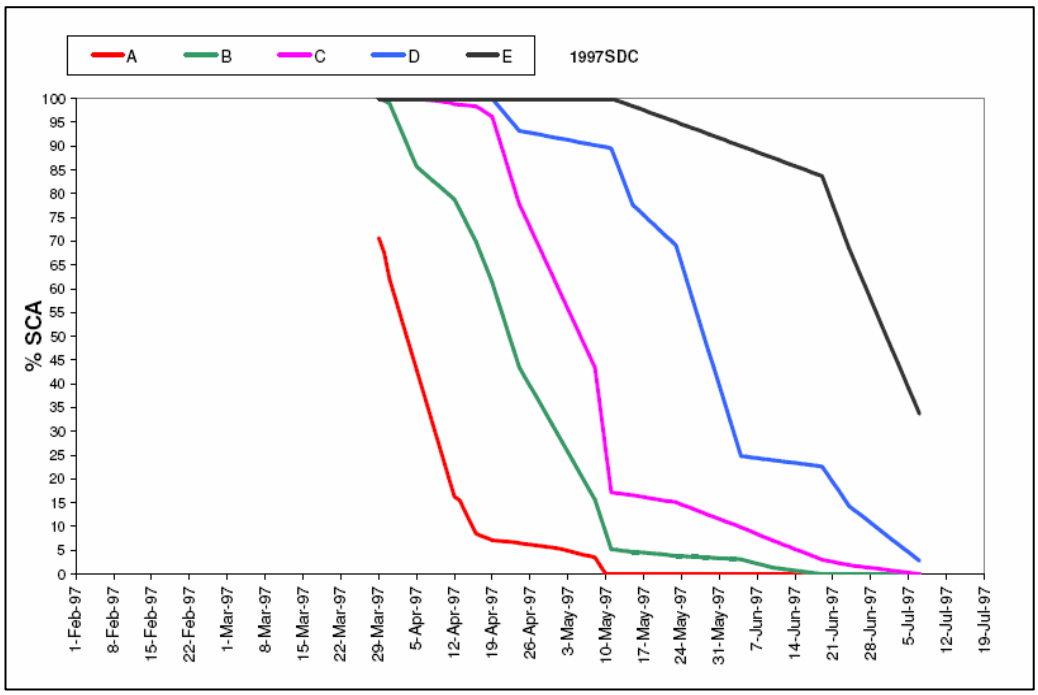

Figure 4.12 Snow depletion curve for the year 1997

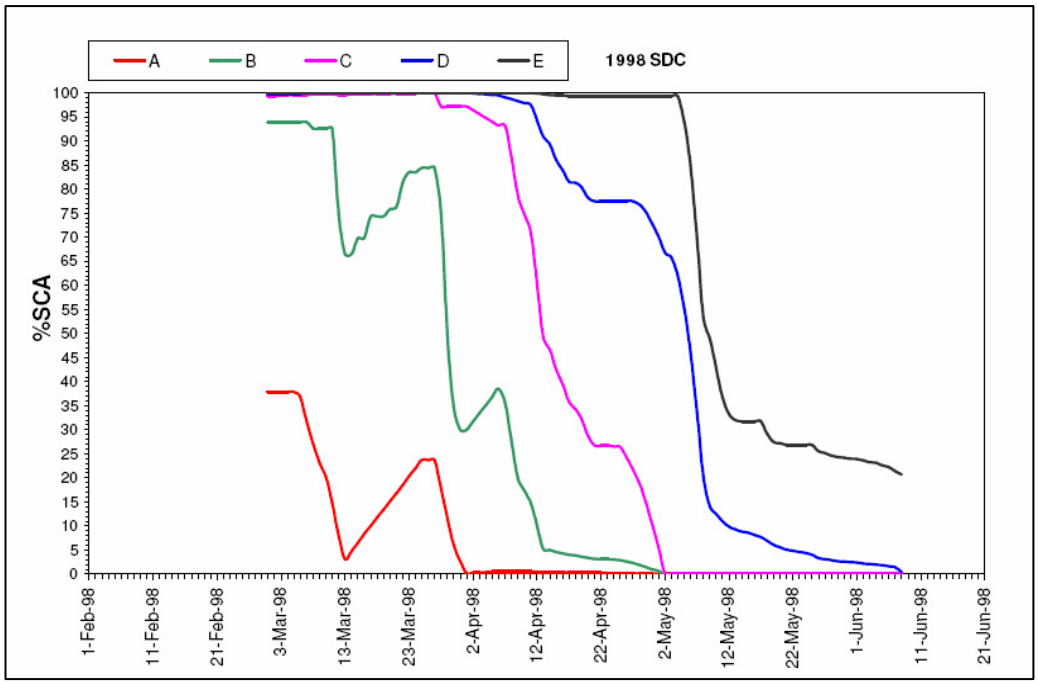

Figure 4.13 Snow depletion curve for the year 1998

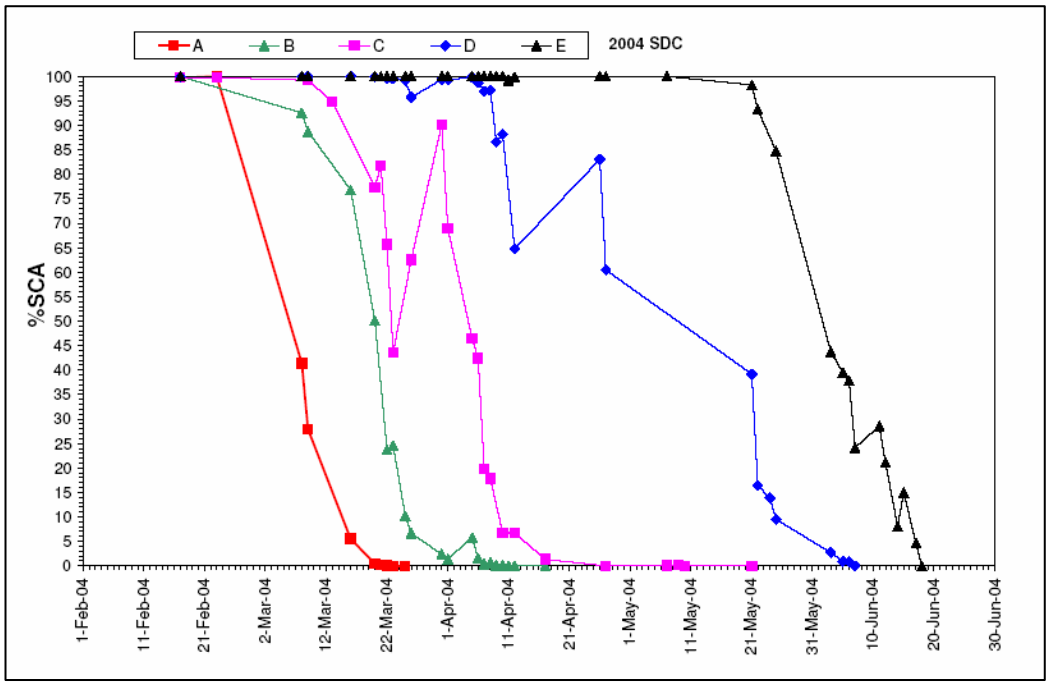

Figure 4.14 Snow depletion curve for the year 2004

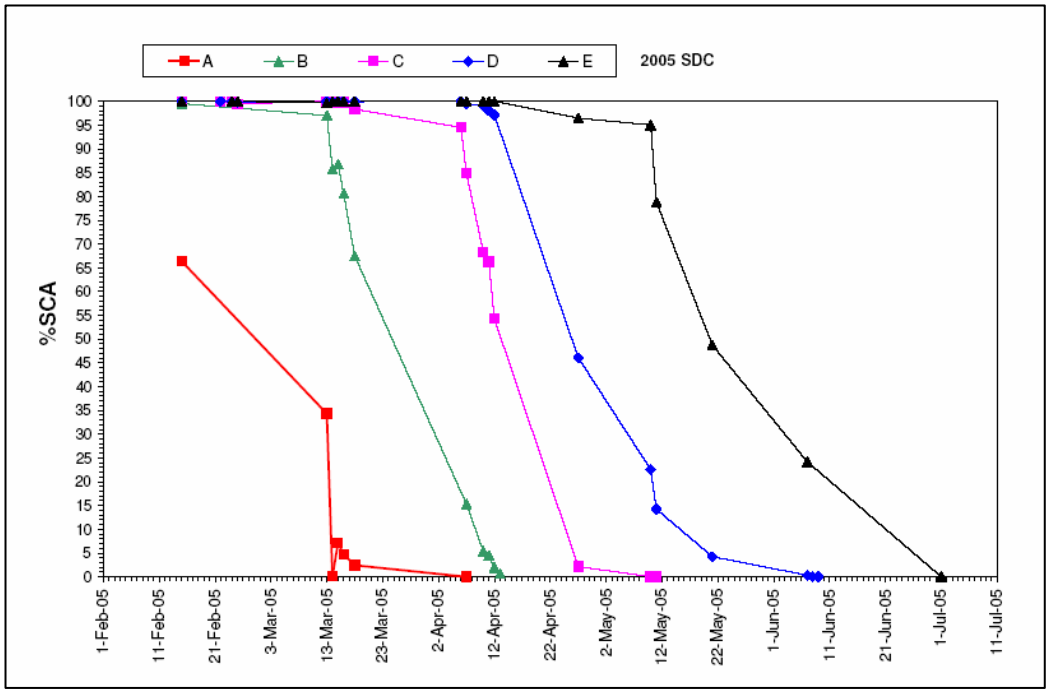

Figure 4.15 Snow depletion curve for the year 2005

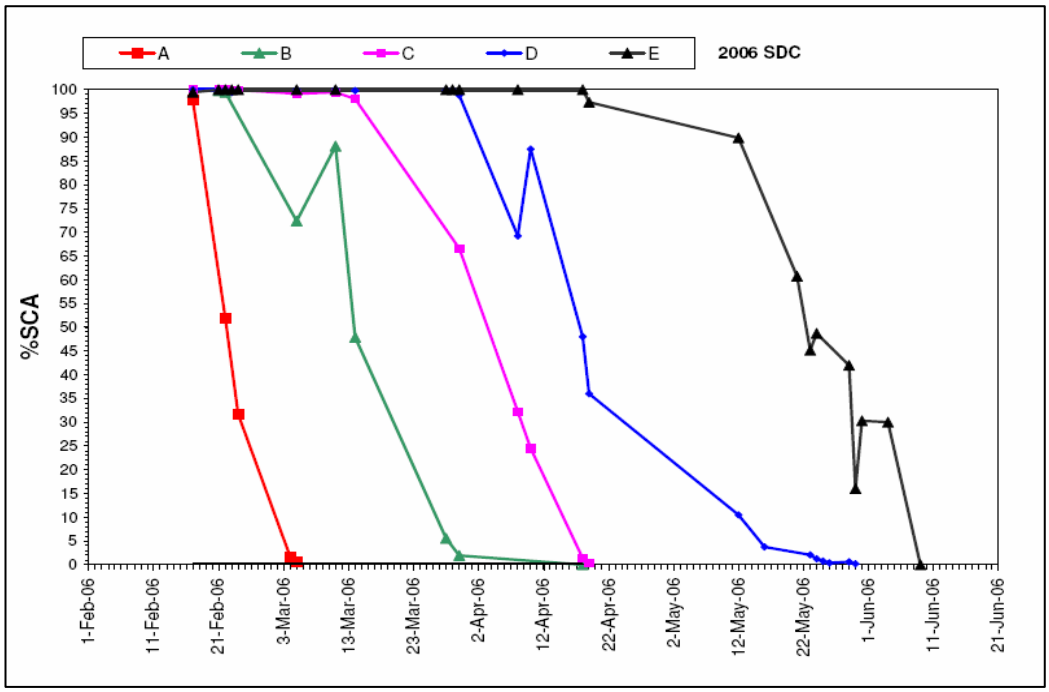

Figure 4.16 Snow depletion curve for the year 2006

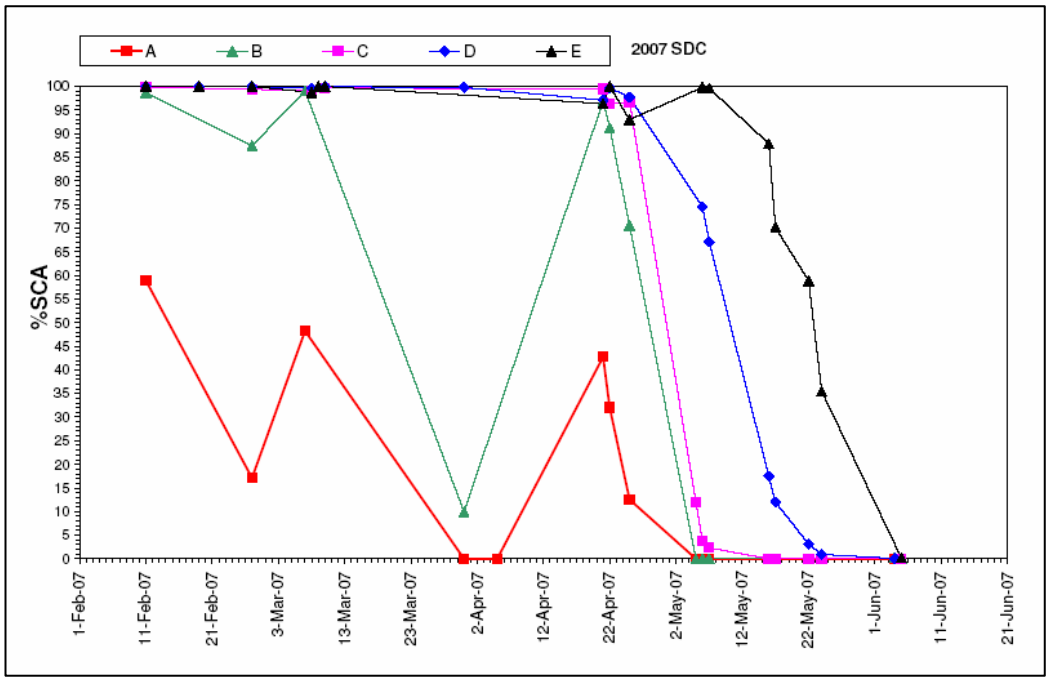

Figure 4.17 Snow depletion curve for the year 2007

As it can be seen from Figures 4.14, 4.15, 4.16 and 4.17, the time period of snow that stays on the ground is increasing from A elevation zone to E elevation zone according to height of elevation zones. If snowmelt season is compared it is seen that snowmelt has started earlier for each year starting from 1997 to 2007 especially in low elevation zones. This may be evidence to global warming and climate changes topics.

In Figures 4.18, 4.19, 4.20, 4.21, 4.22 depletion curves are redrawn according to years; 1997, 1998, 2004, 2005, 2006 and 2007 for each elevation zone. That will serve to have an idea about characteristics of each elevation zone's depletion curves. Moreover it helps defining a depletion curve of each elevation zone for forecast studies.

Total area of B and C elevation zones are 66 % of total basin area. Snow cover area percentages of B and C elevation zones show more recognizable changes than elevation zones D and E. In elevation zone A, snow depletion curve shows different characteristic according to the climate. Snow stays short time in elevation zone A.

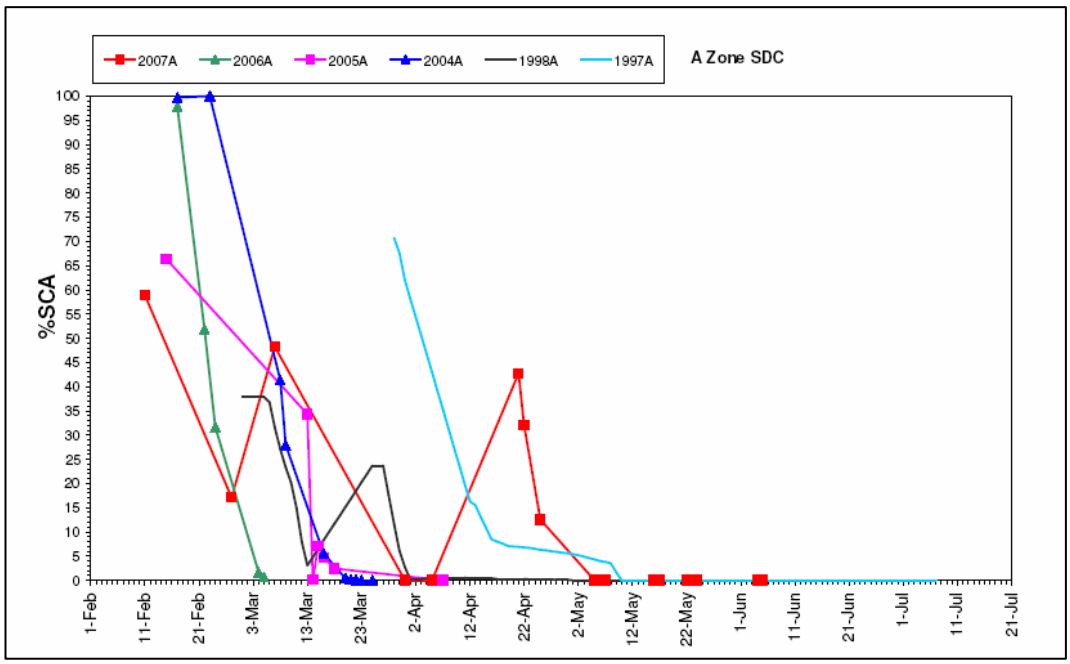

Figure 4.18 Snow depletion curves of A elevation zone

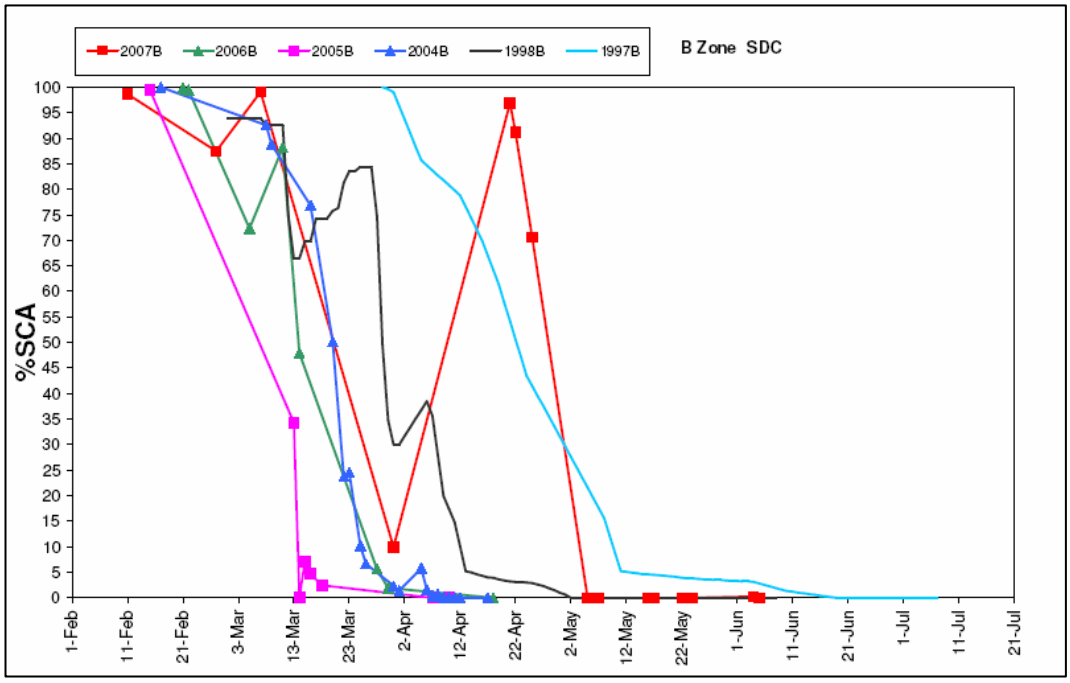

Figure 4.19 Snow depletion curves of B elevation zone

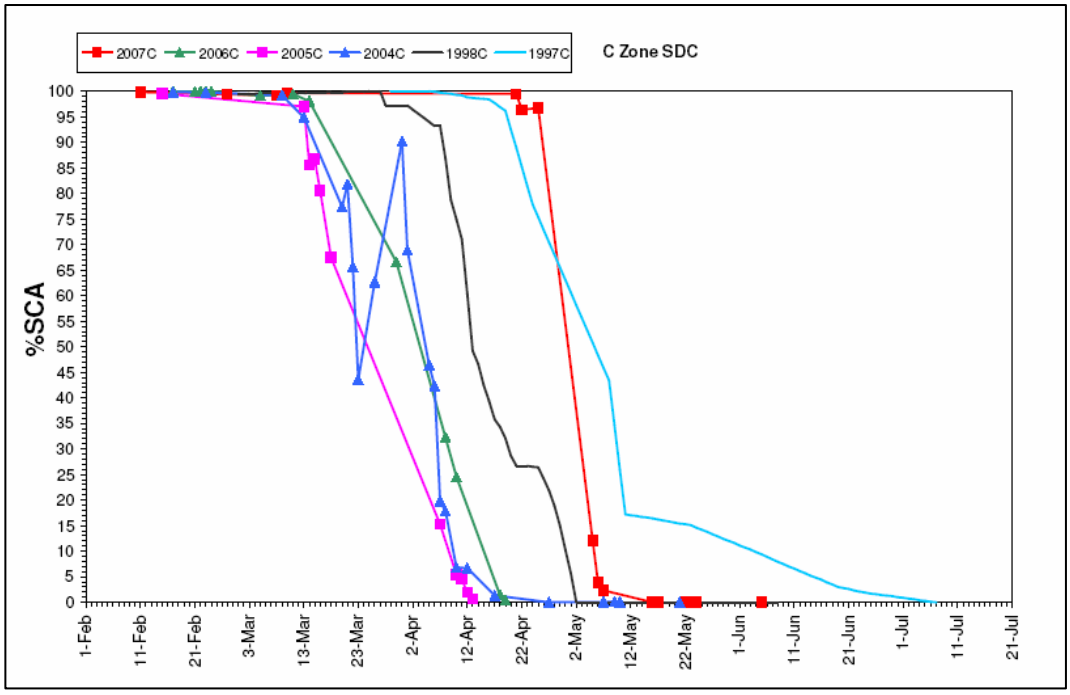

Figure 4.20 Snow depletion curves of C elevation zone

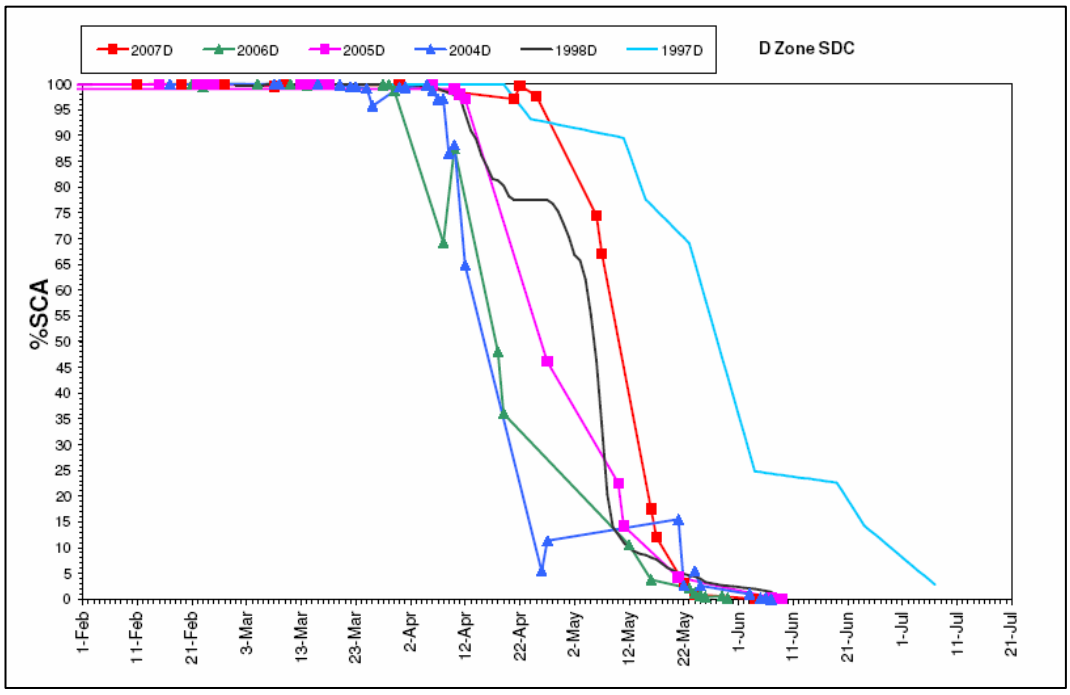

Figure 4.21 Snow depletion curves of D elevation zone

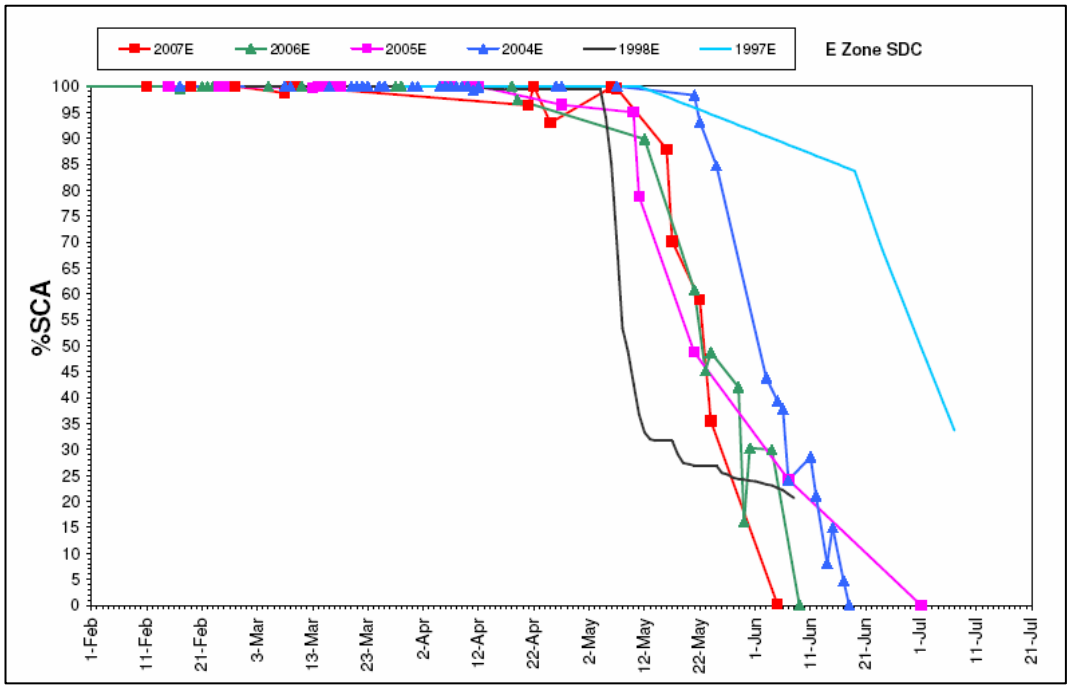

Figure 4.22 Snow depletion curves of E elevation zone

4.4.3. The SRM Parameters

SRM Model Parameters are defined according to previous thesis study on Karasu Basin (Tekeli, 2000&2005 and Kaya, 1999) and SRM Manual (Rango and Martinec , 1998).

The SRM parameters are not calibrated or optimized by historical data (Rango and Martinec, 1998). SRM parameters can be obtained from measurements or hydrological judgments. Adjustments can be done however; can not exceed defined acceptable values. Eight SRM Parameters are listed in Table 4.2. From those parameters adjustment by Temperature Lapse Rate (ΔT) will not be used in this study because the temperature values are distributed for each elevation zone by detrended kriging method. Eight parameters will be detailed in the following sections.

Table 4.2 List of SRM parameters

SRM PARAMETERS
Runoff Coefficients For Snow (Cs)
Runoff Coefficients For Rain (Cr)
Degree Day Factor (a) [$cm \cdot {}^{o}C^{-1} \cdot d^{-1}$]
Critical Temperature (T_{CRIT}) [^{o}C]
Rainfall Contributing Area (RCA)
Recession Coefficient (k)
Time Lag (L) [hr]
The Adjustment by Temperature Lapse Rate (ΔT) [$^{o}C \cdot d$]

4.4.3.1.Runoff Coefficient For Snow (C_S) and Runoff Coefficient For Rain (Cr)

Runoff Coefficients are used to determine losses which are differences between available water volumes and the sum of snowmelt; rainfall and basin outflow. In fact,

runoff coefficients express the ratio of the measured precipitation to measured outflow. That is why historical data; previous precipitation and outflow measurements are good starting point. However, these ratios are not always easily obtained in view of the precipitation catch deficit which particularly affects snowfall and of inadequate precipitation data from mountainous regions (Rango and Martinec, 1998).

Runoff coefficients values are generally changing in a snowmelt season. At the beginning of snowmelt season runoff coefficients are higher than in mid of snowmelt season because losses, evaporations are very small especially at high elevations (Rango and Martinec, 1998). Towards the end of the melting season direct channel flow from snowfield and glaciers on the ground may lead to decrease losses consequently runoff coefficients increase. The graphics of average runoff coefficients (Figure 4.23) from SRM user's manual show seasonal trends of runoff coefficients (Rango and Martinec, 1998). In semiarid basins, losses may be higher especially in the lowest elevation zone of basin.

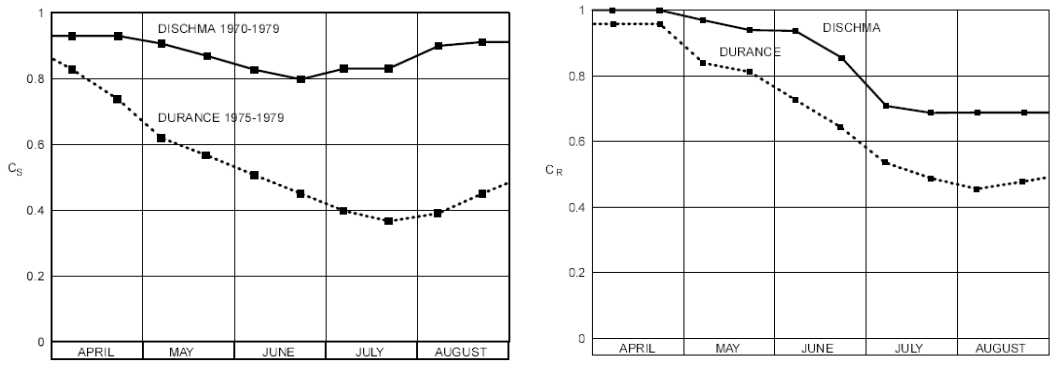

Figure 4.23 Average runoff coefficients for snow (C_S) and rainfall (Cr) (for the alpine basins Dischma (43.3 km^2, 1668-3146 m a.s.l.) and Durance (2170 km^2,786-4105 m a.s.l.) (Martinec & Rango, 1986).

Based on the definitions about runoff coefficients, the formula 4.6 and 4.7 are generated in Kaya's thesis study (1999).Moreover that formula is applied also in Tekeli's thesis study (2000).

$$C_S = \frac{\text{Snowmelt volume contributing to runoff}}{\text{Total snow volume}} \quad (4.6)$$

$$C_R = \frac{\text{Rainfall volume contributing to runoff}}{\text{Total rainfall volume}} \quad (4.7)$$

After that formulization, the hydrograph in the Figure 4.24 is divided according to events and time intervals for C_S and Cr calculations are obtained. The hydrograph for year 2006 is constituted from the measurements that are observed in 2119 runoff gauging station of Electrical Power Resources Survey and Development Administration (EIE).

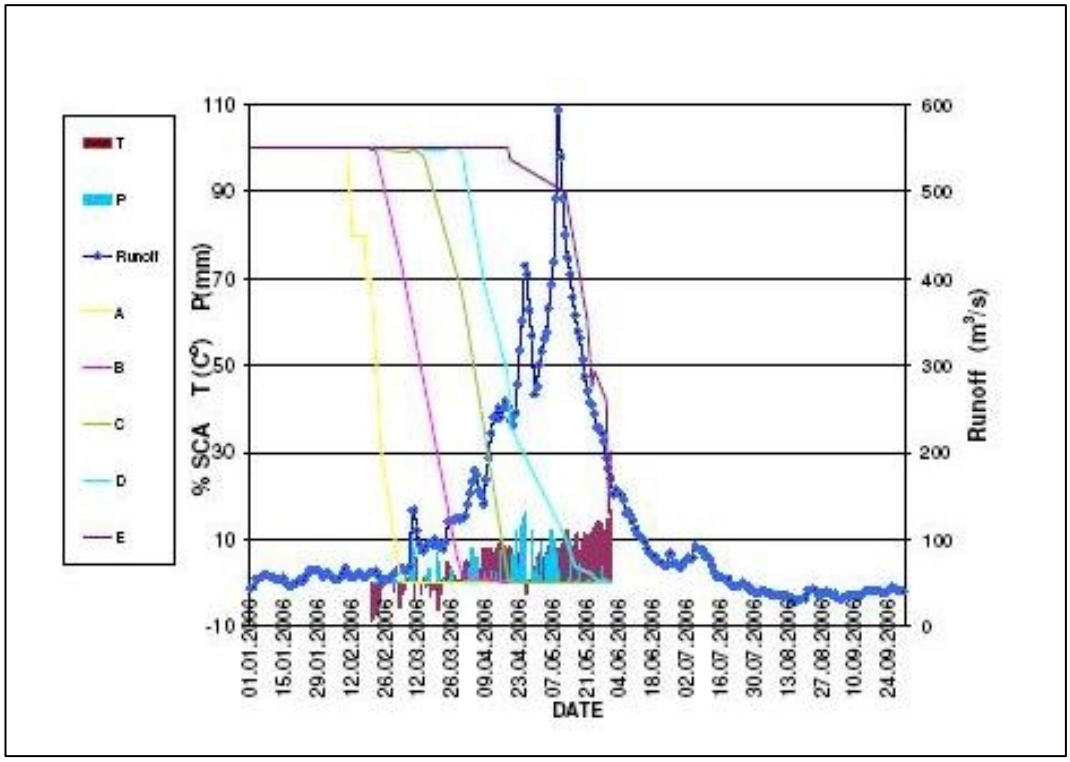

Figure 4.24 Observed hydrograph at 2119 EIE station for year 2006

Temperature and precipitation bar charts are also plotted in Figure 4.24 to use in separating hydrograph into components .The characteristics of rainfall and snowmelt runoff are important for distinguishing the hydrograph. The temperature values help

to distinguish precipitation. Precipitation is defined rain if temperature of zone is above critical temperature (T_{CRIT}). Runoff generated from rainfall makes sharp peaks on hydrograph whereas runoff generated from snowmelt makes smooth peaks. The hydrograph is separated into baseflow, snowmelt and runoff components in Figure 4.25

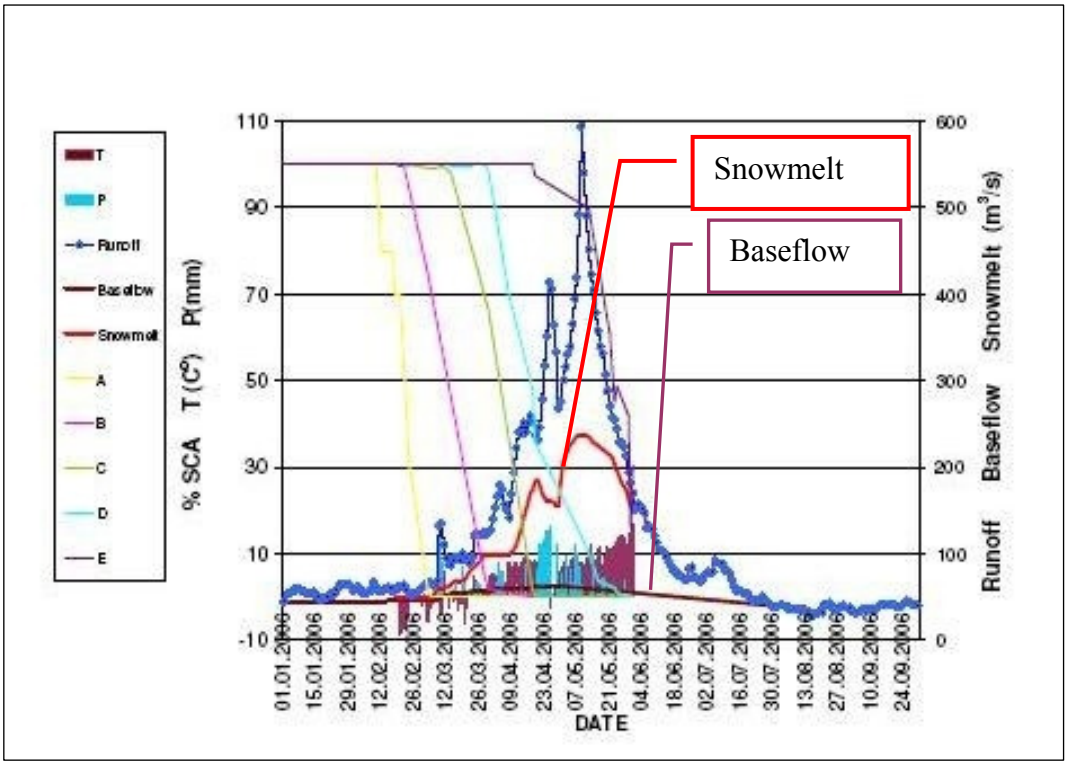

Figure 4.25 Hydrograph separated into components for year 2006

After this subjective separation of hydrograph into components, the volume for snowmelt, baseflow and rainfall is calculated for the related time period. The values obtained in Table 4.3 and will be used in calculations of C_R and C_S.

Table 4.3 Volumes of components of hydrograph

Time Period	Total Hydrograph	**Base Flow**	Surface Flow		**all in m^3**
			Rainfall	**Snowmelt**	Snowmelt+ Baseflow
20 Feb-8 Mar	89398080.00	70502400.00	14964480.00	3931200.00	74433600.00
9 Mar-14 Mar	56047680.00	26697600.00	24373440.00	4976640.00	31674240.00
15 Mar-23 Mar	73526400.00	43027200.00	17297280.00	13201920.00	56229120.00
24 Mar-31 Mar	85363200.00	40159891.53	20217600.00	24985708.47	65145600.00
1 Apr-8 Apr	109209600.00	40876279.32	40089600.00	28243720.68	69120000.00
9 Apr-20 Apr	241228800.00	62948696.95	91843200.00	86436903.05	149385600.00
21 Apr-29 Apr	257558400.00	48498516.61	130999680.00	78060203.39	126558720.00
30 Apr-31 May	916963200.00	162752534.51	334981440.00	419229225.49	581981760.00

The C_R values are calculated by dividing rainfall separated from hydrograph to rainfall volume calculated from spatial and temporal distributed rainfall measurements.

Table 4.4 Calculated C_R values

Time Period For 2006	**Rain From Hydrograph (Table 4.6) (m^3)**	**Rainfall Volume (m^3)**	**C_R**
20 Feb-8 Mar	14964480.00	41391985.00	**0.36**
9 Mar-14 Mar	24373440.00	75439474.00	**0.32**
15 Mar-23 Mar	17297280.00	60024814.00	**0.29**
24 Mar-31 Mar	20217600.00	64707681.00	**0.31**
1 Apr-8 Apr	40089600.00	230140425.00	**0.17**
9 Apr-20 Apr	91843200.00	212338355.00	**0.43**
21 Apr-29 Apr	130999680.00	697250027.00	**0.19**
30 Apr-31 May	334981440.00	832075309.00	**0.40**

Detecting water coming from snowmelt is dependent on the Snow Water Equivalent (SWE) content of the snow. To calculate the snowmelt volume, the SWE measurement of Ovacık and ÇAT stations are used in two different dates; 19 February 2006, 30 March 2006 for ÇAT station and 22 February 2006, 30 March 2006 for Ovacık station. Then the graphs of SWE with respect to the elevation are obtained in Figure 4.26 and 4.27

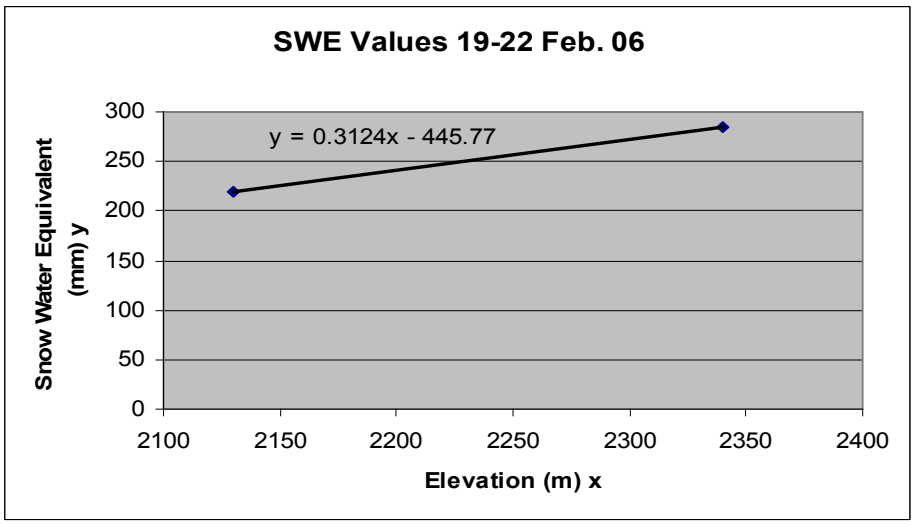

Figure 4.26 SWE for 19-22 February 2006

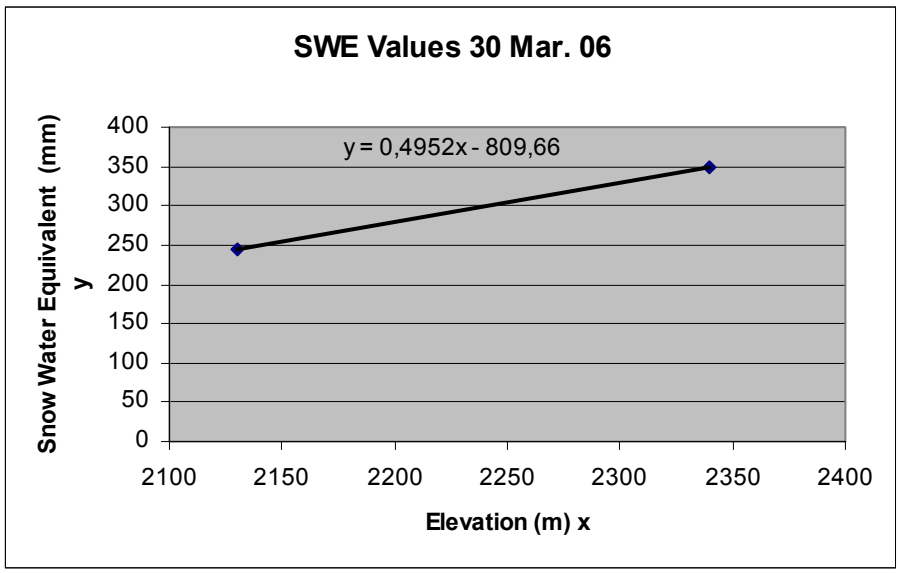

Figure 4.27 SWE for 30 February 2006

C_S value is calculated for the dates between 19-22 February and 30 March 2006. The procedure is defined below:

Step 1 : Snowline for 19-22 February and 30 March 2006 is found as 1426.9 m and 1635 m respectively.

Step 2 : The area above the snowline for 19-22 February and 30 March 2006 is found as 8405.93 km^2 and 9429.13 km^2 respectively. The values are obtained by the help of GIS software which perform classification method to DEM of basin area. The area between these two snowlines is found 1023.21 km^2.

Step 3 : The hypsometric mean elevation of the area is found to be 1542 m.

Step 4 : SWE for hypsometric mean elevation of the area is found by 35.95 mm by applying formula in the Figure 4.26

Step 5: Accumulated snow volume is found 36785130.49 m^3 by multiplication SWE with the area between snowlines.

Step6 : It is assumed that accumulated snow is melted immediately. The new falling snow is added to calculate melted volume. The SWE of new snow is assumed as 10 % of volume of new falling snow. It is calculated as 35093432.5 m^3.Therefore totally 71878562.99 m^3 volume of snow is melted.

Step7 : The snowmelt calculated from hydrograph is 43158117.97 m^3. Therefore C_S is found as:

$$C_s = \frac{\text{Snowmelt volume contributing to runoff}}{\text{Total snowmelt volume}} = \frac{43158117.9}{71878562.9} = 0.60$$

Because there is no SWE measurement obtained for the later time period, the C_S value is calculated to give an idea only for those given time period. The determined C_S and C_R values in previous studies for Karasu Basin Area are shown in the Figure 4.28 and 4.29 should be used in adjustment of runoff coefficients. Average temperature and precipitation values in given time period for the years

1998,2006,2007 and the C_R and C_S values for the years 1997,1998,2005 are plotted in Figures 4.30 and 4.31. Of the SRM parameters, the runoff coefficient appears to be the primary candidate for adjustment if a runoff simulation is not at once successful (Rango and Martinec, 1998).

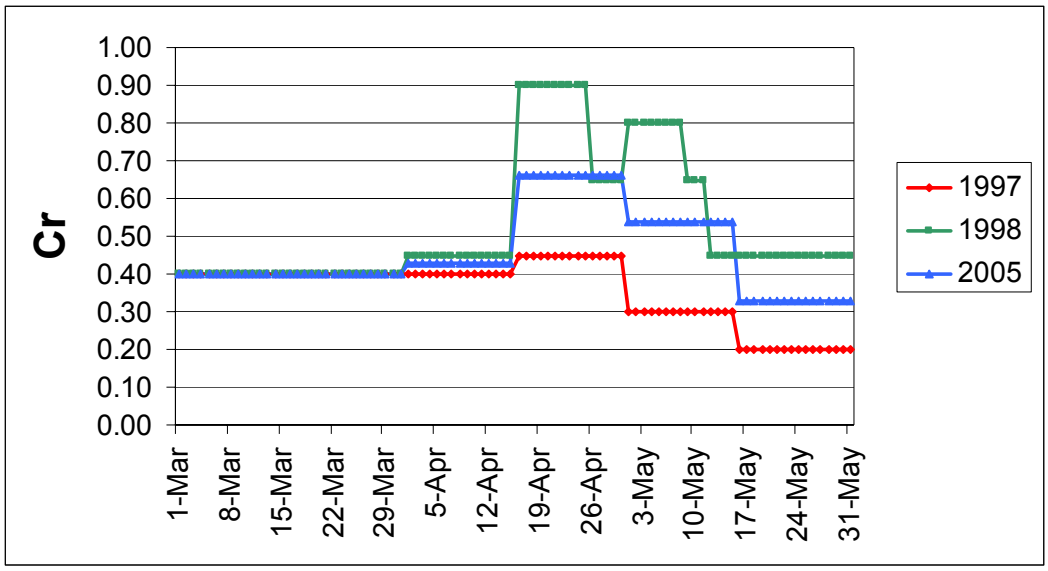

Figure 4.28 Previous C_R values used in SRM

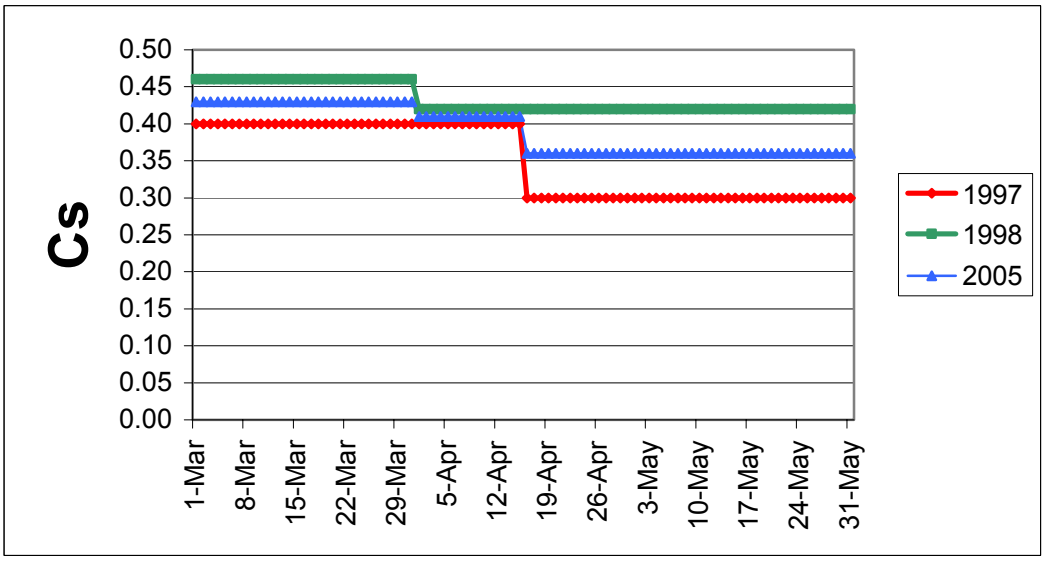

Figure 4.29 Previous C_S values used in SRM

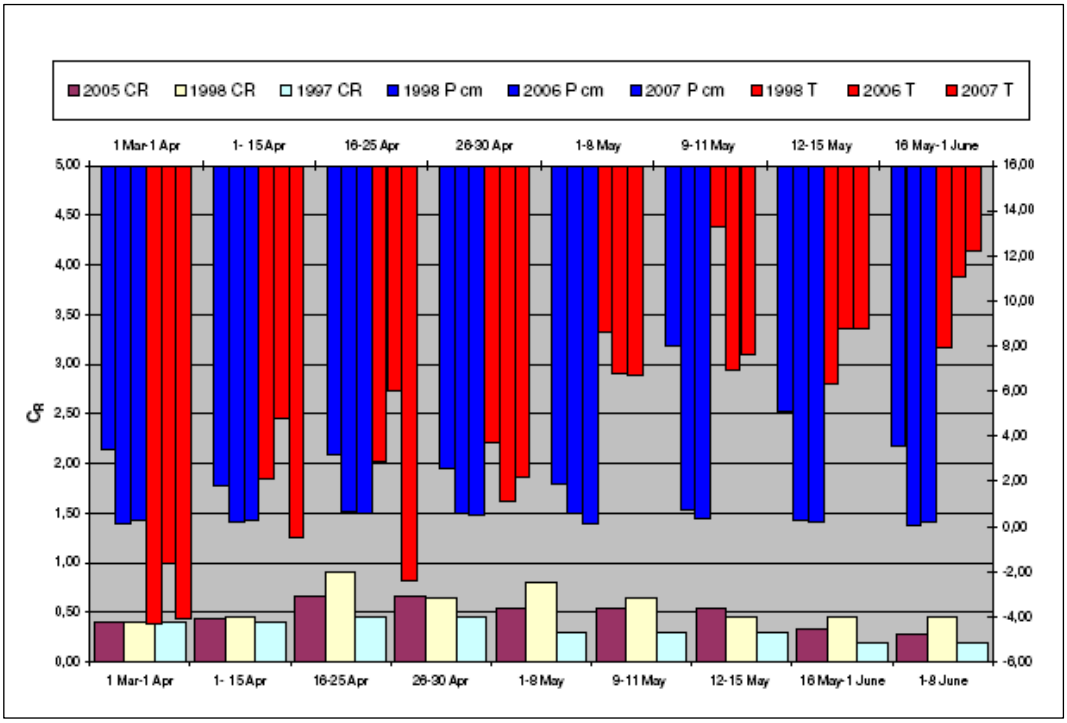

Figure 4.30.Previous C_R values and average precipitation and temperature values

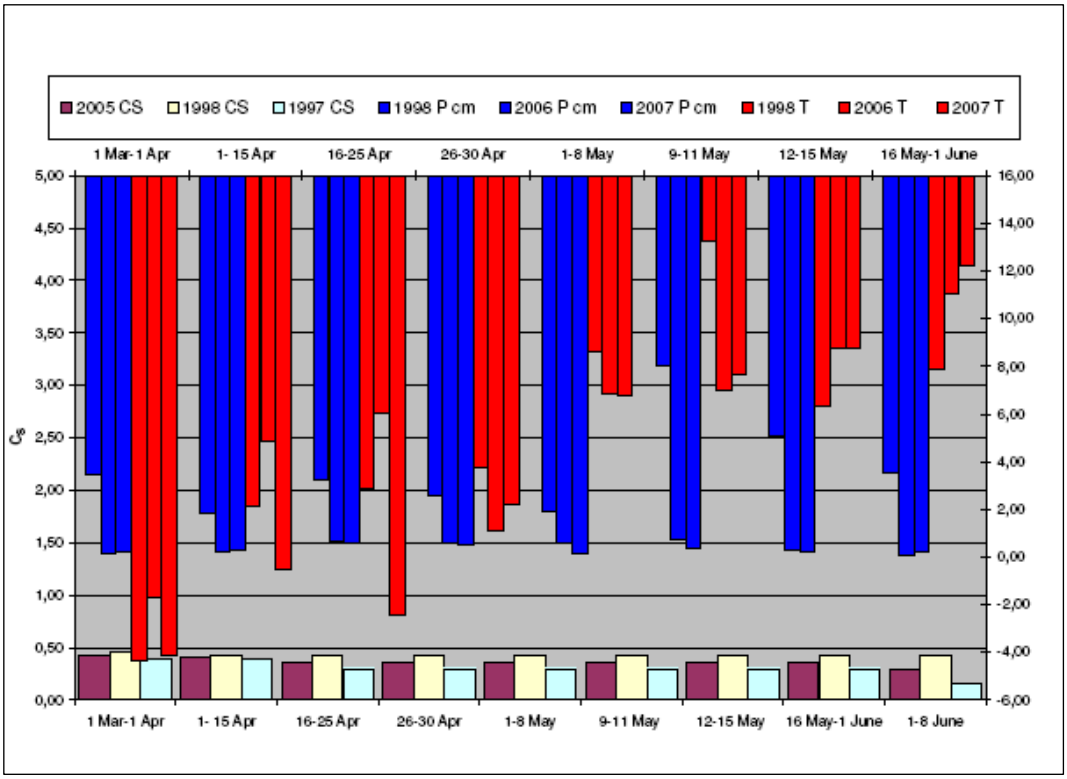

Figure 4.31 Previous C_S values and average precipitation and temperature values

4.4.3.2.Degree Day Factor (a)

The daily snowmelt depth M (cm) is obtained by multiplication of the number of degree days T (^{o}C.d) with degree day factor a (cm.^{o}C $^{-1}$.d^{-1}) :

$$M = a.T \qquad 4.8$$

The degree day factors can be obtained by comparing the degree day values T with the decrease of daily snow water equivalent values. This SWE values can be measured by radioactive snow gauge, snow pillow and a snow lysimeter (Rango and Martinec, 1998). In Karasu basin snow pillows are installed to measure SWE values.

In the absence of sufficient data, an empirical formula can be used (Martinec, 1960):

$$a = 1.1 * \frac{\rho_s}{\rho_w} \qquad 4.9$$

Where ;
a = the degree day factor (cm $^{\circ}$C $^{-1}$ d^{-1})
ρ_s = density of snow
ρ_w = density of water

If the density of snow increases, it means degree day factor also increases and the albedo of snow decreases .That is why liquid water content in snow increases. If snowfall occurs in the late snowmelt season, it produces decreasing of degree day factor for several days.

World Meteorological Organization (WMO) suggests degree day factors according to land cover of area (Table 4.5).In Table 4.5 and Figure 4.32 it is seen that degree day factor is not constant in a season. The seasonal trends of degree day factor values in the Alps and in the Rocky Mountains are shown in Figure 4.32 and in SRM Manual (Rango and Martinec, 1998).

The degree day factor values for this study is obtained from the Tekeli's thesis study (2000) values which are computed values and showed in Table 4.6 .The trend of degree day factor values for elevation zones is plotted in Figure 4.33

Table 4.5 Degree day factors recommended by WMO (1964)

Month	Moderate Forest Cover	Partial Forest Cover	No Forest
April	0.2	0.3	0.4
May	0.3	0.4	0.6
June	0.4	0.6	0.7

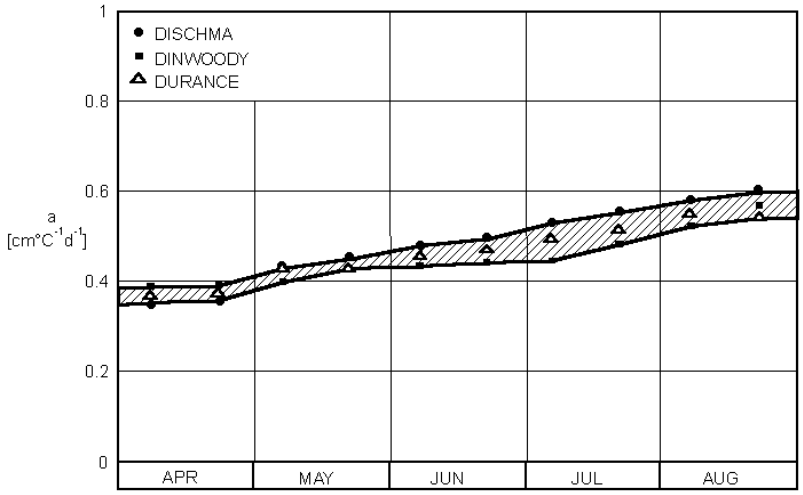

Figure 4.32 Average degree-day ratio (*a*) used in runoff simulations by the SRM model in the basins Dischma (10 years), Durance (5 years) and Dinwoody (228 km2; 1981-4202 m a.s.l.,Wyoming, 2 years) (Martinec & Rango, 1986).

Table 4.6 The degree day factor values for 5 elevation zones

Zone	A	B	C	D	E
March	0.26	0.26	0.28	0.36	0.36
April	0.40	0.40	0.41	0.35	0.35
May	0.42	0.42	0.42	0.42	0.42
June	0.42	0.42	0.42	0.42	0.42

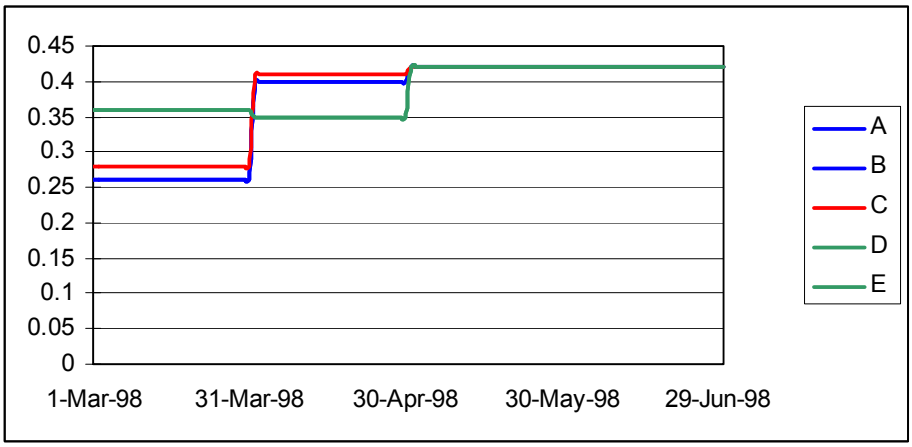

Figure 4.33 The trend of degree day factor values for 5 elevation zones

4.4.3.3. Critical Temperature, T_{CRIT}

The critical temperature is used to define the precipitation type. If daily average temperature value is less than critical temperature, $T<T_{CRIT}$, the precipitation is defined as a snowfall. Whereas if daily average temperature value is higher than critical temperature, $T>T_{CRIT,}$ the precipitation is defined as a rainfall. SRM needs critical temperature to decide if precipitation contributes to runoff as a rainfall or precipitation is stored as a new snowfall. In the $T<T_{CRIT}$ case, snow will be melt in following warm days.

SRM may not catch sharp rainfall runoffs because precipitation can be defined as a snowfall by critical temperature .In such cases, critical temperature and average daily temperature should be reviewed or adjustment should be done to change snowfall to rainfall. Moreover the temperature values for each elevation zone are average daily values and the temperature value when precipitation occurs may be less than critical temperature. That is why, it is difficult to define the precipitation type even in a normal day cycle.

In SRM Manual, in one SRM applied study to alpine basin Dischma , T_{CRIT} started at + 3 ^{o}C in April at the beginning of snowmelt and diminished to + 0.75 ^{o}C in July

(Rango and Martinec, 1998). In Kaya (1999) and Tekeli (2000) where previous studies of Karasu Basin for the years 1997 and 1998 are carried out, the critical temperature value is defined as 0.01 ^{o}C.

4.4.3.4.Rainfall Contributing Area, RCA

After the precipitation is defined as rainfall, it is treated in two different ways:

In option 1, RCA = 0; the time of rain falling on snow is in the early time period of snowmelt season. At that time period, snow is deep and dry. In this case, rainfall runoff is added to snowmelt runoff only from snow –free area. Therefore the rainfall depth is reduced.

In option 2, RCA = 1; after sometimes (the user will decide on that time), the temperature increases then snow becomes ripe and softened. It is assumed that when the rain falls on snow cover, the same amount of water is released and is added to snowmelt .Melting effect of rain is neglected.

In this study, it is assumed that the starting time of melting period is chosen as the dates of snow ripen and softened for the SRM running years 2006 and 2007. In Table 4.7 based on above explanations starting date of RCA=1 for years 2006 and 2007 is shown.

Table 4.7 The determined starting date of RCA

	2006	**2007**
Zone	**Starting date of RCA =1**	**Starting date of RCA =1**
A	1-Mar-06	1-Mar-07
B	1-Mar-06	8-Mar-07
C	15-Mar-06	21-Apr-07
D	1-Apr-06	23-Apr-07
E	15-Apr-06	7-May-07

4.4.3.5.Recession Coefficient, k

The recession coefficient is an important parameter for SRM. The recession coefficient decides the amount of meltwater that will contribute to runoff. As it is well known not all of the meltwater in a day appears in runoff on that day. It may take a period of time. Perzyna (1990) found that a minimum 10 years data is necessary to provide reliable estimates of the recession parameters. To analyze historical data is a good way to determine recession coefficient. The range of daily recession coefficient has been found typically to be (Klaassen and Pilgrim, 1975):
0.20-0.80 for surface runoff
0.70-0.94 for interflow
0.93-0.995 for baseflow.

The SRM uses correlation method for recession calculations and defines the recession coefficient with the following formulas (Martinec, 1998). Q_n and Q_{n+1} are plotted each other on log-log paper to determine x and y coefficients. The lower envelope line shows k values.

$$k = \frac{Q_{n+1}}{Q_n} \qquad 4.10$$

Therefore x and y can be found by solving the equations :

$$k_{n+1} = x.Q_n^{-y} \qquad 4.11$$

$$k_1 = x.Q_1^{-y} \qquad 4.12$$

$$k_2 = x.Q_2^{-y} \qquad 4.13$$

4.4.3.5.1. Recession Coefficient, k for 2006

In this section the hydrograph of 2006 is used to calculate recession coefficients for the year 2006. Figure 4.34 shows the hydrograph of the study area; Karasu basin for year 2006. The hydrograph of EIE 2119 runoff station (Figure 4.34) for year 2007 should be analyzed to obtain recession coefficient.

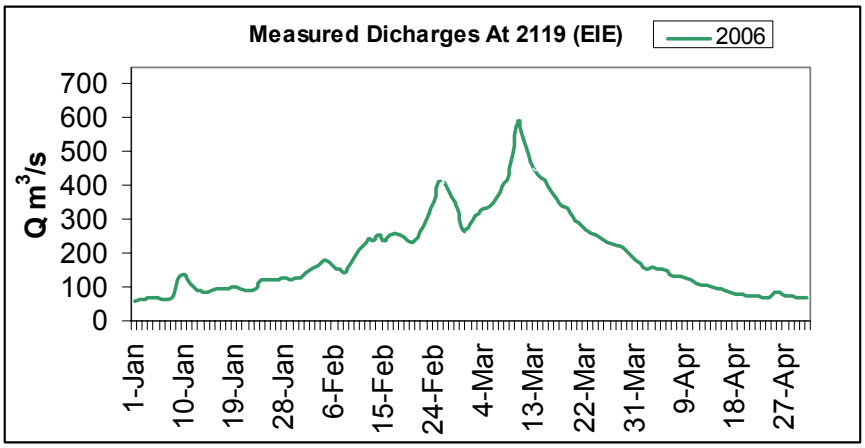

Figure 4.34 The hydrograph of Karasu Basin

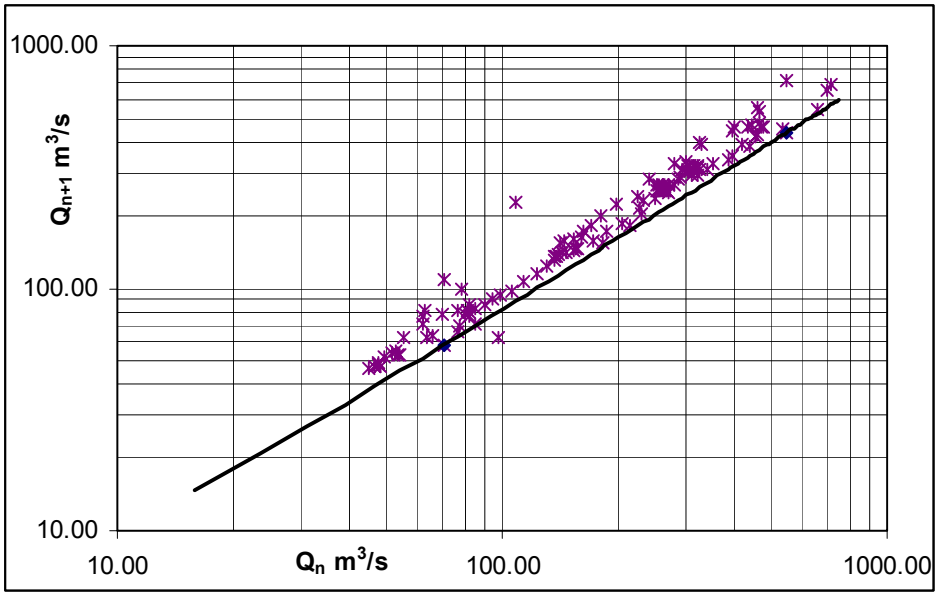

Figure 4.35 Q_n vs. Q_{n+1} for year 2006

Table 4.8 Coefficients of x and y for the year 2006

	SERIES 1						SERIES 2					
	Q_n (m^3)	Q_{n+1} (m^3)	k	x	y		Q_n (m^3)	Q_{n+1} (m^3)	k	x	y	
	15	14.1	0.94	**1.068**	**0.047**		**40**	33.99	0.85	**0.928**	**0.024**	
1	**450**	360.23	0.801			1	**500**	400.02	0.8			
	Q_n (m^3)	Q_{n+1} (m^3)	k	x	y		Q_n (m^3)	Q_{n+1} (m^3)	k	x	y	
	25	22.06	0.882	**0.983**	**0.034**		**40**	33.99	0.85	**0.934**	**0.026**	
2	**450**	360.23	0.801			2	**400**	320.45	0.801			
	Q_n (m^3)	Q_{n+1} (m^3)	k	x	y		Q_n (m^3)	Q_{n+1} (m^3)	k	x	y	
	40	33.99	0.85	**0.931**	**0.025**		**40**	33.99	0.85	**0.938**	**0.027**	
3	**450**	360.23	0.801			3	**350**	280.66	0.802			
	Q_n (m^3)	Q_{n+1} (m^3)	k	x	y		Q_n (m^3)	Q_{n+1} (m^3)	k	x	y	
	100	81.74	0.817	**0.871**	**0.014**		**40**	33.99	0.85	**0.943**	**0.028**	
4	**450**	360.23	0.801			4	**300**	240.88	0.803			
	Q_n (m^3)	Q_{n+1} (m^3)	k	x	y		Q_n (m^3)	Q_{n+1} (m^3)	k	x	y	
	150	121.52	0.81	**0.856**	**0.011**		**40**	33.99	0.85	**0.949**	**0.03**	
5	**450**	360.23	0.801			5	**250**	201.09	0.804			
	Q_n (m^3)	Q_{n+1} (m^3)	k	x	y		Q_n (m^3)	Q_{n+1} (m^3)	k	x	y	
	200	161.31	0.807	**0.847**	**0.009**		**40**	33.99	0.85	**0.958**	**0.032**	
6	**450**	360.23	0.801			6	**200**	161.31	0.807			
	Q_n (m^3)	Q_{n+1} (m^3)	k	x	y		Q_n (m^3)	Q_{n+1} (m^3)	k	x	y	
	250	201.09	0.804	**0.841**	**0.008**		**40**	33.99	0.85	**0.971**	**0.036**	
7	**450**	360.23	0.801			7	**150**	121.52	0.81			
	Q_n (m^3)	Q_{n+1} (m^3)	k	x	y		Q_n (m^3)	Q_{n+1} (m^3)	k	x	y	
	300	240.88	0.803	**0.838**	**0.007**		**40**	33.99	0.85	**0.994**	**0.043**	
8	**450**	360.23	0.801			8	**100**	81.74	0.817			
	Q_n (m^3)	Q_{n+1} (m^3)	k	x	y		Q_n (m^3)	Q_{n+1} (m^3)	k	x	y	
	350	280.66	0.802	**0.835**	**0.007**		**40**	33.99	0.85	**1.01**	**0.047**	
9	**450**	360.23	0.801			9	**80**	65.82	0.823			
	Q_n (m^3)	Q_{n+1} (m^3)	k	x	y		Q_n (m^3)	Q_{n+1} (m^3)	k	x	y	
	400	320.45	0.801	**0.832**	**0.006**		**40**	33.99	0.85	**1.05**	**0.057**	
10	**450**	360.23	0.801			10	**50**	41.95	0.839			
			Ave.	0.89	0.017				**Ave.**	0.968	0.035	
			St.dev.	0.08	0.014				**St.dev.**	0.039	0.011	
			Max*	0.97	0.031				**Max***	1.007	0.046	
			Min*	0.811	0.003				**Min***	0.928	0.024	

* Max-min values are considered as average value +- standard deviation value.

Table 4.9 Overall coefficients of x and y

Overall	x	y
Average	0.929	0.026
St.dev.	0.073	0.015
Max	1.002	0.041
Min	0.856	0.011

.

Q_n and Q_{n+1} are plotted against each other (Figure 4.35) for year 2006. Lower envelope line of all points is considered to indicate the k values (Rango and Martinec, 1998).Based on Equation 4.10-11-12-13 x and y values are calculated for two different series of Q_n values.

In the first series Q_{n2} is fixed in 400 m^3 and Q_n is increased from 15 to 400 m^3 in ten steps. The average, standard deviation and max-min values of the first series' x and y coefficients are given in Table 4.8.

In the second series, opposite of first series, Q_n is fixed in 40 m^3 and Q_{n2} is decreased from 500 to 50 m^3 in ten steps. The average, standard deviation and max-min values of second series' x and y coefficients are given in Table 4.8 also. Overall average, standard deviation and max-min values of x and y coefficients are given in Table 4.9

4.4.3.5.2. Recession Coefficient, k for 2007

In this section the hydrograph of 2007 is used to calculate recession coefficients for the year 2007. Figure 4.36 shows the hydrograph of the study area; Karasu basin for year 2007.

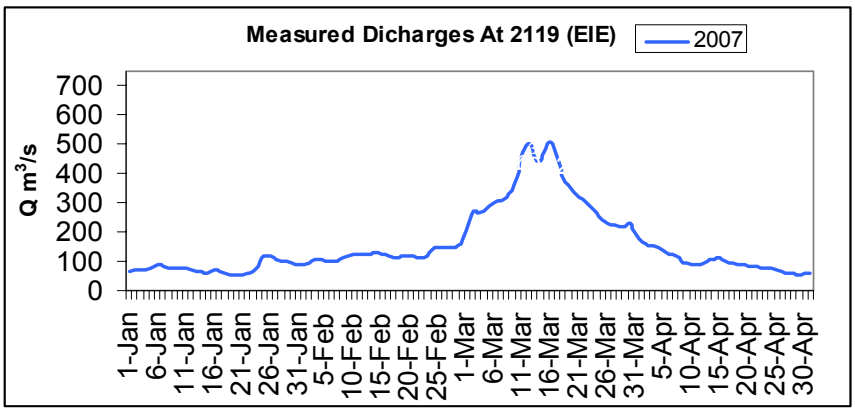

Figure 4.36 The hydrograph of Karasu Basin

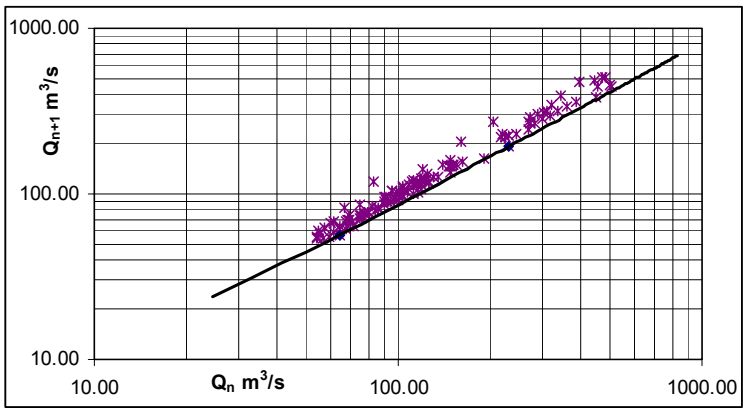

Figure 4.37 Q_n vs Q_{n+1} for year 2007

Q_n and Q_{n+1} are plotted against each other (Figure 4.37) for year 2007. Lower envelope line of all points is considered to indicate the k values (Rango and Martinec, 1998).Based on Equation 4.10-11-12-13 x and y values are calculated for two different series of Qn values.

In this section, same procedure is applied as in previous section 4.4.3.5.1.The same Q_{n2} and Q_n values are used to calculate x and y values. The average, standard deviation and max-min values of the **first** series' x and y coefficients are given in Table 4.10.The average, standard deviation and max-min values of the **second** series' x and y coefficients are given in Table 4.10 also. Overall average, standard deviation and max-min values of x and y coefficients for 2007 are given in Table 4.11.

Table 4.10 Coefficients of x and y for the year 2007

	SERIES 1						SERIES 2					
	Q_n (m^3)	Q_{n+1} (m^3)	k	x	y		Q_n (m^3)	Q_{n+1} (m^3)	k	x	y	
	15	16.45	1.096	1.374	0.083		**40**	36.87	0.922	1.083	0.044	
1	**450**	371.8	0.826			1	**500**	412.64	0.825			
	Q_n (m^3)	Q_{n+1} (m^3)	k	x	y		Q_n (m^3)	Q_{n+1} (m^3)	k	x	y	
	25	24.62	0.985	1.197	0.061		**40**	36.87	0.922	1.096	0.047	
2	**450**	371.8	0.826			2	**400**	330.95	0.827			
	Q_n (m^3)	Q_{n+1} (m^3)	k	x	y		Q_n (m^3)	Q_{n+1} (m^3)	k	x	y	
	40	36.87	0.922	1.089	0.045		**40**	36.87	0.922	1.104	0.049	
3	**450**	371.8	0.826			3	**350**	290.11	0.829			
	Q_n (m^3)	Q_{n+1} (m^3)	k	x	y		Q_n (m^3)	Q_{n+1} (m^3)	k	x	y	
	100	85.88	0.859	0.967	0.026		**40**	36.87	0.922	1.115	0.052	
4	**450**	371.8	0.826			4	**300**	249.26	0.831			
	Q_n (m^3)	Q_{n+1} (m^3)	k	x	y		Q_n (m^3)	Q_{n+1} (m^3)	k	x	y	
	150	126.73	0.845	0.935	0.02		**40**	36.87	0.922	1.128	0.055	
5	**450**	371.8	0.826			5	**250**	208.42	0.834			
	Q_n (m^3)	Q_{n+1} (m^3)	k	x	y		Q_n (m^3)	Q_{n+1} (m^3)	k	x	y	
	200	167.57	0.838	0.918	0.017		**40**	36.87	0.922	1.147	0.059	
6	**450**	371.8	0.826			6	**200**	167.57	0.838			
	Q_n (m^3)	Q_{n+1} (m^3)	k	x	y		Q_n (m^3)	Q_{n+1} (m^3)	k	x	y	
	250	208.42	0.834	0.907	0.015		**40**	36.87	0.922	1.175	0.066	
7	**450**	371.8	0.826			7	**150**	126.73	0.845			
	Q_n (m^3)	Q_{n+1} (m^3)	k	x	y		Q_n (m^3)	Q_{n+1} (m^3)	k	x	y	
	300	249.26	0.831	0.899	0.014		**40**	36.87	0.922	1.225	0.077	
8	**450**	371.8	0.826			8	**100**	85.88	0.859			
	Q_n (m^3)	Q_{n+1} (m^3)	k	x	y		Q_n (m^3)	Q_{n+1} (m^3)	k	x	y	
	350	290.11	0.829	0.893	0.013		**40**	36.87	0.922	1.259	0.084	
9	**450**	371.8	0.826			9	**80**	69.55	0.869			
	Q_n (m^3)	Q_{n+1} (m^3)	k	x	y		Q_n (m^3)	Q_{n+1} (m^3)	k	x	y	
	400	330.95	0.827	0.889	0.012		**40**	36.87	0.922	1.348	0.103	
10	**450**	371.8	0.826			10	**50**	45.04	0.901			
			Ave.	1.007	0.031				**Ave.**	1.168	0.064	
			St.dev.	0.163	0.024				**St.dev.**	0.085	0.019	
			Max*	1.17	0.055				**Max***	1.253	0.083	
			Min*	0.843	0.006				**Min***	1.083	0.044	

* Max-min values are considered as average value +- standard deviation value.

Table 4.11 Overall coefficients of x and y

Overall	**x**	**y**
Average	1.087	0.047
St.dev.	0.151	0.027
Max	1.239	0.074
Min	0.936	0.020

It can be seen in Table 4.9 and 4.11 as max-min values are considered as average value +- standard deviation value .From these results it is seen that for the **first** series of 2006, x and y values can be in the range (0.811-0.970) , (0.003-0.031) respectively. For the **second** series of 2006, x and y can be in the range (0.928-1.007), (0.024-0.046) respectively. For the **overall** series, x and y can be in the range (0.856-1.002) , (0.011-0.041) respectively.

Beside the resultant x and y coefficients of 2006, for the **first** series of 2007, x and y values can be in the range (0.843- 1.170), (0.006-0.055) respectively. For the **second** series of 2007, x and y can be in the range (1.083-1.253), (0.044-0.083) respectively. For the **overall** series, x and y can be in the range (0.936-1.239), (0.020-0.074) respectively.

Table 4.12 The summary range of x and y coefficients

	x	y	
2006	**0.811**-0.970	**0.003**-0.031	**1.series**
	0.928-1.007	0.024-0.046	**2.series**
	0.856-1.002	0.011-0.041	**Overall**
2007	0.843-1.17	0.006-0.055	**1.series**
	1.083-1.253	0.044-**0.083**	**2.series**
	0.936-**1.239**	0.020-0.074	**Overall**

Consequently, for years both 2006 and 2007, x and y can be in the range (0.811-1.239), (0.003-0.083) respectively (Table 4.12). If the previous studies are investigated, it is that from Kaya's thesis study (1999), x = 1.1140± 0.1128 y = 0.0505± 0.0233 average values are found from year 1954 to 1997. Therefore it is concluded from those calculations and examining previous studies, x and y values can show variations even in single year. In SRM manual it is clearly explained that recession coefficients which may be right for snowmelt period are usually too low for the winter months (Rango, 1998).It is also clarified in manual that user can decide to increase or decrease the k values according to basin response. If k value is low, basin will response too quickly. A quick improvement is possible by deriving new x and y values (Rango, 1998). Therefore, in this study, as a starting point **0.8555 and 0.011** values for x and y values respectively which are in the lower part of ranges (Table 4.12) are taken for the first run. It would be improved according to simulation basin response.

4.4.3.6.Time Lag, L

One of the main purposes of SRM is to catch the timing of the floods and also to calculate volume of simulated runoff correctly. The time lag in SRM is used to match the time of simulated runoff with measured runoff.

The characteristic daily fluctuations of snowmelt runoff enable the time lag to be determined directly from the hydrographs of the past years (Rango and Martinec, 1998). There is a procedure detailed in SRM Manual (1998) but that procedure is preferable for mountain basins whose area is less than 5000 km^2. As a second option, in case the hydrographs are not available and hydrographs are distorted by reservoir operations, the time lag can be estimated according to area of basin. In the Table 4.13, there are some examples of time lag values and areas of basins taken from World Meteorological Organization intercomparison test (WMO, 1986).

Table 4.13 Basin areas and lag time values

Basin Name	Basin Area (km^2)	Lag Time (h)
Basin W-3	8.42	3
Dischma	43.3	7.2
Dunajec	680	10.5
Durance	2170	12.4

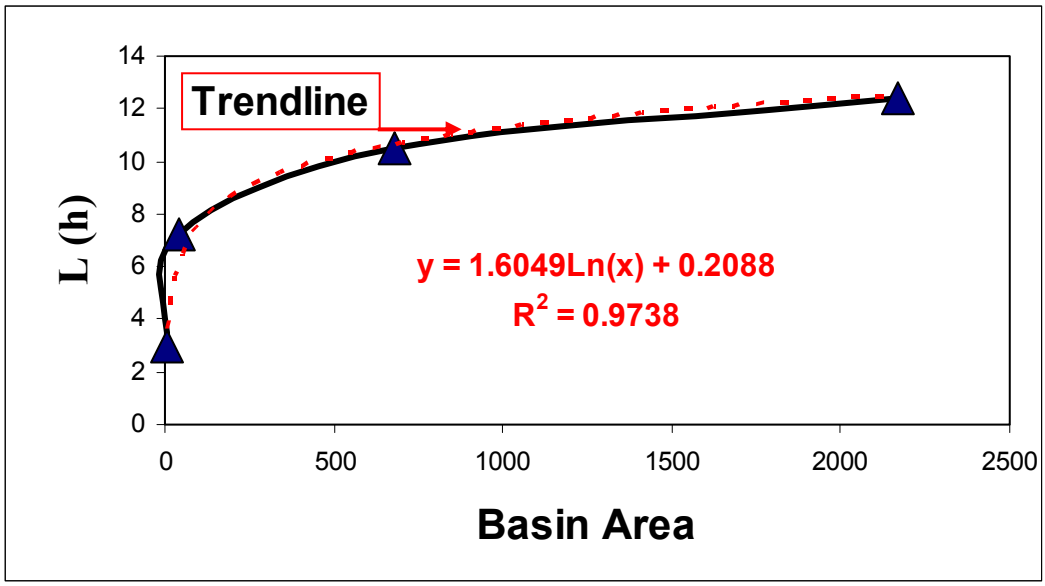

Figure 4.38 Lag time vs Basin Area

The time lag is plotted against to the basin area values in Figure 4.38 .The logarithmic trend line gives the best result; higher R^2 value. Then the time lag is calculated for Karasu Basin (10215.7 km^2) by applying the trend line formula; y = 1.6049Ln(x) + 0.2088. **The time lag is found 15 h**.

CHAPTER 5

SNOWMELT RUNOFF MODEL RESULTS

In this chapter first of all, the parameters and variable defined in chapter 4 is performed in case 1 (Section 5.1) for 2006. In case 2 (Section 5.2), model parameters are calibrated for 2006 and then SRM is performed with calibrated 2006 parameters. In case 3 (Section 5.3) the SRM is performed for 2007 without changing any parameter obtained in case 2. In case 4 (Section 5.4), only x and y coefficients are improved for both years and resultant parameters and simulation of this thesis is shown in this section.

5.1. Case 1 : Model Run with Calculated Parameters For Year 2006

In case 1, parameters and variables explained in chapter 4 are used for year 2006. The performed parameters for case 1 can be seen in Table 5.1. Moreover, measured-simulated runoff results and graph for year 2006 can be seen in Figure 5.1 and 5.2.From the results obtained for case 1 (Figure 5.1&5.2), it is clearly understood that SRM parameters should be calibrated for year 2006. The parameters are calibrated in the following cases.

Table 5.1 The parameters for the year 2006

	Runoff Coef. For Snow (Cs)	Runoff Coef. For Rain (Cr)	Degree Day Factor (a)*	Critical Temp. (T_{CRIT})	Rainfall Cont. Area (RCA)*	Recession Coefficient (x)	Recession Coefficient (y)	Time Lag (L)
20 feb-28 feb	0.6	0.36	0.26	0.01	0	0.8555	0.011	15
1 mar-8 mar	0.6	0.36	0.26	0.01	1	0.8555	0.011	15
9 mar - 14 mar	0.6	0.32	0.26	0.01	1	0.8555	0.011	15
15 mar-23 mar	0.6	0.32	0.29	0.01	1	0.8555	0.011	15
24 mar-31 mar	0.6	0.31	0.29	0.01	1	0.8555	0.011	15
1 apr-8 apr	0.6	0.17	0.4	0.01	1	0.8555	0.011	15
9 apr - 20 apr	0.6	0.43	0.4	0.01	1	0.8555	0.011	15
21 apr - 30 apr	0.6	0.19	0.4	0.01	1	0.8555	0.011	15
1 may - 31 may	0.6	0.19	0.42	0.01	1	0.8555	0.011	15

* RCA and a values are the values of elevation zone A.

Statistics	Run Results
Measured Runoff Volume (10^6 m³)	1829.295
Average Measured Runoff (m³/s):	209.628
Computed Runoff Volume (10^6 m³)	1320.824
Average Computed Runoff (m³/s):	151.360
Volume Difference (%):	27.7960
Coefficient of Determination (R^2):	0.4303

Figure 5.1 Simulation Result For Case 1

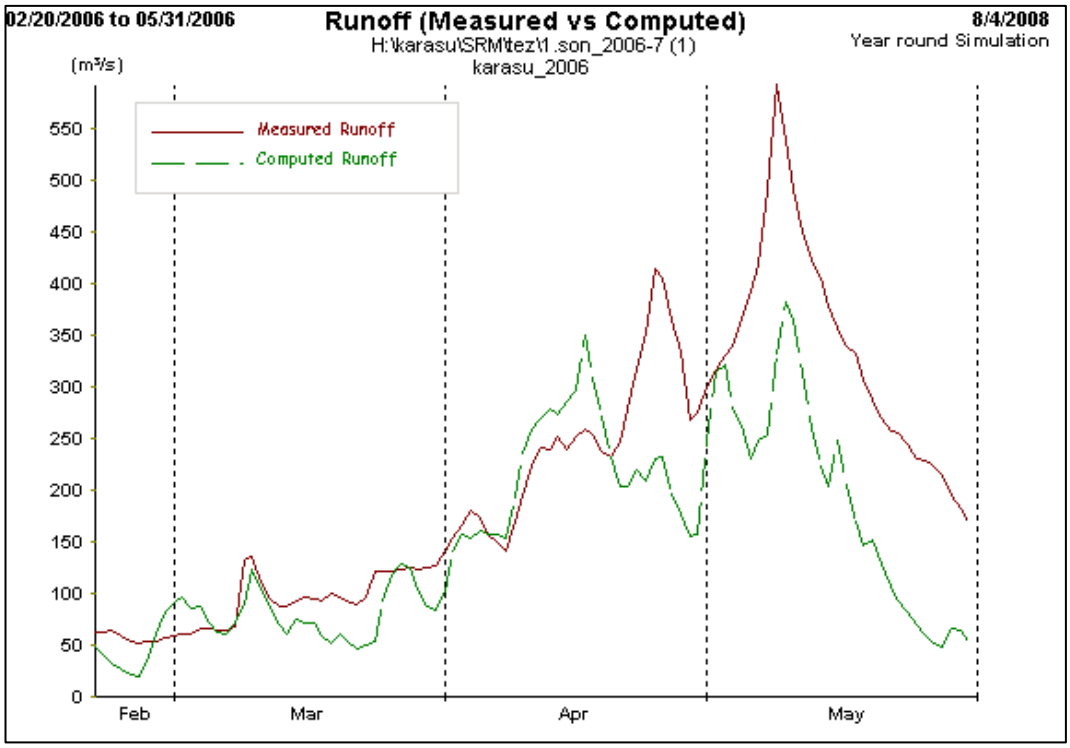

Figure 5.2 Simulated hydrograph for case 1

5.2. Case 2 : Model Run with Calibrated Parameters For Year 2006

In this case runoff coefficients, C_R and C_S; degree day, a; and recession coefficients x and y is calibrated or improved:

5.2.1. Calibration of Runoff Coefficients C_R and C_S

Runoff coefficients are calibrated according to SRM Manual and parameter values of previous studies. The characteristic of runoff coefficient described in section 4.4.3.1 and are also shown in Figure 4.23. The both graphic of calculated and calibrated runoff coefficients can be seen in Figures 5.3 and 5.4.The Figure 5.5 and 5.6 shows

comparison of the calibrated C_S and C_R with the C_S and C_R values that used in previous model run for the years 1997, 1998 and 2005.

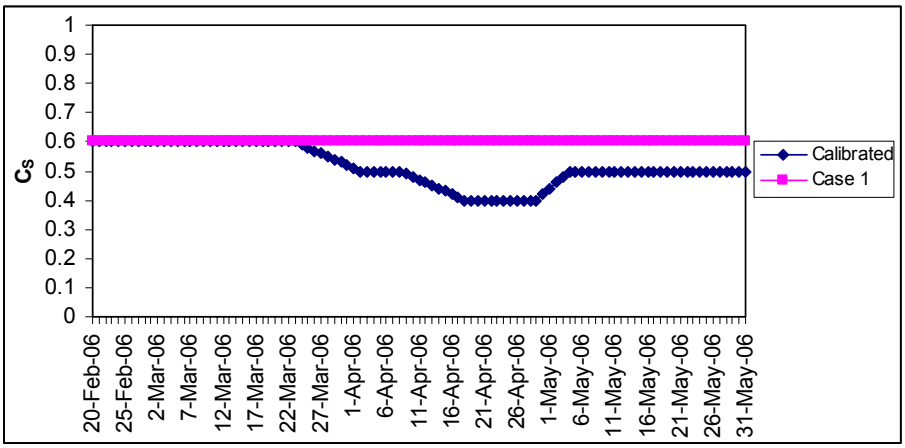

Figure 5.3 Calculated, calibrated C_S for year 2006

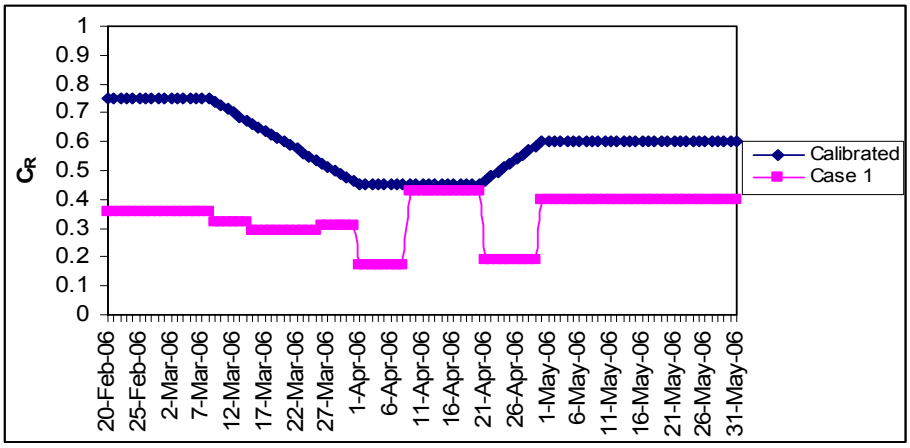

Figure 5.4 Calculated, calibrated C_R for year 2006

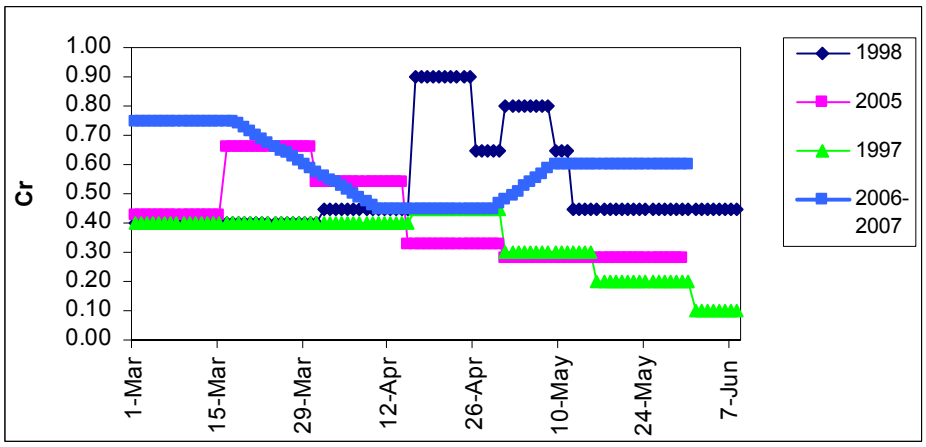

Figure 5.5 The comparison of the calibrated C_R with the years 1997, 1998, 2005

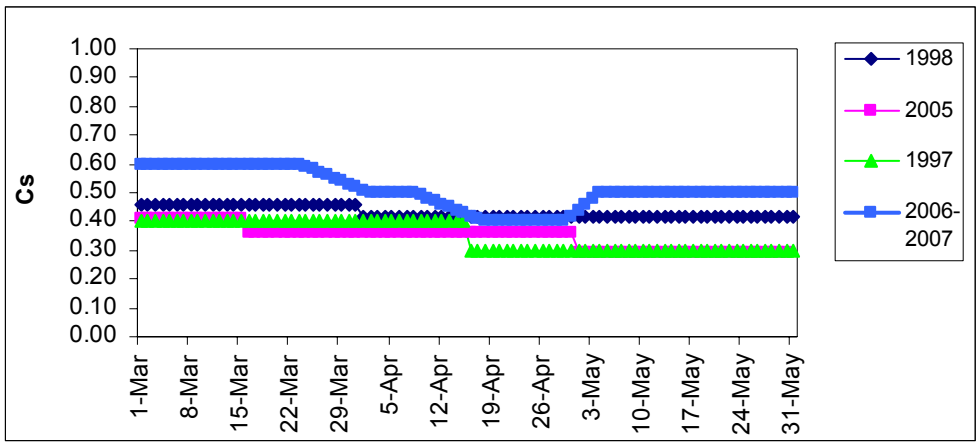

Figure5.6 The comparisons of the calibrated CS with the years 1997, 1998, 2005

5.2.2. Degree Day Factor (a) For Case 2

The degree day factor was decided in case 1 according to a previous thesis study (Tekeli A.E., 2000). The degree day factors for each elevation zone in that study are calculated from snow density measurements obtained from snow pillows. The values obtained for each elevation zone in Table 4.6 are changed as in Table5.2 according to the Kaya's thesis study (1999).The degree day factors are also assumed to be areal values for Karasu Basin, that is they are entered to model as basin wide (Kaya,

1999).Therefore, the same degree day factor values for each elevation zone as a basin wide are used in case 2.

Table 5.2 Changed degree day factor (a) values

Date Range	a
20 Feb - 14 Apr	0.35
15 Apr -2 May	0.40
3 May - 31 May	0.45

5.2.3. Calibration of Recession Coefficient, k

The recession coefficient is a very effective parameter in SRM. 1-k portion of daily meltwater is seen in runoff. From Figure 5.2 it is seen that calculated recession coefficients should be calibrated. Basin response is very quick. Therefore k value would be decreased. To decrease k value x value can be increased. For this case, x value is **increased from 0.8555 to 0.9883** which is used by Tekeli (2000), in his thesis study.

The other parameters remain same. In Table5.3 the parameters of case 2 are shown. The model is performed with those calibrated parameters and the results for year 2006 in Figure 5.7 and 5.8 are obtained.

Table 5.3 Parameters of case 2

	Runoff Coef. For Snow (Cs)	Runoff Coef. For Rain (Cr)	Degree Day Factor (a)	Critical Temp. (T_{CRIT})	Rainfall Cont. Area (RCA)**	Recession Coefficient (x)	Recession Coefficient (y)	Time Lag (L)
20 feb-28 feb	0.6	0.75	0.35	0.01	0	0.9883	0.011	15
1 mar-8 mar	0.6	0.75	0.35	0.01	1	0.9883	0.011	15
9 mar - 14 mar	0.6	0.706*	0.35	0.01	1	0.9883	0.011	15
15 mar-23 mar	0.6	0.613*	0.35	0.01	1	0.9883	0.011	15
24 mar-31 mar	0.55*	0.51*	0.35	0.01	1	0.9883	0.011	15
1 apr-8 apr	0.5	0.45	0.35	0.01	1	0.9883	0.011	15
9 apr - 20 apr	0.44*	0.45	0.375*	0.01	1	0.9883	0.011	15
21 apr - 30 apr	0.4	0.53*	0.40	0.01	1	0.9883	0.011	15
1 may - 31 may	0.50	0.6	0.45	0.01	1	0.9883	0.011	15

* Obtained by averaging the values within the given time interval
** RCA values are the values of elevation zone A.

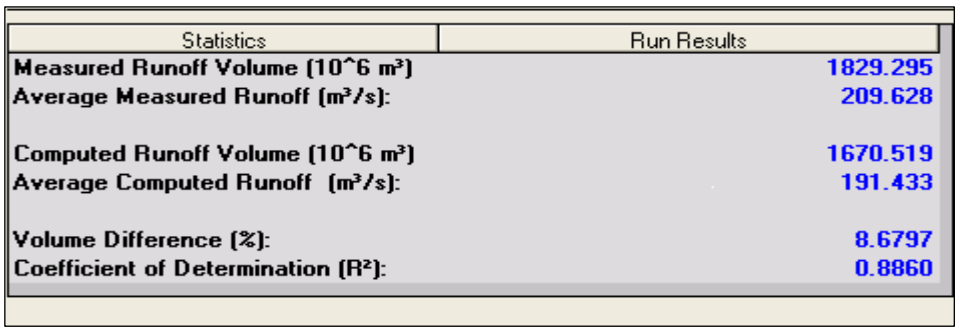

Figure 5.7 Simulation result for case 2

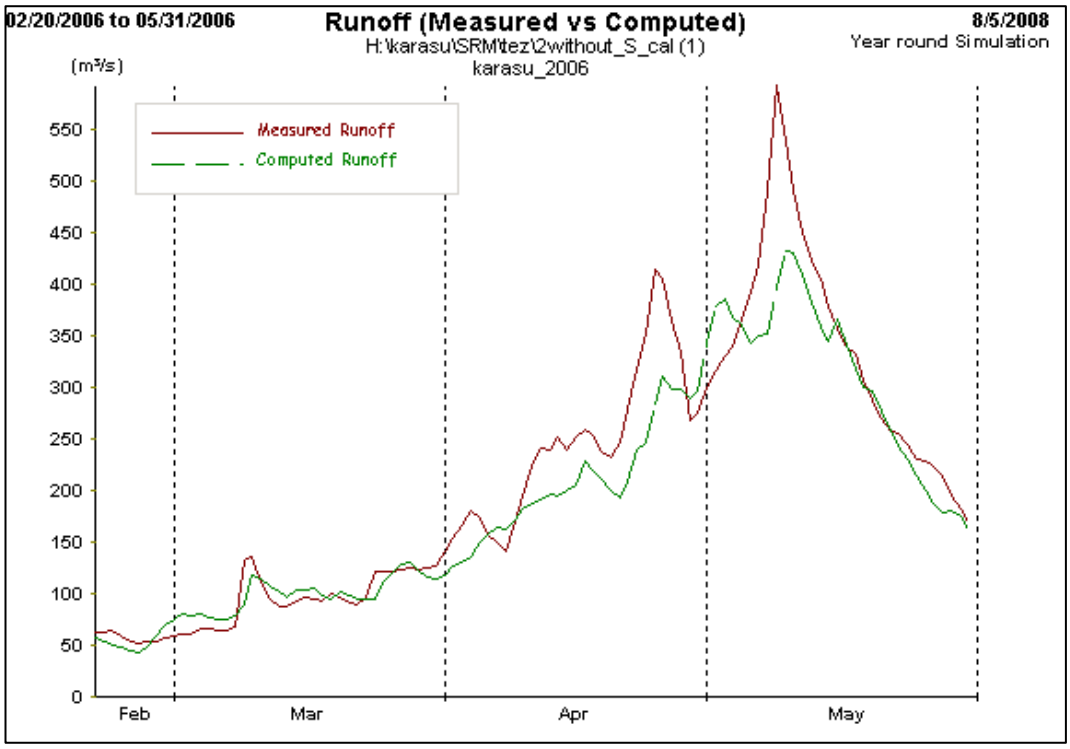

Figure 5.8 Simulated hydrograph for case 2

5.3. Case 3: Model Run with 2006 Calibrated Parameters For Year 2007

The model is performed for year 2007 with 2006 with calibrated parameters. The results are obtained as in Figure 5.9 and 5.10

Statistics	Run Results
Measured Runoff Volume (10^6 m³)	1444.064
Average Measured Runoff (m³/s):	165.482
Computed Runoff Volume (10^6 m³)	1427.978
Average Computed Runoff (m³/s):	163.639
Volume Difference (%):	1.1139
Coefficient of Determination (R²):	0.8790

Figure 5.9 Simulation result for case 3

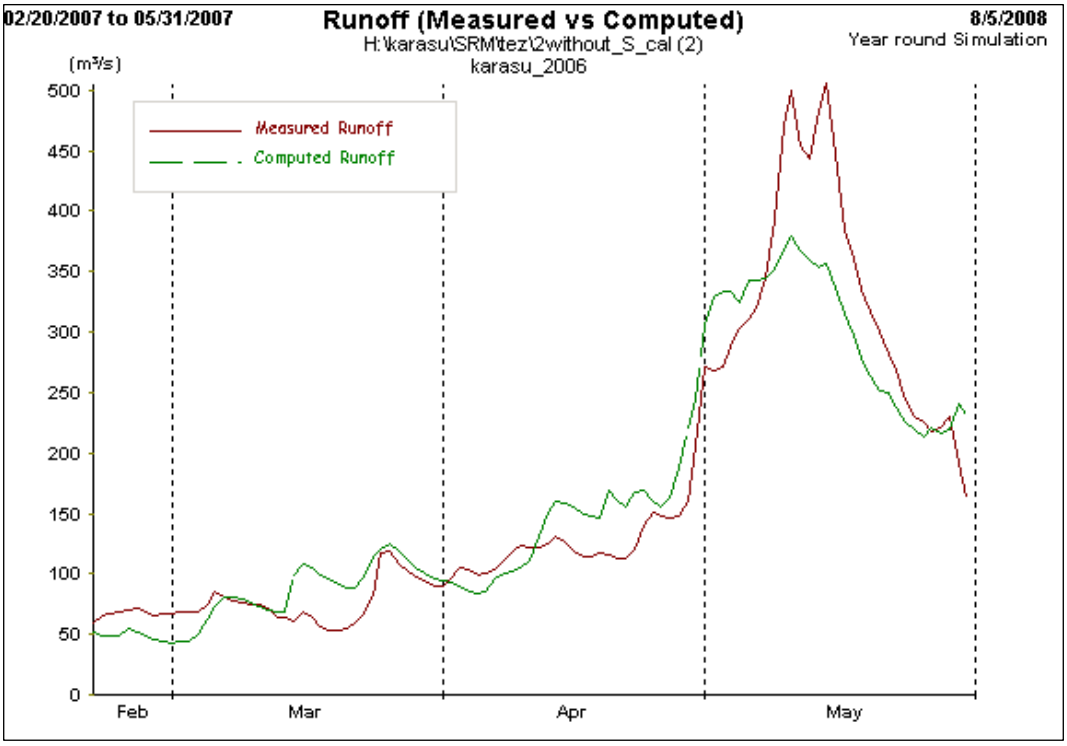

Figure 5.10 Simulated hydrograph for case 3

5.4. Case 4: One More Calibration of Both 2006 and 2007 Model Runs For The Years 2006 and 2007

It can be seen from case 2 and case 3 results (Figure 5.8 and 5.10) that both simulated hydrographs values are low at the peak time interval of hydrograph.

At that time intervals for both years 2006 and 2007, simulation basin response is low. Therefore, as an improvement, at that time interval; 4-11 may of each year, y value is **increased from 0.011 to 0.050 gradually**. By doing this, and the recession coefficient is decreased so that basin response to input becomes faster. The results are shown in Table 5.4. From those results y= **0.040** is chosen for both year 2006 and 2007.

At last, the results of this thesis study are shown in Figures 5.11-5.14 for the years 2006 and 2007. Moreover the resultant parameters of two successive run for the years 2006 and 2007 can be seen in the Table5.5.

Table 5.4 The simulation results with gradually increased y values for 4-11 may

	2006		2007	
"y" values	R^2	Volume Difference (%)	R^2	Volume Difference (%)
0.11	0.8860	8.67	0.8790	1.11
0.20	0.8978	6.61	0.8995	-0.33
0.30	0.8950	4.40	0.9131	-1.69
0.40	**0.8784**	**2.35**	**0.9226**	**-2.84**
0.50	0.8513	0.46	0.9287	-3.82

Statistics	Run Results
Measured Runoff Volume (10^6 m³)	1829.295
Average Measured Runoff (m³/s):	209.628
Computed Runoff Volume (10^6 m³)	1786.286
Average Computed Runoff (m³/s):	204.699
Volume Difference (%):	2.3512
Coefficient of Determination (R²):	0.8784

Figure 5.11 Simulation result for case 4 for year 2006

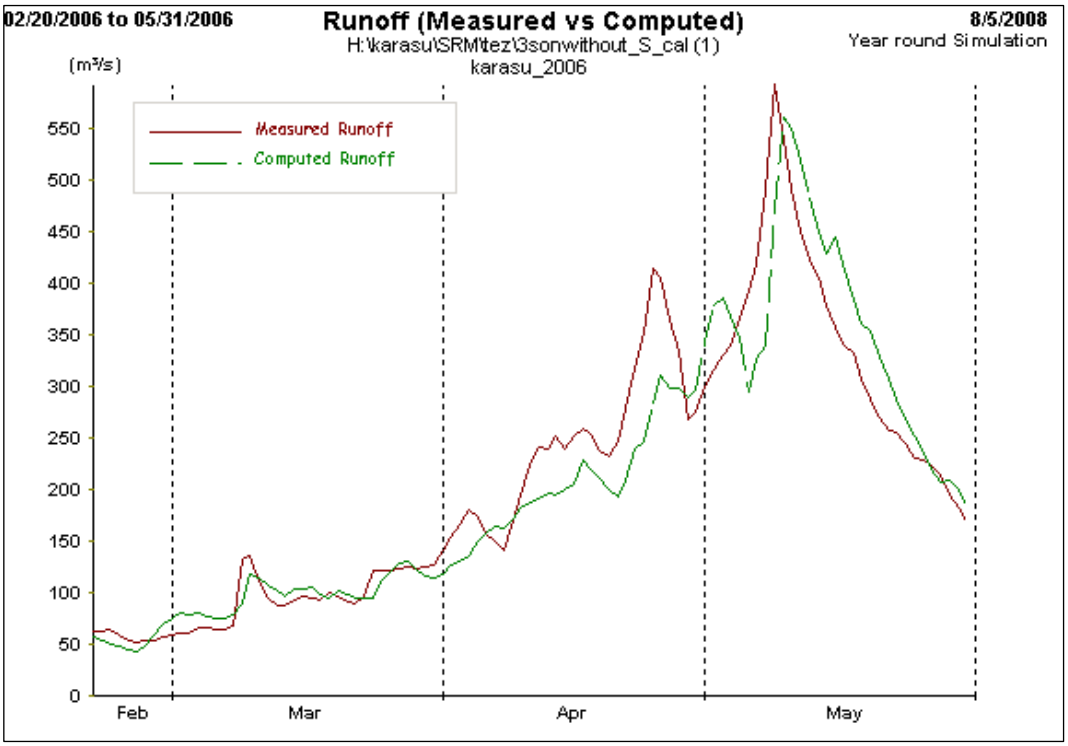

Figure 5.12 Simulated hydrograph for case 4 for year 2006

Statistics	Run Results
Measured Runoff Volume (10^6 m³)	1444.064
Average Measured Runoff (m³/s):	165.482
Computed Runoff Volume (10^6 m³)	1485.093
Average Computed Runoff (m³/s):	170.184
Volume Difference (%):	-2.8413
Coefficient of Determination (R²):	0.9226

Figure 5.13 Simulation result for case 4 for 2007

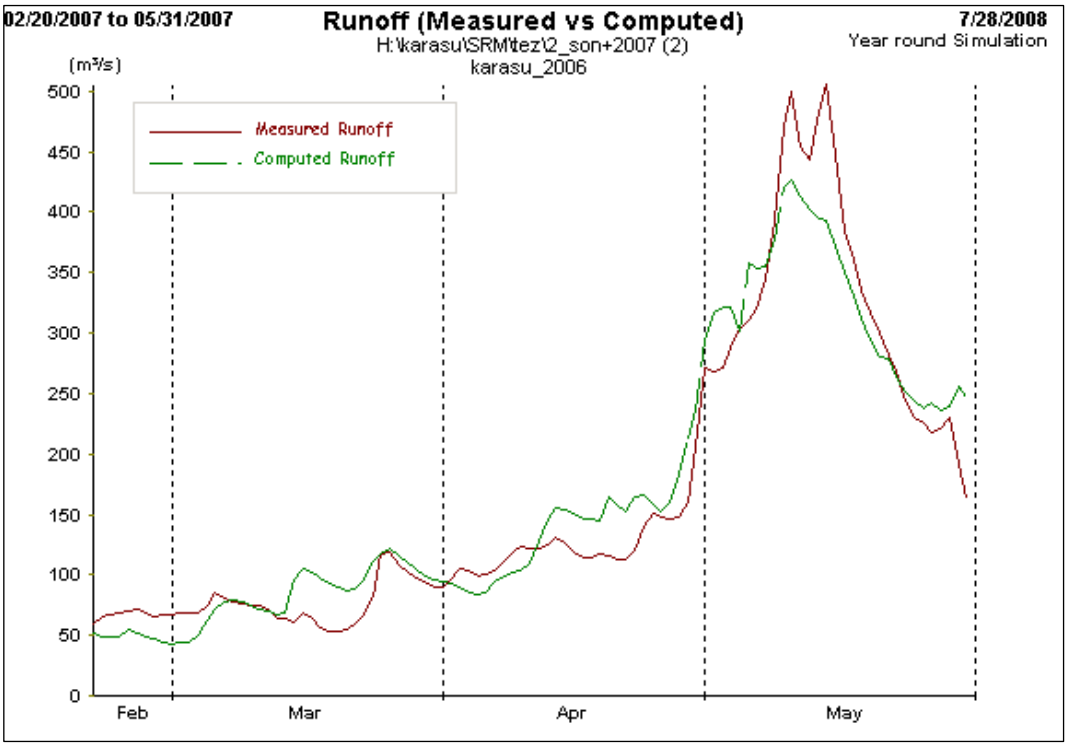

Figure 5.14 Simulated hydrograph for case 4 for year 2007

Table 5.5 The resultant SRM parameters for the years 2006, 2007

	Runoff Coef. For Snow (Cs)	**Runoff Coef. For Rain (Cr)**	**Degree Day Factor (a)***	**Critical Temp. (T_{CRIT}) ***	**Rainfall Cont. Area (RCA)****	**Recession Coefficient (x)**	**Recession Coefficient (y)**	**Time Lag (L)**
20 feb-28 feb	0.6	0.75	0.35	0.01	0	0.9883	0.011	15
1 mar-8 mar	0.6	0.75	0.35	0.01	1	0.9883	0.011	15
9 mar - 14 mar	0.6	0.706*	0.35	0.01	1	0.9883	0.011	15
15 mar-23 mar	0.6	0.613*	0.35	0.01	1	0.9883	0.011	15
24 mar-31 mar	0.55*	0.51*	0.35	0.01	1	0.9883	0.011	15
1 apr-8 apr	0.5	0.45	0.35	0.01	1	0.9883	0.011	15
9 apr - 20 apr	0.44*	0.45	0.375*	0.01	1	0.9883	0.011	15
21 apr - 30 apr	0.4	0.53*	0.4	0.01	1	0.9883	0.011	15
1 may - 4 may	0.47*	0.6	0.425*	0.01	1	0.9883	0.011	15
5 may - 10 may	0.5	0.6	0.45	0.01	1	0.9883	0.04	15
10 may 31 may	0.5	0.6	0.45	0.01	1	0.9883	0.011	15

*Obtained by averaging the values within the given time interval

** RCA values are the values of elevation zone A.

CHAPTER 6

CONCLUSIONS AND RECOMMENDATIONS

The following conclusions and recommendations are derived from this study. The recommendations are hoped to be a useful guideline to future studies on this subject.

In this study, snow depletion curves (SDC) for five elevation zones for years 2004, 2005, 2006 and 2007 are obtained by Remote Sensing Techniques and GIS applications. SDC for years 1997 and 1998 is used that is obtained from previous studies made in this basin area (Kaya, 1999 and Tekeli 2000). All of them gathered and compared for each elevation zone. Thus, snow cover area percentages of B and C elevation zones show more recognizable changes than D and E elevation zones since these last two zones have higher elevations. In elevation zone A, snow stays short time and SDC show more variations than the other elevation zones. Snow generally melts already in zone A at the beginning of April. In elevation zone B, snow stays till the second half of April, whereas in elevation zone C snow stays till May generally. Total area of B and C elevation zones is 66 % of total basin area that is why SDC of B and C elevation zone is very effective in snowmelt modelling process. In elevation zone D, snow usually melts till beginning of June whereas snow stays till the second half of June in elevation zone E. If all years are compared it is seen that the time period of snowmelt is shorter in elevation zones D and E than that of elevation zones A, B and C. Forecasting SDC is difficult matter for Karasu Basin. Because of the cloud problem of optic satellites, the cloud free days can not be caught easily that is why observing the changes in SDC for each year of the same region is useful for runoff forecast studies. According to observation on snowmelt

periods for each year the effect of global warming can not be seen clearly. However, the changes of SDC in different years may be an indicator for changes on climate if there is.

In this study, SRM was run for two different years 2006 and 2007. After 2006 parameters were recomputed and good result was obtained, SRM performed for 2007 with unchanged model parameters of 2006. Quite good result is obtained for the year 2007 with unchanged model parameters of 2006. More number of years should be evaluated to perform in the same basin area to obtain more reliable SRM parameters. The variation of SRM parameters is analysed for different years. Especially, the recession coefficient is computed by physically in this study. The forecasting studies depend mainly on reliability of model parameters. Obtaining parameters from field measurements are better for accuracy of the model in stead of calculating parameters from empiric methods.

The relation between precipitation and runoff is observed for the years 2006 and 2007. The amount and timing of snowmelt is detected by the help of SRM property that SDC is directly included to model. The model runoff results are compared with measured runoff. This helps to determine model accuracy, model performance and to verify model parameters. There were 1997, 1998 and 2004 calibrated parameters from previous studies for Karasu Basin. Calibrated parameters are also added for the years 2006 and 2007 by this study. Therefore the reliability of future forecast studies are increased Basin characteristics such as forested area, soil conditions if available are also useful for determination of model parameters. In future studies, seasonal and short term runoff forecasts can be done after determination of model parameters. Modified depletion curves which relate snow cover areas to cumulative snow depths can be derived. .

The performance of SRM depends on how sufficient and accurate data is obtained. The success of the model is limited to improvement in quality of input variables; SCA percentages, especially temporarily and spatially distributed precipitation and temperature data. The precipitation and temperature data is not available in higher

elevations. Maximum height of station is 2340 m. whereas the maximum altitude in the basin area is 3487 m. The number of stations should be increased and located in higher elevations to obtain high quality of distributed precipitation and temperature data.

In this study, MODIS daily snow product, MODIS10A1 is used for obtaining snow cover area percentages. Approximately 10 images that have less than 30 % area of cloud are detected in a snowmelt season for each year. If the number of cloud free images is improved, the better SDC would be obtained. There is also one method that improves the cloud covered images (Tekeli et al, 2005). In that method, an exponential curve dependant on temperature is calculated for cloud covered days.
That kind of methods will improve SDC. Optical images have problem with cloud. That is why, microwave images which are used together with optical images would improve detecting cloud free days in the basin area.

MODIS snow product, MODIS10A1 gives information only in binary format whether there is snow in pixel or not. The percentages of snow cover area in pixel area can not be found with their product. Fractional Snow Cover Area (FSCA) would serve that kind of information. By the help of FSCA, the quality of snow depletion curves would increase. Thus, that would provide more accurate simulated runoff hydrographs.

Temperature is an important meteorological variable that determine snowmelt process and type of precipitation. It also affects snow accumulation. Therefore it should be taken extreme care to spatially and temporarily distribution of temperature

The precipitation and temperature data is distributed by using **Detrended Kriging Program** which applies kriging / detrended kriging method. Kriging method is well known in literature as objective, statistically rigorous and performs as well as or better than other estimation techniques. The other techniques can not handle with orographic effects. Using slope and aspect characteristic of basin area could improve

the quality of distributed temperature and precipitation data by Detrended Kriging Program.

Recession coefficients x and y values can show variation among different snowmelt years even in a year. In SRM manual it is clearly explained that recession coefficients which may be right for snowmelt period are usually too low for the winter months (Rango, 1998). It is also clarified in user manual of SRM that user can decide to increase or decrease the k values according to basin response. If k value is low, basin will response too quickly. Therefore if user detects something wrong with basin response, a quick improvement is possible by deriving new x and y values. In previous studies recession coefficients are taken average values whereas in this study the recession coefficients are calculated and obtained more carefully according to basin model response.

The runoff coefficients for snow (C_S) and for rain (C_R) are calculated according to previous studies and empiric methods. Determining C_S and C_R with isotope methods could improve the parameterization of SRM and model results.

T_{CRIT} value is assumed as 0.01 in this study. Although it provides good results, the variation of this value with elevation change should be taken care. The ground measurement may improve T_{CRIT} values. The base temperature is taken 0 ^{o}C by SRM. However it can change in snowmelt season .This would be taken care in the future by SRM program build upper.

Consequently, the improvements in the new algorithms prosper the studies for that region. The modelling studies in that region contribute the information database of planning of water resources. In order to obtain a good planning of water resources, the region would be well known especially the timing of snowfall and snowmelt should be well known. There are more then 200 dams in Turkey which are operated by governmental organizations for irrigation, water supply and energy. With regarding management of water resources, modelling studies are hoped to be performed more widespread.

REFERENCES

Armstrong RL., Brodzik MJ. (2001). Recent Northern Hemisphere snow extent: a comparison of data derived from visible and microwave satellite sensors, Geophysical Research Letters, 28 : 3673–3676.

Aronoff S. (1993).Geographic Information Systems : A Management perspective, WDC Publications

Aytemiz L., Kodaman T. (2006). Sınır Aşan Sular Kullanımı ve Türkiye- Süriye İlişkileri, TMMOB Su Politikaları Kongresi

Barnes WL, Pagano TS, Salomonson VV. (1998). Prelaunch characteristics on the moderate resolution imaging spectroradiometer (MODIS) on EOS-AM1. IEEE Transactions on Geoscience and Remote Sensing, 36: 1088–1100.

Bitner D, Carroll T, Cline D, Romanov R. (2002). An assessment of the differences between three satellite snow cover mapping techniques, Hydrological Processes, 16: 3723–3733.

Chang ATC, Foster JL, Hall DK. (1987). Nimbus-7 SMMR derived global snow cover parameters, Annals of Glaciology, 9: 39–44.

Ferguson RI. (1999). Snowmelt runoff models, Progress in Physical Geography, 23: 205–227.

Garen D. (1994). Mean Areal Precipitation For Daily Hydrologic Modeling In Mountainous Regions, Water Resources Bulletin, 30:481-491.

Garen D. (2003). Detrended Kriging Program (DK) User's Guide

Hall DK, Andrew BT, James LF, Alfred TCC, Milan A. (2000). Intercomparison of satellite-derived snow-cover maps, Annals of Glaciology, 31: 369–376.

Hartman RK, Rost AA, Anderson DM. (1996). Operational processing of multi-source snow data, In Third International Conference/Workshop on Integrating Geographic Information Systems and Environmental Modeling, National Center for Geographic Information and Analysis, Santa Barbara, CA.

International River Basin Management Congress (2007) Antalya ,General Directorate of State Hydraulic Works, 1: 7-21

Kaya I. (1999).Application of Snowmelt Runoff Model Using Remote Sensing and Geographic Information Systems ,Master of Science Thesis, Water Resources Laboratory, Civil Engineering Department, Graduate School of Natural and Applied Sciences, Middle East Technical University.

GIS World (1991). MKS-ASPECT Enhances Color Surface Renderings, GIS World, 4(October): 30-32.

Klaassen, B., Pilgrim,D.H. (1975). Hydrograph recession constants for New South Wales streams , Inst.Eng.Civ.Eng.Trans., CE17, 43-49

Klein AG, Barnett AC. (2003). Validation of daily MODIS snow cover maps of the Upper Rio Grande river basin for the 2000–2001 snow year, Remote Sensing of Environment, 86: 162–176.

Martinec, J. (1960). The degree-day factor for snowmelt runoff forecasting. IUGG General Assembly of Helsinki, IAHS Commission of Surface Waters, IAHS Publ. no. 51, 468-477.

Martinec J, Rango A, Robert R. (2003). Snow Runoff Model (SRM) User's Manual.

Maurer EP, Rhoads JD, Dubayah RO, Lettenmaier DP. (2003). Evaluation of the snow-covered area data product from MODIS, Hydrological Processes, 17: 59–71.

Mitchell KM, DeWalle DR. (1998). Application of the snowmelt runoff model using multiple-parameter landscape zones on the Towanda Creek basin, Pennsylvania, Journal of the American Water Resources Association, 34: 335–346.

Moellering, H., and Kimerling A.J. (1990). A New Digital Slope-Aspect Display Process, Cartography and Geographic Information Systems, 17(2): 151-159.

National Aeronautics and Space Administration (NASA), http://modis.gsfc.nasa.gov/about/specifications.php, 20.08.2008

National Aeronautics and Space Administration (NASA), http://modis-snow-ice.gsfc.nasa.gov/val-df.html, 17. 06.2008

National Aeronautics and Space Administration (NASA), http://modis-snow-ice.gsfc.nasa.gov/MOD10A1.html, 15.07.2008

National Aeronautics and Space Administration (NASA), http://landweb.nascom.asa.gov/cgi-bin/browse/browse.cgi, 15.07.2008

National Snow and Ice Data Center (NSIDC), http://nsidc.org/~imswww/pub/imswelcome/index.html, 15.06.2008

National Snow and Ice Data Center (NSIDC), http://nsidc.org/cgi-bin/get_metadata.pl?id=mod10a1, 10.07.2008

Perzyna , G.,Parameter estimation from short observation serious of low flows , Dr.Sci.Thesisi İnst.Geophys.,University of Oslo , Oslo, Norway,1993

Pivot F.C., Duguay C.R., Brown R.D.,Duchiron B.,Kergomard C. (2002). Remote sensing of snow cover for climate monitoring in the Canadian Subarctic, A comparison between SMMR–SSM/I and NOAA–AVHRR sensors.

Potts HL. (1937). Snow surveys and runoff forecasting from photographs, Transactions of the American Geophysical Union, South Continental Divide Snow-Survey Conference, 658–660.

Rango A, Martinec J. (1981). Accuracy of snowmelt runoff simulation, Nordic Hydrology, 12: 265–274.

Rango A. (1986). Progress in snow hydrology remote-sensing research, IEEE Transactions on Geoscience and Remote Sensing, 24: 47–53.

Rango A. (1996). Spaceborne remote sensing for snow hydrology applications, Hydrological Science Journal, 41: 477–494.

Romanov P, Gutman G, Csiszar I. (2000). Automated monitoring of snow cover over North America with multispectral satellite data, Journal of Applied Meteorology, 39: 1866–1880.

Şensoy A. (2000). Spatially distributed hydrologic modeling approach using geographic information systems, Thesis submitted to the Graduate School of Natural and Applied Sciences of Middle East Technical University.

Şensoy A. (2005). Physically based point snowmelt modeling and its distribution in Euphrates basin, Thesis submitted to the Graduate School of Natural and Applied Sciences of Middle East Technical University.

Şorman A. (1999). A remote sensing and geographic information systems approach in hydrologic modeling, Thesis submitted to the Graduate School of Natural and Applied Sciences of Middle East Technical University.

Şorman A. (2005). Use of satellite observed seasonal snow cover in hydrological modeling and snowmelt runoff prediction in upper Euphrates basin, Turkey, Thesis submitted to the Graduate School of Natural and Applied Sciences of Middle East Technical University.

UNEP (2001) The Mesopotamian Marshlands: Demise of an Ecosystem, Early Warning and Assessment Technical Report No.3, UNEP/DEWA/TR.0103, Geneva.

Tabios G.Q., III and J.D. Salas. (1985).A comparative Analysis of Techniques for Spatial Interpolation of Precipitation, Water Resources Bulletin, 21(3):365-380.

Tekeli A.E. (2000). Integration of Remote Sensing and Geographic Information Systems on Snow Hydrology Modeling.

Tekeli A.E., Akyürek Z., Sensoy A., Sorman A.A., Sorman A.Ü. (2005). Modelling the temporal variation in snow-covered area derived from satellite images for simulating/forecasting of snowmelt runoff in Turkey, Hydrological Sciences Journal, 50 (4) : 669-682.

Tekeli A.E. (2005). Operational Hydrological Forecasting of Snowmelt Runoff by Remote Sensing and Geographic Information Systems Integration

WMO (1986) Intercomparison of Models of Snowmelt Runoff, Operational Hydrol. Report 23, World Meteorological Organization, Geneva, Switzerland.

APPENDIX A

TEMPORARILY–SPATIALLY DISTRIBUTED TEMPERATURE, PRECIPITATION AND SNOW COVERAGE DATA FOR 2006 AND 2007

Table A.1, A.2 and A.3 shows the values of main input variables to SRM; temperature, precipitation and snow coverage for 2006 and 2007 respectively.

Table A.1 Daily average temperatures values for each elevation zone

T	A		B		C		D		E	
Date	2006	2007	2006	2007	2006	2007	2006	2007	2006	2007
20-Feb	-3.4	0.2	-6.7	-3.9	-9.6	-7.6	-12.9	-16.8	-16.8	-19.3
21-Feb	-3.6	3	-6.5	-0.3	-8.9	-3.2	-11.7	-10.5	-15	-8.4
22-Feb	-2.8	3.4	-5.6	0.1	-8	-2.8	-10.7	-10	-14	-8
23-Feb	-2.6	5.2	-5.5	1.9	-8.1	-1.1	-11	-8.4	-14.6	-6.2
24-Feb	0.1	-0.1	-2.9	-3.5	-5.5	-6.5	-8.5	-13.9	-12.1	-11.1
25-Feb	4.5	-5.7	1.1	-11.4	-1.8	-16.4	-5.1	-28.8	-9.1	-27.6
26-Feb	6.6	-6.2	2.7	-12.1	-0.7	-17.3	-4.5	-30.1	-9.2	-28.3
27-Feb	6.3	-4.2	2.9	-9.7	0	-14.5	-3.3	-26.5	-7.4	-25
28-Feb	5.4	-0.3	2.1	-5.2	-0.8	-9.4	-4.1	-20	-8.1	-13.9
29-Feb	5.2	2.8	2.2	-1.2	-0.5	-4.7	-3.5	-13.5	-7.2	-6.9
1-Mar	4.1	3.2	0.4	-0.7	-2.8	-4.1	-6.4	-12.6	-10.8	-8.5
2-Mar	5.4	4.7	2	1	-1	-2.2	-4.4	-10.4	-8.5	-9.2
3-Mar	1.1	6.1	-3	2.8	-6.6	-0.2	-10.6	-7.5	-15.5	-5.6
4-Mar	4.6	4	0.3	1.7	-3.5	-0.3	-7.8	-5.2	-13	-3.8
5-Mar	5.4	2.8	1.1	-0.3	-2.7	-3.1	-7	-10.1	-12.2	-10.2
6-Mar	7.2	2.4	2.6	-1.8	-1.4	-5.5	-5.9	-14.7	-11.4	-16.2
7-Mar	5.4	3.8	2.8	-1.2	0.6	-5.7	-1.9	-16.7	-5	-18
8-Mar	4.6	2.2	1.8	-3.2	-0.6	-8	-3.3	-19.8	-6.6	-18.5
9-Mar	1.5	2	-2.1	-3.7	-5.2	-8.7	-8.8	-21.1	-13	-20.5
10-Mar	2.6	2.5	-2.2	-3.3	-6.5	-8.4	-11.2	-21.2	-17	-20.9
11-Mar	4.2	3.1	-0.7	-2.5	-5	-7.4	-9.8	-19.5	-15.7	-17.3

Table A.1 Continued

12-Mar	5	1.2	0.1	-2.7	-4.1	-6.1	-8.9	-14.5	-14.7	-12.1
13-Mar	8.2	4.9	3.7	1.7	-0.2	-1.1	-4.7	-8	-10	-5.1
14-Mar	4.9	5.2	1.2	1.6	-2	-1.6	-5.7	-9.6	-10.1	-6.3
15-Mar	5.4	2.1	1.6	-1.9	-1.8	-5.4	-5.6	-14.2	-10.2	-12.5
16-Mar	3.4	1.1	-0.7	-3.8	-4.3	-8.1	-8.3	-18.7	-13.3	-18.4
17-Mar	4.1	3.9	0.6	-1.1	-2.4	-5.5	-5.9	-16.6	-10	-13.6
18-Mar	2.9	3.1	0.3	-1.3	-2.1	-5.1	-4.7	-14.6	-7.8	-9.7
19-Mar	0.2	2.8	-3.8	-1.3	-7.4	-4.9	-11.4	-13.8	-16.2	-5.4
20-Mar	4.9	4.7	0.3	0.5	-3.7	-3.1	-8.3	-12.2	-13.8	-5.5
21-Mar	6.2	8.4	2.7	3.9	-0.4	-0.1	-3.9	-9.9	-8.1	-7.6
22-Mar	7.4	9.5	3.4	4.9	-0.1	0.8	-4	-9.2	-8.8	-6.1
23-Mar	11.9	6.6	7.3	3.6	3.4	0.9	-1.1	-5.8	-6.5	-3.8
24-Mar	8	5.1	5.3	1.6	3	-1.5	0.4	-9	-2.8	-6.9
25-Mar	7.5	4.6	4.1	0.7	1.2	-2.7	-2.1	-11.1	-6.1	-9
26-Mar	7.1	3	3.7	-0.9	0.8	-4.3	-2.5	-12.8	-6.5	-10.8
27-Mar	7.2	3.3	3.1	-0.7	-0.5	-4.3	-4.6	-13.1	-9.5	-9.3
28-Mar	6.9	3.5	3	-0.7	-0.4	-4.4	-4.2	-13.5	-8.8	-10.9
29-Mar	9.3	4.1	5	0.3	1.2	-3	-3	-11.3	-8.1	-9
30-Mar	11.1	6.6	7.1	2.6	3.5	-1	-0.5	-9.7	-5.3	-7.6
31-Mar	11	7.4	7.5	3.6	4.4	0.4	1	-7.8	-3.2	-5
1-Apr	10.2	4.1	6.8	1.3	3.8	-1.3	0.4	-7.6	-3.8	-7.6
2-Apr	6	2.5	3.6	-0.4	1.5	-2.9	-0.8	-9.2	-3.7	-9.2
3-Apr	5.9	2.6	3.6	-0.8	1.6	-3.7	-0.7	-11.1	-3.4	-11.1
4-Apr	6.9	6.3	3.8	1.3	1.1	-3.1	-1.9	-14	-5.6	-14
5-Apr	8.4	6.8	4.7	3.7	1.5	0.9	-2.2	-5.9	-6.6	-5.9
6-Apr	9.6	7.1	5.7	3.4	2.2	0.1	-1.7	-8.1	-6.5	-8.1
7-Apr	13.7	8.6	9.9	3.9	6.6	-0.1	2.9	-10.2	-1.6	-10.2
8-Apr	12.4	6.9	9	3.2	6	0	2.7	-7.9	-1.4	-7.9
9-Apr	13.8	6.1	10.2	2.7	7.1	-0.4	3.5	-7.9	-0.8	-7.9
10-Apr	12.4	8.4	9.5	4.7	7	1.5	4.1	-6.4	0.6	-6.4
11-Apr	12.8	8.1	9.1	5	5.9	2.4	2.3	-4.2	-2.1	-4.2
12-Apr	13.1	7	9.8	3.5	6.9	0.4	3.7	-7.3	-0.3	-7.3
13-Apr	14.7	4.9	11	1.8	7.7	-0.9	4.1	-7.6	-0.4	-7.6
14-Apr	13.7	5	11.3	1.5	9.2	-1.5	6.8	-9.2	4	-9.2
15-Apr	12.4	3	10	-0.6	7.8	-3.7	5.4	-11.5	2.4	-11.5
16-Apr	13.8	4.6	10.5	0.5	7.5	-3.2	4.3	-12.3	0.3	-12.3
17-Apr	13.7	1.6	10.2	0	7.2	-1.4	3.8	-4.9	-0.4	-4.9
18-Apr	13.9	3.9	10.4	1.5	7.3	-0.7	3.9	-6	-0.3	-6
19-Apr	13.3	2.5	10	-0.8	7.1	-3.7	3.8	-11.1	-0.1	-11.1
20-Apr	11	4.5	7.9	-0.1	5.2	-4.1	2.1	-14.1	-1.6	-14.1
21-Apr	11.6	8.8	8.6	4.1	6	0.1	3.1	-10.1	-0.5	-10.1
22-Apr	11.8	5	8.7	2.6	5.9	0.6	2.8	-4.5	-0.9	-4.5
23-Apr	10.4	1.8	7.9	-1.3	5.7	-4	3.2	-10.6	0.2	-10.6
24-Apr	5.2	4.2	2.8	-0.2	0.6	-4	-1.8	-13.4	-4.8	-13.4

Table A.1 Continued

25-Apr	3	8.5	-0.4	3.4	-3.3	-1.1	-6.7	-12.2	-10.8	-12.2
26-Apr	7.3	9.2	3.2	5.8	-0.4	2.8	-4.5	-4.7	-9.4	-4.7
27-Apr	7.6	10.1	4.2	6.3	1.2	3.1	-2.1	-5	-6.2	-5
28-Apr	8.4	9.9	5.5	6.5	3.1	3.5	0.3	-4.1	-3.1	-4.1
29-Apr	10.7	8.4	7.7	5.4	5	2.7	2	-3.9	-1.7	-3.9
30-Apr	11.4	11.4	8.6	7.5	6.2	4.1	3.4	-4.4	0.1	-4.4
1-May	11.4	11.2	9.1	7.9	7.1	5.1	4.9	-2	2.2	-2
2-May	10.4	10.4	7.4	7.4	4.7	4.8	1.7	-1.6	-1.9	-1.6
3-May	12.9	10.1	9.2	6.7	5.9	3.8	2.2	-3.5	-2.3	-3.5
4-May	12.2	14.6	9.8	10.2	7.7	6.3	5.3	-3.2	2.5	-3.2
5-May	13.1	16.9	10.3	12.6	7.9	8.9	5.2	-0.5	2	-0.5
6-May	12.8	17.8	10.1	13.5	7.6	9.7	4.9	0.3	1.6	0.3
7-May	11.5	18.8	9.3	14.8	7.4	11.2	5.2	2.4	2.6	2.4
8-May	12.7	13.3	9.6	10.5	6.9	8	3.8	1.8	0	1.8
9-May	13.2	15.6	9.5	11.6	6.3	8.1	2.6	-0.6	-1.8	-0.6
10-May	14.6	14.2	10.9	10.2	7.7	6.8	4.1	-1.8	-0.3	-1.8
11-May	17	14.7	13.1	11.4	9.7	8.4	5.8	1.2	1.1	1.2
12-May	15.8	15.1	13.4	12.3	11.3	9.8	9	3.7	6.1	3.7
13-May	13.4	14.3	9.8	11	6.7	8	3.2	0.7	-1	0.7
14-May	14.1	15.4	10.5	11.9	7.3	8.8	3.6	1.1	-0.7	1.1
15-May	16.8	17	13.2	13	10.1	9.5	6.6	0.8	2.4	0.8
16-May	17.3	18.7	13.7	14.8	10.5	11.3	6.9	2.7	2.5	2.7
17-May	11.8	18.9	9	14.8	6.5	11.1	3.8	2	0.4	2
18-May	14.6	17.9	11.2	14.1	8.3	10.9	5	2.7	1	2.7
19-May	16.8	18.8	13.6	15.1	10.8	11.8	7.6	3.8	3.7	3.8
20-May	16.7	19.9	13	16.1	9.7	12.8	6	4.6	1.6	4.6
21-May	16.7	20.8	13.2	16.8	10.1	13.3	6.7	4.5	2.5	4.5
22-May	17.3	18.6	13.8	15.4	10.8	12.6	7.5	5.7	3.4	5.7
23-May	18	22.6	14.7	19.1	11.8	16.1	8.5	8.5	4.6	8.5
24-May	18.7	17.1	15.4	14.3	12.6	11.9	9.3	5.8	5.4	5.8
25-May	19.8	19.2	16.2	16.5	13	14.2	9.5	8.3	5.2	8.3
26-May	17.6	17.9	15.2	15	13.1	12.3	10.7	5.8	7.8	5.8
27-May	14.7	17.1	11.7	14.1	9.1	11.5	6.1	5.1	2.4	5.1
28-May	17.3	19.3	14.1	15.8	11.3	12.7	8.2	5	4.3	5
29-May	19.7	18.6	16.4	15.4	13.5	12.7	10.3	5.8	6.4	5.8
30-May	21.9	17.9	18.6	14.1	15.8	10.8	12.6	2.6	8.7	2.6

TableA.2 Daily totally precipitation values for each elevation zone

Precipitation (cm)	A		B		C		D		E	
Date	2006	2007	2006	2007	2006	2007	2006	2007	2006	2007
20-Feb	0	0	0	0	0	0	0	0	0	0
21-Feb	0	0	0	0	0	0	0	0	0	0
22-Feb	0	0	0	0	0	0	0	0	0	0
23-Feb	0	0	0	0	0	0	0	0	0	0
24-Feb	0	0.4	0	0.4	0	0.4	0	0.4	0	0.4
25-Feb	0	0.4	0	0.4	0	0.4	0	0.4	0	0.4
26-Feb	0	0	0	0	0	0	0	0	0	0
27-Feb	0	0	0	0	0	0	0	0	0	0
28-Feb	0	0	0	0	0.1	0	0.1	0	0.1	0
29-Feb	0	0	0	0	0	0	0.1	0.1	0.2	0.1
1-Mar	0	0	0	0	0.1	0	0.1	0	0.1	0
2-Mar	0	0	0	0	0	0	0	0	0	0
3-Mar	0.1	0.1	0.1	0.1	0.1	0.2	0.1	0.2	0.1	0.3
4-Mar	0	0.7	0	0.7	0	0.7	0	0.7	0	0.7
5-Mar	0	1.7	0	1.7	0	1.7	0	1.7	0	1.7
6-Mar	0	0.6	0	0.7	0	0.8	0	1	0	1.1
7-Mar	0	0	0	0	0	0	0	0	0	0
8-Mar	1.4	0	1.4	0	1.4	0	1.4	0	1.4	0
9-Mar	0.8	0	0.8	0	0.8	0	0.8	0	0.8	0
10-Mar	0	0	0	0	0	0	0	0	0	0
11-Mar	0	0	0	0	0	0	0	0	0	0
12-Mar	0	0	0	0	0	0.1	0	0.1	0	0.2
13-Mar	0	1.1	0	1.4	0	1.6	0	1.9	0	2.3
14-Mar	0.1	0.4	0.1	0.4	0.2	0.4	0.3	0.4	0.3	0.4
15-Mar	0.3	0.5	0.3	0.5	0.3	0.5	0.3	0.5	0.3	0.5
16-Mar	0	0.1	0	0.1	0	0.1	0	0.1	0	0.1
17-Mar	0	0	0	0	0.1	0	0.2	0	0.3	0
18-Mar	0.6	0.2	0.7	0.2	0.7	0.2	0.8	0.2	0.8	0.2
19-Mar	0.4	0	0.4	0	0.4	0	0.4	0	0.4	0
20-Mar	0	0	0	0	0	0	0	0	0	0
21-Mar	0	0.1	0	0.1	0	0.1	0	0.1	0	0.1
22-Mar	0	0.3	0	0.3	0	0.3	0	0.3	0	0.3
23-Mar	0	0	0	0	0	0	0	0	0	0
24-Mar	0	0.5	0	0.6	0	0.8	0	0.9	0	1.1
25-Mar	0.3	0	0.3	0	0.3	0	0.3	0	0.3	0
26-Mar	0.2	0	0.2	0	0.3	0	0.3	0	0.4	0
27-Mar	0	0.1	0	0.1	0	0.1	0	0.1	0	0.1
28-Mar	0	0.2	0	0.2	0	0.2	0	0.2	0	0.2
29-Mar	0	0	0	0	0	0	0	0	0	0
30-Mar	0	0.1	0	0.1	0	0.1	0	0.1	0	0.1
31-Mar	0	0.1	0	0.1	0	0.1	0	0.1	0	0.1

Table A.2 Continued

1-Apr	0	0	0	0.1	0	0.2	0	0.2	0	0.3
2-Apr	0.3	0.3	0.3	0.5	0.3	0.6	0.3	0.8	0.3	1
3-Apr	0.7	0.8	0.8	0.8	0.8	0.8	0.8	0.8	0.8	0.8
4-Apr	0.4	0.1	0.5	0.1	0.6	0.1	0.7	0.1	0.8	0.1
5-Apr	0.5	0	0.6	0.1	0.6	0.1	0.6	0.1	0.6	0.2
6-Apr	0.1	0.3	0.1	0.3	0.1	0.4	0.1	0.4	0.2	0.4
7-Apr	0	0	0	0	0	0	0	0	0	0
8-Apr	0.2	0.1	0.2	0.1	0.2	0.1	0.2	0.1	0.2	0.1
9-Apr	0	0.3	0	0.4	0	0.4	0	0.5	0	0.6
10-Apr	0	0.5	0	0.5	0	0.5	0	0.5	0	0.5
11-Apr	0.3	0.2	0.3	0.3	0.3	0.4	0.3	0.4	0.3	0.5
12-Apr	0	0.4	0	0.5	0	0.6	0	0.8	0	1
13-Apr	0.2	0.2	0.2	0.2	0.2	0.2	0.2	0.3	0.2	0.3
14-Apr	0	0	0	0	0	0	0	0	0	0
15-Apr	0.2	0.7	0.6	0.7	0.9	0.8	1.3	0.8	1.8	0.9
16-Apr	0	0.2	0	0.3	0	0.4	0	0.5	0	0.6
17-Apr	0	0.9	0.1	0.9	0.1	1	0.1	1.1	0.1	1.2
18-Apr	0	1.7	0	1.7	0	1.7	0	1.7	0	1.7
19-Apr	0	0.2	0	0.2	0	0.2	0	0.2	0	0.2
20-Apr	0.2	0.2	0.5	0.2	0.8	0.2	1.2	0.2	1.6	0.2
21-Apr	1.1	0	1.1	0	1.2	0.2	1.3	0.4	1.4	0.6
22-Apr	0.1	0	0.3	0	0.5	0	0.7	0	1	0
23-Apr	1.3	0.6	1.3	0.6	1.3	0.6	1.3	0.6	1.3	0.6
24-Apr	1.5	0.5	1.5	0.5	1.5	0.5	1.5	0.5	1.5	0.5
25-Apr	1.6	0	1.6	0	1.6	0	1.6	0	1.6	0
26-Apr	0	0.1	0.1	0.2	0.1	0.2	0.1	0.3	0.1	0.3
27-Apr	0	0.5	0	0.5	0	0.5	0	0.5	0	0.5
28-Apr	0	0	0	0	0	0	0	0	0	0.1
29-Apr	1.1	1.2	1.2	1.5	1.2	1.8	1.3	2.1	1.4	2.5
30-Apr	0.3	0.4	0.7	0.4	1.1	0.4	1.5	0.4	2	0.4
1-May	0.5	0	0.5	0	0.5	0.1	0.5	0.1	0.5	0.2
2-May	0.2	0	0.2	0	0.2	0	0.2	0.1	0.2	0.1
3-May	0.4	0	0.4	0	0.4	0.1	0.4	0.1	0.4	0.1
4-May	0	0.6	0	0.6	0	0.6	0	0.6	0	0.6
5-May	0.6	0.1	0.6	0.1	0.6	0.1	0.6	0.1	0.6	0.1
6-May	0.1	0	0.3	0	0.4	0	0.6	0	0.8	0
7-May	1.2	0	1.3	0	1.3	0	1.4	0	1.4	0
8-May	1.2	0.3	1.3	0.4	1.3	0.4	1.4	0.4	1.4	0.4
9-May	0.6	0.5	0.6	0.5	0.6	0.5	0.6	0.5	0.6	0.5
10-May	0.2	0.2	0.2	0.2	0.2	0.2	0.2	0.2	0.2	0.2
11-May	0	0.1	0	0.2	0	0.2	0	0.3	0	0.5
12-May	0	0.2	0	0.2	0	0.2	0	0.2	0	0.2
13-May	0.1	0.5	0.1	0.5	0.1	0.5	0.1	0.5	0.1	0.5
14-May	0.7	0	0.9	0	1.1	0	1.3	0	1.5	0

Table A.2 Continued

15-May	0	0	0	0	0	0	0	0	0	0
16-May	0	0	0	0	0	0	0	0	0	0
17-May	0	0	0	0	0.1	0	0.1	0	0.1	0
18-May	0.4	0	0.4	0	0.4	0	0.4	0	0.4	0
19-May	0	0	0	0	0	0	0	0	0	0
20-May	0	0.3	0	0.3	0	0.3	0	0.3	0	0.3
21-May	0	0	0	0	0	0	0	0	0	0
22-May	0.1	0	0.1	0	0.1	0	0.1	0	0.1	0
23-May	0	0.1	0	0.2	0	0.2	0	0.2	0	0.2
24-May	0	0	0	0.1	0	0.2	0	0.3	0	0.4
25-May	0	0	0	0.3	0	0.5	0	0.8	0	1.2
26-May	0	0	0	0	0	0.2	0	0.4	0	0.7
27-May	0.3	0.3	0.3	0.3	0.3	0.3	0.3	0.3	0.3	0.3
28-May	0.1	0.8	0.1	0.8	0.1	0.8	0.1	0.8	0.1	0.8
29-May	0	0	0	0	0	0	0	0	0	0
30-May	0	1.1	0	1.1	0	1.2	0	1.2	0	1.2

Table A.3 Zonal snow cover area percentages

S (%)	A		B		C		D		E	
Date	2006	2007	2006	2007	2006	2007	2006	2007	2006	2007
20-Feb	70.2	35.4	99.8	92.4	100	99.6	100	100	99.9	100
21-Feb	61	32.8	99.8	91.7	100	99.6	100	100	100	100
22-Feb	51.9	30.2	99.4	91	100	99.5	100	100	100	100
23-Feb	41.8	27.6	97	90.2	99.9	99.5	99.5	100	100	100
24-Feb	31.7	25	94.5	89.5	100	99.5	100	100	100	100
25-Feb	27.9	22.4	92	88.8	99.9	99.5	100	100	100	100
26-Feb	24.2	19.7	89.6	88.1	99.8	99.4	100	99.9	100	100
27-Feb	20.4	17.1	87.1	87.4	99.7	99.4	100	99.9	100	100
28-Feb	16.7	21	84.6	88.9	99.6	99.4	100	99.9	100	99.9
29-Feb	12.9	24.9	82.2	90.4	99.5	99.3	100	99.9	100	99.7
1-Mar	9.2	28.8	79.7	91.8	99.4	99.3	100	99.8	100	99.6
2-Mar	5.4	32.7	77.3	93.3	99.3	99.3	100	99.8	100	99.4
3-Mar	1.6	36.6	74.8	94.7	99.2	99.2	100	99.7	100	99.3
4-Mar	0.6	40.5	72.3	96.2	99.1	99.2	100	99.7	100	99.1
5-Mar	0	44.3	69.4	97.6	99.2	99.2	100	99.7	100	99
6-Mar	0	48.2	66.5	99.1	99.2	99.2	100	99.6	100	98.8
7-Mar	0	46.2	63.6	95.3	99.3	99.1	100	99.6	100	98.7
8-Mar	0	44.2	60.7	91.6	99.4	99.4	100	99.8	100	100
9-Mar	0	42.2	57.8	87.9	99.4	99.7	100	100	100	100

Table A.3 Continued

10-Mar	0	40.2	54.9	84.2	99.5	99.7	100	100	100	99.9
11-Mar	0	38.2	52	80.5	99	99.7	99.9	99.9	100	99.8
12-Mar	0	36.2	49.1	76.8	98.5	99.7	99.9	99.9	100	99.7
13-Mar	0	34.2	46.2	73.1	98	99.7	99.8	99.9	100	99.7
14-Mar	0	32.2	43.3	69.4	96.1	99.7	99.8	99.9	100	99.6
15-Mar	0	30.1	40.4	65.6	94.1	99.7	99.8	99.9	100	99.5
16-Mar	0	28.1	37.5	61.9	92.1	99.7	99.8	99.9	100	99.4
17-Mar	0	26.1	34.6	58.2	90.2	99.7	99.8	99.9	100	99.3
18-Mar	0	24.1	31.7	54.5	88.2	99.6	99.8	99.9	100	99.2
19-Mar	0	22.1	28.8	50.8	86.2	99.6	99.8	99.9	100	99.1
20-Mar	0	20.1	25.9	47.1	84.3	99.6	99.8	99.9	100	99
21-Mar	0	18.1	23	43.4	82.3	99.6	99.8	99.9	100	99
22-Mar	0	16.1	20.1	39.6	80.3	99.6	99.8	99.9	100	98.9
23-Mar	0	14.1	17.2	35.9	78.4	99.6	99.9	99.8	100	98.8
24-Mar	0	12.1	14.3	32.2	76.4	99.6	99.9	99.8	100	98.7
25-Mar	0	10	11.4	28.5	74.4	99.6	99.9	99.8	100	98.6
26-Mar	0	8	8.5	24.8	72.5	99.6	99.9	99.8	100	98.5
27-Mar	0	6	5.6	21.1	70.5	99.6	99.9	99.8	100	98.4
28-Mar	0	4	3.7	17.4	68.5	99.6	99.3	99.8	100	98.3
29-Mar	0	2	1.9	13.7	66.6	99.6	98.8	99.8	100	98.3
30-Mar	0	0	1.8	9.9	63.1	99.6	95.5	99.8	100	98.2
31-Mar	0	0	1.7	14.1	59.7	99.6	92.2	99.7	100	98.1
1-Apr	0	0	1.6	18.2	56.3	99.6	88.9	99.5	100	98
2-Apr	0	0	1.5	22.4	52.8	99.6	85.7	99.4	100	97.9
3-Apr	0	0	1.4	26.5	49.4	99.6	82.4	99.3	100	97.8
4-Apr	0	0	1.3	30.6	46	99.6	79.1	99.1	100	97.7
5-Apr	0	2.7	1.2	34.8	42.6	99.6	75.8	99	100	97.6
6-Apr	0	5.3	1.1	38.9	39.1	99.6	72.5	98.9	100	97.6
7-Apr	0	8	1	43.1	35.7	99.5	69.2	98.8	100	97.5
8-Apr	0	10.7	0.9	47.2	32.3	99.5	67.1	98.6	100	97.4
9-Apr	0	13.4	0.8	51.3	28.8	99.5	65	98.5	100	97.3
10-Apr	0	16	0.7	55.5	25.4	99.5	62.9	98.4	100	97.2
11-Apr	0	18.7	0.6	59.6	22	99.5	60.8	98.3	100	97.1
12-Apr	0	21.4	0.5	63.8	18.5	99.5	58.6	98.1	100	97
13-Apr	0	24.1	0.4	67.9	15.1	99.5	56.5	98	100	96.9
14-Apr	0	26.7	0.3	72	11.7	99.5	54.4	97.9	100	96.9
15-Apr	0	29.4	0.2	76.2	8.2	99.5	52.3	97.7	100	96.8
16-Apr	0	32.1	0.1	80.3	4.8	99.5	50.2	97.6	100	96.7
17-Apr	0	34.7	0	84.5	1.4	99.5	48	97.5	100	96.6
18-Apr	0	37.4	0	88.6	0.3	99.5	36	97.4	97.4	96.5
19-Apr	0	40.1	0	92.7	0	99.5	34.9	97.2	97.1	96.4
20-Apr	0	42.8	0	96.9	0	99.5	33.8	97.1	96.7	96.3
21-Apr	0	32	0	91.2	0	96.4	32.7	99.7	96.4	100
22-Apr	0	25.5	0	84.3	0	96.5	31.6	99	96.1	97.7

Table A.3 Continued

23-Apr	0	19	0	77.5	0	96.6	30.5	98.4	95.7	95.3
24-Apr	0	12.5	0	70.6	0	96.7	29.4	97.7	95.4	93
25-Apr	0	11.3	0	63.5	0	88.3	28.3	95.6	95.1	93.6
26-Apr	0	10	0	56.5	0	79.8	27.1	93.5	94.8	94.2
27-Apr	0	8.8	0	49.4	0	71.3	26	91.4	94.4	94.8
28-Apr	0	7.5	0	42.4	0	62.9	24.9	89.3	94.1	95.4
29-Apr	0	6.3	0	35.3	0	54.4	23.8	87.1	93.8	96.1
30-Apr	0	5	0	28.2	0	45.9	22.7	85	93.4	96.7
1-May	0	3.8	0	21.2	0	37.5	21.6	82.9	93.1	97.3
2-May	0	2.5	0	14.1	0	29	20.5	80.8	92.8	97.9
3-May	0	1.3	0	7.1	0	20.5	19.4	78.7	92.5	98.6
4-May	0	0	0	0	0	12.1	18.3	76.6	92.1	99.2
5-May	0	0	0	0	0	3.8	17.2	74.5	91.8	99.8
6-May	0	0	0	0	0	2.3	16.1	67.1	91.5	99.6
7-May	0	0	0	0	0	2.1	15	61.6	91.2	98.3
8-May	0	0	0	0	0	1.8	13.8	56.1	90.8	97
9-May	0	0	0	0	0	1.5	12.7	50.5	90.5	95.7
10-May	0	0	0	0	0	1.3	11.6	45	90.2	94.4
11-May	0	0	0	0	0	1	10.5	39.5	89.8	93.1
12-May	0	0	0	0	0	0.8	8.8	34	86.6	91.8
13-May	0	0	0	0	0	0.5	7.1	28.5	83.4	90.5
14-May	0	0	0	0	0	0.3	5.5	23	80.1	89.2
15-May	0	0	0	0	0	0	3.8	17.5	76.9	87.9
16-May	0	0	0	0	0	0	3.5	12	73.7	70.1
17-May	0	0	0	0	0	0	3.3	10.2	70.5	67.9
18-May	0	0	0	0	0	0	3.1	8.5	67.2	65.6
19-May	0	0	0	0	0	0	2.8	6.7	64	63.4
20-May	0	0	0	0	0	0	2.6	4.9	60.8	61.1
21-May	0	0	0	0	0	0	2.4	3.1	53	58.8
22-May	0	0	0	0	0	0	2.1	2	45.2	47.2
23-May	0	0	0	0	0	0	1.2	1	48.7	35.5
24-May	0	0	0	0	0	0	0.8	0.9	47.4	32.5
25-May	0	0	0	0	0	0	0.4	0.8	46.1	29.6
26-May	0	0	0	0.1	0	0	0.5	0.7	44.7	26.7
27-May	0	0	0	0.1	0	0	0.5	0.6	43.4	23.7
28-May	0	0	0	0.1	0	0	0.6	0.6	42	20.8
29-May	0	0	0	0.1	0	0	0.2	0.5	16	17.8
30-May	0	0	0	0.2	0	0	0	0.4	30.3	14.9